Investigating Activation of the cGAS STING Pathway in Primary and Metastatic Uveal Melanoma

Katie Louise Mitchinson

MSc by Research Biomedical Science

Supervised by Dr Andrew Fielding and Dr Leonie Unterholzner

Biomedical and Life Sciences

Faculty of Health and Medicine

Lancaster University

October 2025

Abbreviations

Absent in Melanoma 2 – AIM2

Ataxia Telangiectasia Mutated – ATM

Apoptosis Associated Speck Like Protein – ASC

Ammonium Persulfate - APS

BRCA-1 Associated Protein - BAP1

v-raf murine sarcoma viral oncogene homolog B1 – BRAF

Bovine serum albumin – BSA

Bicinchoninic Acid assay - BCA

Chimeric Antigen receptor natural killer – CAR-NK

Centrosome Amplification - CA

Cyclic GMP-AMP Synthase - cGAS

Cyclic Guanosine Monophosphate- Adenosine Monophosphate - cGAMP

Cysteinyl Leukotriene Receptor Two - CYSTLTR2

Chromosomal Instability - CIN

Cyclic di-andenosine monophosphate – C-di-AMP

C-X-C motif chemokine ligand 10 – CXCL10

C-C- motif chemokine ligand 5 – CCL5

7,12-Dimethylbenz(a)anthracene – DMBA

5.6-dimethylaxanthenone-4 acetic acid - DMXAA

Damage Associated Molecular Pattern – DAMP

Dimethyl Sulfoxide – DMSO

Dulbecco's Modified Eagle Medium - DMEM

Enzyme Linked Immunosorbent Assay - ELISA

Eukaryotic Translation Initiation Factor 1A X-Linked - EIF1AX

Endoplasmic Reticulum – ER

Ectonucleotide Pyrophosphatase Phosphodiesterase 1 - ENPP1

False Discovery Rate – FDR

Foetal Bovine Serum - FBS

Fragments per kilobase of transcript per million mapped reads - FPKM

G protein-alpha subunit 11 - GNA11

G protein-alpha subunit Q – GNAQ

Human Immortalised Keratinocytes - HaCaT

High Mobility Group Box 1 - HMGB1

Heat Shock Protein – HSP

Horseradish Peroxidase - HRP

Herrings Testis DNA – (HT) DNA

Indoleamine-2,3-dioxygenase - IDO

IFN – Interferons

Interferon Regulatory Factor 3 – IRF3

Interferon Regulatory Factor 7 – IRF7

Interferon Stimulated Genes – ISG

Interferon Gamma Inducible Protein 16 – IFI16

Interleukin-6 -IL-6

Interleukin-8 - IL-8

Interleukin- 18 – IL-18

Interleukin- 1 beta – IL-1β

Interleukin 2 – IL-2

Kinesin Family Member C1 – KIFC1

KIT proto-oncogene, receptor tyrosine kinase – KIT

Mitochondrial Associated Membranes - MAMS

Mitochondrial Anti-viral Signalling Protein – MAVS

Microtubule Organising Centre - MTOC

Melanoma Differentiation Associated Protein 5 – MDA5

Mitogen Activated Protein Kinase - MAPK

Micronuclei – MN

Mitochondrial DNA – Mt DNA

Milli-Q Water – MQW

3-(4,5-Dimethylthiazol-2-yl)-5-(3-carboxymethoxyphenyl)-2-(4-sulfophenyl)-2H-tetra-zolium – MTS

Nod-like receptor protein 3 - NLRP3

Nuclear Factor Kappa- Light-Chain Enhancer of Activated B Cells - NF-κB

Natural Killer Cells – NK cells

Neuroblastoma RAS viral oncogene – N-RAS

Pattern Recognition Receptor - PRR

Pathogen Associated Molecular Pattern – PAMP

Penicillin/streptomycin – Pen/strep

Poly- [ADP-ribose] Polymerase 1 – PARP-1

Pericentriolar Material - PCM

Polo-Like Kinase 4 - plk4

Phosphatidylinositol 3 Kinase - PIK3

Phospholipase C Beta 4 - PLCB4

Phosphate Buffered Saline - PBS

Programmed Cell Death Ligand 1 - PD-L1

Ras-related C3 botulinum toxin substrate 1 – RAC1

Retinoic Acid Inducible Gene I – RIG-I

Room Temperature – RT

Reactive oxygen Species – ROS

Revolutions per minute – RPM

Sodium Dodecyl Sulfate-Polyacrylamide Gel Electrophoresis – SDS-PAGE

Sodium Dodecyl Sulfate - SDS

Splicing factor 3B subunit 1 - SF3B1

Serine/arginine-rich splicing factor 2 - SRFS2

Stimulator of Interferon Genes – STING

Tetramethylethylenediamine – TEMED

3,3′,5,5′-Tetramethylbenzidine -TMB

TANK Binding kinase 1 – TBK1

TNF-receptor associated factor 6 - TRAF6

Tumour Necrosis Factor Receptor - TNFR

Three Prime Repair Exonuclease 1 – TREX1

Triss buffered saline - TBST

Toll Like Receptor 3 and 4 – TLR3/ TLR4

Uveal Melanoma - UM

List of Figures

List of Tables

Acknowledgements

I would like to express my deepest gratitude to my supervisors Dr Andrew Fielding and Dr Leonie Unterholzner for their invaluable guidance and continuous support throughout the year. I would also like to thank members of their research groups, particularly Dr Joshua-Northecote Smith from the Fielding lab for taking the time to help me learn new lab techniques.

A special thank you, also goes to my fellow master's students and close friends for their support throughout the year.

I owe my biggest thank you to my mum and dad who truly are my biggest supporters and the reason I am where I am today. None of this would have been possible without your endless words of encouragement and the actions you take daily. I will always be grateful to the both of you.

Authors Declaration

This thesis is entirely my own work and has not been submitted in whole or in part for the award of a higher degree at any other educational institution. No sections of this thesis have been published.

Contents

Abstract

Centrosome amplification (CA) is a common feature in many cancers and can act as a double-edged sword, both increasing oncogenic phenotypes and acting as a potential Achilles' Heel. Cancer cells can use a process called centrosome clustering to survive but this can also promote genomic instability, leading to micronuclei (MN) formation. These MN can activate the Cyclic GMP-AMP Synthase, Stimulator of Interferon genes (cGAS-STING) pathway, promoting an innate immune response, whose canonical function is to recognise cytoplasmic DNA and trigger a downstream inflammatory response. Some cancers may downregulate or alter cGAS-STING signalling to evade recognition by the immune system, yet the relationship between CA and the innate immune system remains under-explored. Therefore, this project explores the relationship between CA, MN and the cGAS-STING pathway in primary and metastatic uveal melanoma (UM).

Confocal microscopy revealed that there was increased MN formation in metastatic UM cells, with MN exhibiting DNA damage. Interestingly, both primary and metastatic UM cells contained MN that were devoid of cGAS at baseline and after DNA transfection. Using western blotting we showed that expression of other DNA sensing components including STING and interferon gamma Inducible protein 16 (IFI16) were variable and cell line-dependent, with STING only being found in primary UM. Further use of confocal microscopy and Enzyme Linked Immunosorbent Assay (ELISA), demonstrated a lack of downstream signalling activation in both cell lines, indicated by impaired Nuclear Factor Kappa- Light-Chain Enhancer of Activated B Cells (NF-κB) and Interferon Regulatory Factor 3 (IRF3) translocation and minimal secretion of Interleukin-6 (IL-6) or C-X-C motif chemokine ligand 10 (CXCL10) in response to DNA transfection or etoposide treatment. However, these cells retained responsiveness to RNA transfection, suggesting a specific suppression of DNA-sensing pathways.

Our findings indicate that UM cells, particularly those with high levels of CA and genome instability may evade immune detection by suppressing the cGAS-STING pathway, but the extent of this suppression may vary dependent on the levels of genome instability, warranting further investigation. These findings have implications for emerging therapeutic strategies and highlight the need to further investigate innate immune pathway modulation in UM.

1. Introduction

1.1. Uveal Melanoma

1.1.1. Epidemiology

Uveal Melanoma (UM) although rare, at 5-7 per million per year overall (Ramasamy et al., 2014) is the most common intraocular malignancy in adults, arising from the melanocytes of the uveal tract which comprises the choroid, ciliary body and iris (Jager et al., 2020). Tumours predominantly localise to the choroid (in around 90% of cases), followed by the ciliary body (6%) and the iris (4%) (Kaliki and Shields, 2017). The median age of diagnosis is approximately 62 years, with incidence showing variation across gender, race and country (Krantz et al., 2017). Males display a 30% greater incidence compared to females, and UM is more common in non-Hispanic whites (6.02 per million), followed by Hispanics (1.67 per million) (Krantz et al., 2017). The lowest incidence is observed in individuals of black descent and Asians (0.31 and 0.39 per million respectively) (Krantz et al., 2017). Even though ultraviolet radiation is not a widely accepted risk factor for UM, differences in the incidence of UM could be attributed to the lower levels of melanin present in individuals of the white population (Kaliki and Shields, 2017). Therefore, the protective effects that melanin offers from ultraviolet radiation may be lost in these individuals (Kaliki and Shields, 2017). Agreeing with this finding is a study conducted by Johansson et al., (2020) who demonstrates that ultraviolet mutation signatures do exist in individuals with UM, but these specifically occur in the iris of the eye.

1.1.2. Genetic Mutations

Both UM and cutaneous melanoma arise from melanocytes, but vary considerably in their mutations, cytogenetic aberrations as well as their sites of metastasis (Fig; 1) (Ortega et al., 2020). Both cutaneous melanoma and UM show overactivation in the mitogen-activated protein kinase (MAPK) pathway. However, in comparison to cutaneous melanoma, UM has a much lower mutational burden and a more narrowly defined mutational landscape (Fig; 1) (Ortega et al., 2020). Gene expression profiling has characterised two molecular subtypes of UM, that differ in their mutations, metastatic risk and prognostic outcomes (Kaliki and Shields, 2017). Class 1 tumours are associated with disomy 3, and chromosome 6p gain and display a good prognosis, due to a lower metastatic risk (Kaliki and Shields, 2017). In contrast, Class two

tumours, which make up most cases of UM, have monosomy 3 and have poorer prognostic outcomes due to a greater metastatic risk (Kaliki and Shields, 2017).

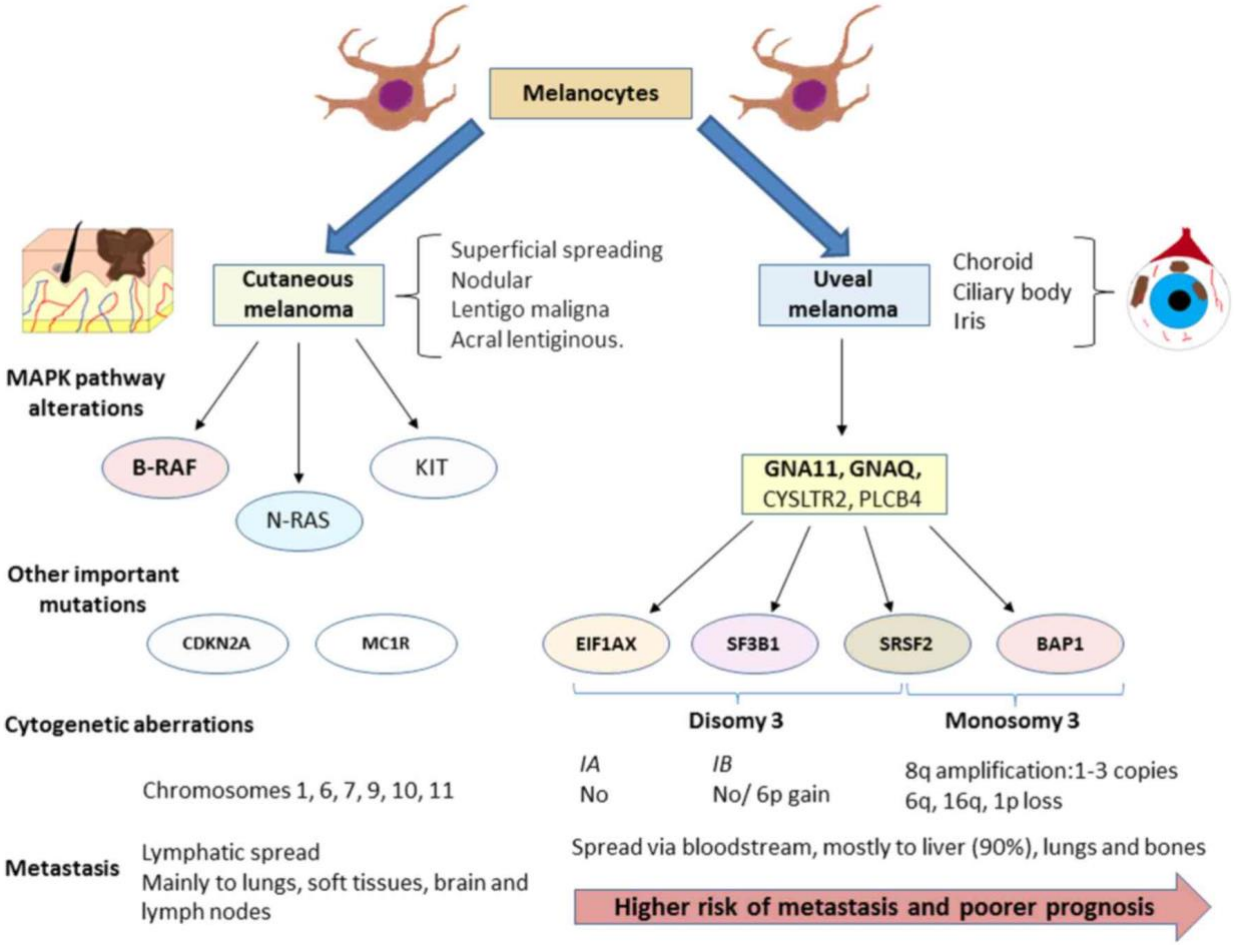

Figure 1: Diagnostic Features of Cutaneous and Uveal Melanoma.

Even though both cutaneous and uveal melanoma originate from melanocytes and typically display alterations in the mitogen-activated protein kinase (MAPK) pathway, they show differences elsewhere. Cutaneous Melanoma mostly has mutations in the genes v-raf murine sarcoma viral oncogene homolog B1 (B-RAF), neuroblastoma RAS viral oncogene (N-RAS) and KIT proto-oncogene, receptor tyrosine kinase (KIT), whilst uveal melanoma displays a much more defined set of mutations that enables classification of tumours into molecular subtypes based on their risk of metastasis and prognostic outcomes. The spread also differs between cutaneous melanoma and uveal melanoma. For cutaneous melanoma, metastasis is commonly through the

lymphatics to the lungs, soft tissue, brain and lymph nodes, whereas for uveal melanoma, metastasis mainly occurs to the liver via the bloodstream. Figure adapted from (Ortega et al., 2020).

Nearly all individuals with UM harbour mutations in the genes G protein-alpha subunit 11 (GNA11) and G protein alpha-subunit Q (GNAQ), which are both alpha subunits of G-proteins; with metastatic risk then defined mostly by monosomy 3 and or (BRCA1)-associated protein (BAP1) loss that are associated with high-risk metastatic class two tumours (Silva-Rodríguez et al., 2022, Robertson et al., 2017). These mutations lead to constitutive activation of the G protein and overactivation of both the MAPK and phosphatidylinositol 3-kinase (PI3K) pathways. Consequently, there is over-proliferation of cells and ignorance of anti-apoptotic signals, promoting tumorigenesis (Silva-Rodríguez et al., 2022). Furthermore, in a small proportion of patients that do not display mutations in GNA11 and GNAQ, mutations instead occur in cysteinyl leukotriene receptor two (CYSLTR2) and phospholipase C beta 4 (PLCB4) which also causes overactivation of the MAPK pathway (van de Nes et al., 2017). These mutations occur in a mutually exclusive manner of GNA11 and GNAQ mutations and are only found in UM, not cutaneous melanoma (van de Nes et al., 2017).

In approximately 84% patients with metastatic disease, inactivating mutations of the BAP1 gene occurs (Harbour et al., 2010). This type of mutation is also associated with high-risk class two tumours and typically involves loss of chromosome three (Kwon et al., 2023). BAP1 functions as a tumour suppressor deubiquitinase and so mutations can lead to alterations in protein function and subsequent tumour development (Kwon et al., 2023).

Other mutations are less common and relate to class one tumours, therefore leading to improved prognostic outcomes. Eukaryotic Translation Initiation Factor 1A X-Linked (EIF1AX) mutations arise in around 15-20% of cases of UM and as EIF1AX functions in the initiation of translation, it is thought that a mutation may cause alternative start codon recognition and indirectly affect tumour suppressor function (Martin et al., 2013). Missense mutations that occur in key splicing proteins such as Splicing factor 3B subunit 1 (SF3B1) (23% of cases) and Serine/arginine-rich splicing factor 2 (SRFS2) (4% of cases), all lead to alternative splicing and consequently widespread

dysregulation of gene expression, promoting tumorigenesis (Helgadottir and Höiom, 2016). Even though SF3B1 and SRFS2 mutations are low-risk, they can still indicate a potential for late-onset metastasis (Yavuzyigitoglu et al., 2016).

1.1.3. Treatment

There are various treatment options available for primary UM (Fig; 2), with surgical intervention considered to be the gold standard approach (Bai et al., 2023).

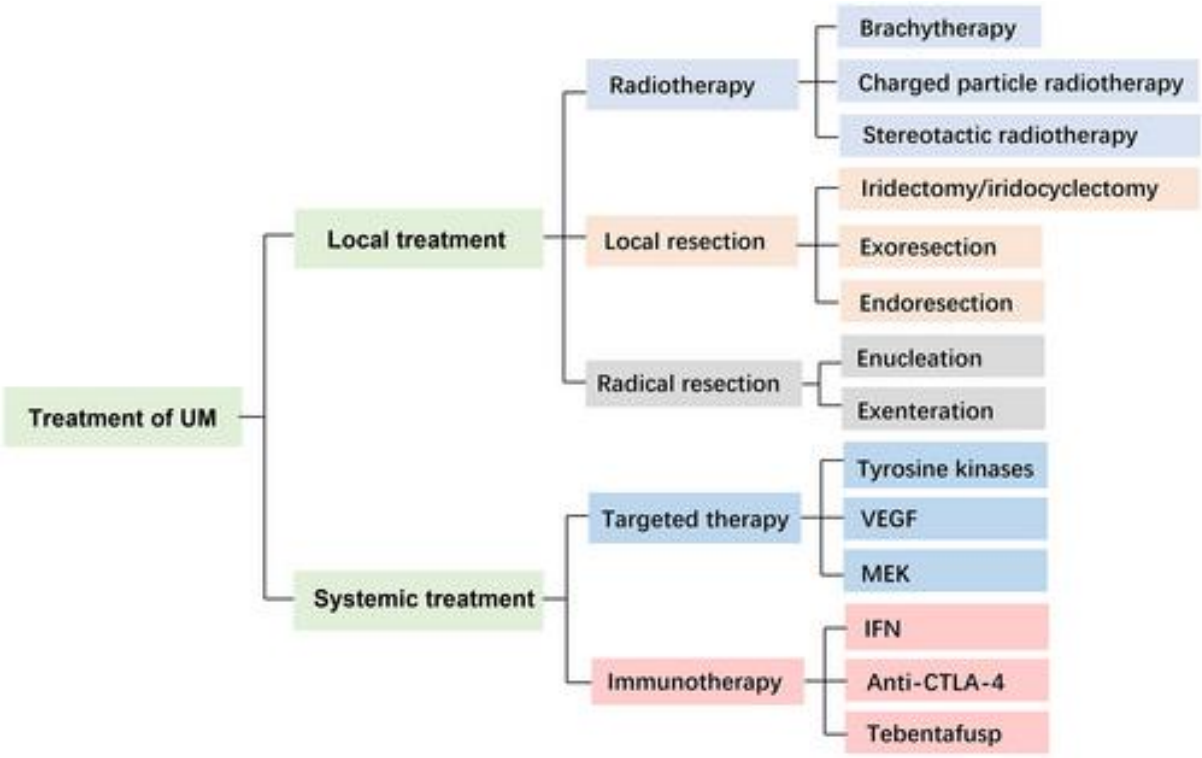

Figure 2: Therapeutic interventions for the Management of Uveal Melanoma. These are mostly effective for primary uveal melanoma alone and involve local treatments and systemic treatments. For metastatic uveal melanoma, there are no definitive therapies available and even though the above treatments have been trailed for metastatic disease, this has come with limited success. Figure adapted from (Bai et al., 2023).

Surgical intervention can involve either enucleation (removing the whole eye) or local resection, which can preserve some of the eye's function, using surgery, brachytherapy, radiation or laser therapy (Relimpio-López et al., 2022). The type of

treatment method used, depends on the size and the location of the tumour itself, as well as other factors such as patient age and physical conditions (Bai et al., 2023). Whilst these therapies are effective for primary UM, 50% of patients still progress to incurable metastatic disease, mostly to the liver, which is usually fatal within one year (Jager et al., 2020).

The high mortality rate is attributed to the fact that metastatic disease cannot be treated using the same methods as used for primary UM. For instance, as multiple tumours arise with metastatic disease, this has hindered the effectiveness of surgery (Li et al., 2020). Similarly, even though Immunotherapy has shown great success for cutaneous melanoma, this has not been the case for UM, perhaps due to a lower mutational burden, enabling tumour evasion of the immune system (Fu et al., 2022, Koch et al., 2024). More recently, the FDA approved tebentafusp for unresectable or metastatic UM (U.S. Food and Drug Administration (FDA)., 2022). Many types of tumours are often rich in tumour associated macrophages, particularly M2 macrophages that function to suppress T cell activity. FDA approved Tebentafusp is a T cell engager that when given to T cells in combination with Interleukin-2 (IL-2), has been shown to drive M2 to M1 macrophage polarisation, and overcome T cell immunosuppression (Güç et al., 2025). In a phase 3 trial of previously untreated metastatic UM patients who expressed the correct allele for Tebentafusp binding, treatment with tebentafusp resulted in a 1 year overall survival rate of 73%, compared to just 59% for standard therapy (Nathan et al., 2021). Furthermore, in a phase 1/2 trial of previously treated metastatic UM patients, tebentafusp achieved 1-year, 2-year, 3-year, 4-year survival rates of 62%, 40%, 23% and 14% respectively (Sacco et al., 2024). Despite this, it is also important to note that the immunotherapy drug has only been effective within a subset of patients, and more than 30% patients have experienced adverse side effects (U.S. Food and Drug Administration (FDA)., 2022). Inhibition of various pathways such as MAPK and PI3K, as well as the use of checkpoint inhibitors have been trialled, but overall response rates have remained low (Yang et al., 2018, Leonard-Murali et al., 2024). Despite this, a study conducted by Onken et al., (2021) showed that inhibition of GNA11 and GNAQ using a specific G-protein inhibitor, strongly inhibited primary and metastatic tumour growth, but despite this, the inhibitor was still not efficient at directly killing tumours.

Despite the many treatment options available, no efficacious therapies have improved survival rates of metastatic disease or reduced the risk of metastasis itself (Rantala et al., 2019). Research to improve our understanding of the disease, particularly in the context of metastasis will enable new potential targets to be identified that could improve treatment options. Fortunately, the fact that Centrosome Amplification (CA) occurs in UM (Sabat-Pośpiech et al., 2022) (section 1.2) and the fact that this could potentially lead to the activation of an innate immune response (Wheeler and Unterholzner, 2023) (section 1.3) could provide a potential target.

1.2. Centrosome Amplification

1.2.1. Centrosome Structure and Replication

Centrosomes are intracellular organelles that serve as microtubule organising centres (MTOCs) and play important roles in a variety of cell functions including cell division, polarity and migration (Conduit et al., 2015). They contain a pair of centrioles, enveloped by pericentriolar material (PCM) (Fig; 3) (Ryniawec and Rogers, 2021).

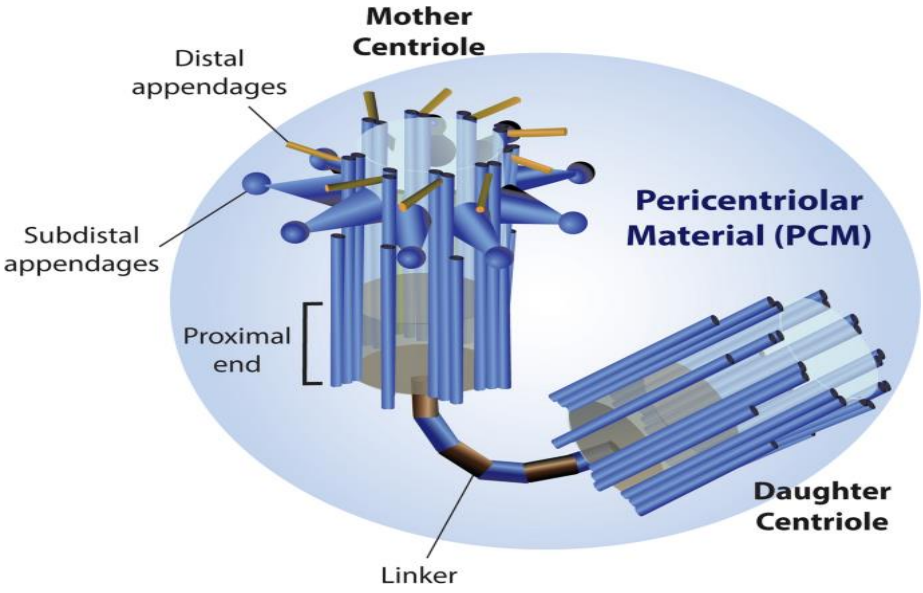

Figure 3: Structure of the Centrosome.
Centrosomes function as microtubule-organizing and nucleating centres of cells**.** They consist of a mother-daughter centriole pair that is surrounded by the peri-centriolar material. Figure adapted from (Ryniawec and Rogers, 2021)**.**

Centrosome duplication is a tightly regulated process that occurs once during the cell cycle, ensuring that there are two centrosomes present at the time of mitosis. This enables accurate formation of a bipolar spindle, which ensures that sister chromatids are accurately segregated into daughter cells during anaphase (Sabat-Pośpiech et al., 2019). This prevents aneuploidy and maintains genome stability (Sabat-Pośpiech et

al., 2019). The centrosome also performs a variety of functions in the organisation of microtubules during interphase. This includes; determining cell polarity for processes such as cell migration, assembling cilia for processes such as signal transduction as well as aiding the function of newly differentiated cells to support different cell specific functions (Holland et al., 2010).

In contrast, cancer cells frequently possess supernumerary centrosomes, which is termed centrosome amplification (CA) (Sabat-Pośpiech et al., 2019). Several aberrant processes can drive CA, and this includes, but is not limited to, centriole overduplication, centriole fragmentation, cytokinesis failure, and cell-cell fusion (Piemonte et al., 2021). Interestingly, CA is typically referred to as a 'double-edged sword' for cancer cells as it can both promote oncogenic phenotypes but can also be an 'Achilles heel', as cancer cells need to find ways of coping with the extra number of centrosomes, they possess to prevent multipolar mitosis and enable their survival (Sabat-Pośpiech et al., 2019).

1.2.2. Centrosome Amplification Induces Tumorigenesis

CA is observed in a wide variety of cancers and correlates with poor prognosis (Chan, 2011). More than a century ago, Boveri proposed that extra centrosomes could induce tumorigenesis (Boveri, 2008). Despite this, for a long time, it was not clear whether CA was a cause or consequence of cancer (Raff and Basto, 2017).There is now increasing evidence supporting Boveri's hypothesis that CA alone is sufficient to induce tumorigenesis. In a study conducted by Basto et al., (2008), using transgenic drosophila overexpressing polo-like kinase 4 (plk4) (key inducer of centrosome duplication); flies demonstrated developmental delay but remained viable. This suggested that CA was tolerated and could be attributed to the process of centrosome clustering by ncd (human homologue Kinesin Family Member C1; KIFC1) (Basto et al., 2008). Interestingly, transplantation assays revealed developing brain tissue of these flies' formed tumours, through CA altering asymmetric division of neural progenitors, but normal brain tissue did not (Basto et al., 2008). This suggested that CA alone was sufficient to induce tumorigenesis, but the exact mechanism by which this occurred remained unclear. Interestingly, in another study conducted by Sabino et al., (2015) using transplanted wing tissue from flies overexpressing plk4, tumorigenesis occurred, even in the absence of any asymmetrically dividing

progenitors, but again suggested that CA could induce tumorigenesis. In contrast, a study conducted by Marthiens et al., (2013) showed that developing mice brains engineered to overexpress plk4 displayed CA but did not spontaneously form tumours. Interestingly however, brains did display microcephaly, suggesting that CA was driving tissue degeneration, rather than cancer (Marthiens et al., 2013). In contrast, a study conducted by Levine et al., (2017) demonstrated that plk4 overexpression to drive CA in mice, exhibited spontaneous formation of lymphomas, sarcomas and carcinomas, and these tumours also displayed chromosomal instability (CIN).

Taken together, this suggests that whilst CA can promote tumorigenesis, likely through aneuploidy, it is still unclear the mechanism behind which this occurs, particularly considering the differences observed between different tissues (Raff and Basto, 2017). Interestingly, it is important to consider how CA could also be promoting tumorigenesis through other mechanisms, including invasion and metastasis (Godinho et al., 2014, Singh et al., 2020).

1.2.3. Centrosome Amplification Promotes Invasion and Metastasis

CA can promote invasion in a cell-autonomous and a non-cell autonomous manner. Non-cell autonomous invasion can be attributed to a range of factors including increased interleukin- 8 (IL-8) secretion, as well as increased generation of reactive oxygen species (ROS) that in turn promotes secretion of pro-invasive factors (Arnandis et al., 2018). In contrast, cell-autonomous invasion is thought to occur because of increased Ras-related C3 botulinum toxin substrate 1 (Rac1, member of the Rho family of GTPases) activity, which disrupts cell-cell adhesion and promotes invasion (Prakash et al., 2023, Godinho et al., 2014). CA can also promote metastasis, and this has been observed using time-lapse imaging. In a study conducted by Pannu et al., (2015), human MDA-MB-231 breast cancer cells with amplified centrosomes were found to display enhanced migratory ability. Similarly, pharmacological induction of CA in human pancreatic cancer cells showed increased motility after a wound healing assay was performed (Mittal et al., 2015).

1.2.4. Coping Mechanisms of Centrosome Amplification

Cancer cells displaying CA are vulnerable to death either through multipolar mitosis and subsequent large-scale aneuploidy or apoptosis through prolonged mitotic arrest (Sabat-Pośpiech et al., 2019). To avoid this, cancer cells can use a number of coping mechanisms to enable them to survive (Fig; 4) (Sabat-Pospiech et al., 2019).

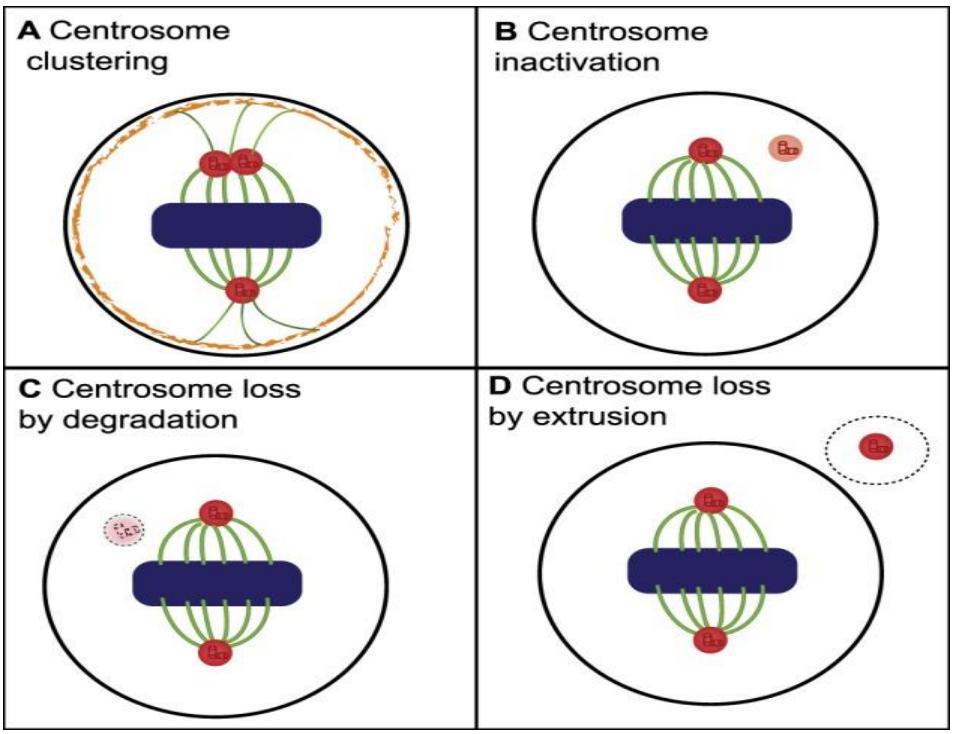

Figure 4: Coping Mechanisms of Centrosome Amplification.
Cancer cells displaying centrosome amplification may use one of the four mechanisms to prevent multipolar mitosis and cell death. Of these, the most well characterised is centrosome clustering. Figure adapted from (Sabat-Pośpiech et al., 2019).

Multipolar anaphases are rare which can be attributed to centrosome clustering, the most well understood coping mechanism, of cancer cells displaying CA (Sabat-Pospiech et al., 2019). This involves reshaping of the transient multipolar spindle into a pseudo-bipolar spindle structure through clustering of supernumerary centrosomes, enabling cancer cells with CA to proliferate and survive (Milunović-Jevtić et al., 2016). Most of the current research in the field has looked at targeting centrosome clustering for cancer therapy, with the idea that cancer cells no longer able to cluster their

centrosomes will undergo prolonged mitotic arrest and eventual apoptosis or death through large-scale aneuploidy (Sabat-Pośpiech et al., 2019). One promising target is the key centrosome clustering protein KIFC1. KIFC1 is a member of the kinesin-14 family that facilitates clustering of centrosomes via its microtubule motor protein activity (Xiao et al., 2017). Therefore, inhibiting or depleting KIFC1 can prevent centrosome clustering, leading to multipolar mitosis and cancer cell death. In a study conducted by Wang et al., (2019) overexpression of KIFC1 promoted proliferation of human hepatocellular carcinoma cells. Similarly, findings from Li et al., (2020) revealed that silencing of KIFC1 inhibited proliferation of human ovarian cancer cells. These studies have therefore highlighted the importance of targeting centrosome clustering, specifically the motor protein KIFC1 as an attractive area of research. Despite this, small molecule inhibitors that have been developed so far lack the potency and specificity to be used clinically, despite their effectiveness at inducing multipolar spindle formation (Zhang et al., 2016, Sekino et al., 2019). Therefore, this and other approaches to targeting CA, should continue to be explored.

Interestingly, even though centrosome clustering can promote cancer cell survival, it can also generate low-level CIN (section 1.2.5.) (Milunović-Jevtić et al., 2016). However, this could provide an opportunity for exploitation as an alternative therapeutic target, due to its potential to activate an innate immune response (Section 1.3) (Mackenzie et al., 2017, Harding et al., 2017).

1.2.5. Centrosome Clustering and Chromosomal Instability

During centrosome clustering, the formation of transient multipolar intermediates can generate merotelic kinetochore attachments (single kinetochore attached to multiple spindle poles) (Gregan et al., 2011, Ganem et al., 2009). Not all cancer cells displaying CA will have spindles containing merotelic attachments (Milunović-Jevtić et al., 2016) Despite this, those that do often generate lagging chromosomes at anaphase, which display high levels of damage and mis-segregation (Fig; 5) (Milunović-Jevtić et al., 2016).

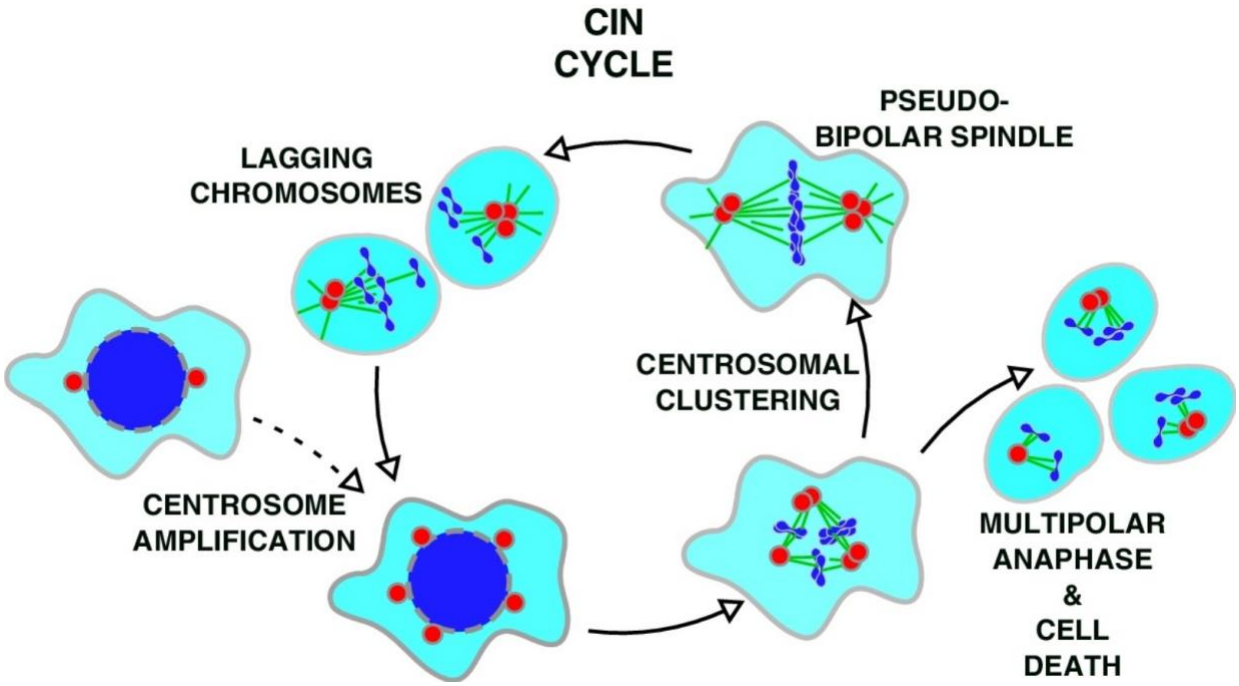

Figure 5: Chromosomal Instability Arising from Centrosome Clustering. Dysregulation of the cell cycle drives centrosome amplification in cancer cells, leading to the formation of transient multipolar intermediates, multipolar anaphases and subsequent apoptosis. To avoid this fate, cancer cells can cluster their centrosomes and form pseudo-bipolar spindles. Whilst this, can enable cancer cells displaying centrosome amplification to survive, some cells will develop merotelic kinetochore attachments and lagging chromosomes, often resulting in aneuploidy and chromosomal instability. Figure adapted from (Milunović-Jevtić et al., 2016).

Importantly, these lagging chromosomes can give rise to chromatin bridges and micronuclei (MN) (Krupina et al., 2021, Kwon et al., 2020). MN arise from lagging chromosomes or chromosomal fragments, that fail to be incorporated into newly formed daughter cells upon mitotic exit and so are associated with dividing cells (Fig; 6) (Kwon et al., 2020). MN recruit their own nuclear envelopes and are spatially separate from the primary nucleus (Krupina et al., 2021). MN have long been recognised as a hallmark of CIN and arise in a cell cycle dependent manner. This was evidenced in a study conducted by Crasta et al., (2012) who showed that irradiated human retinal pigment epithelial and osteosarcoma cells in S-phase of the cell cycle showed lower levels of DNA damage in MN compared to cells in G2 phase. As MN

frequently possess defective nuclear envelopes, due to a defective laminar network, they are prone to rupture (Krupina et al., 2021). Upon doing so, MN release their double stranded DNA into the cytosol, which is thought to potentially activate an innate immune response (Kwon and Bakhoum, 2020).

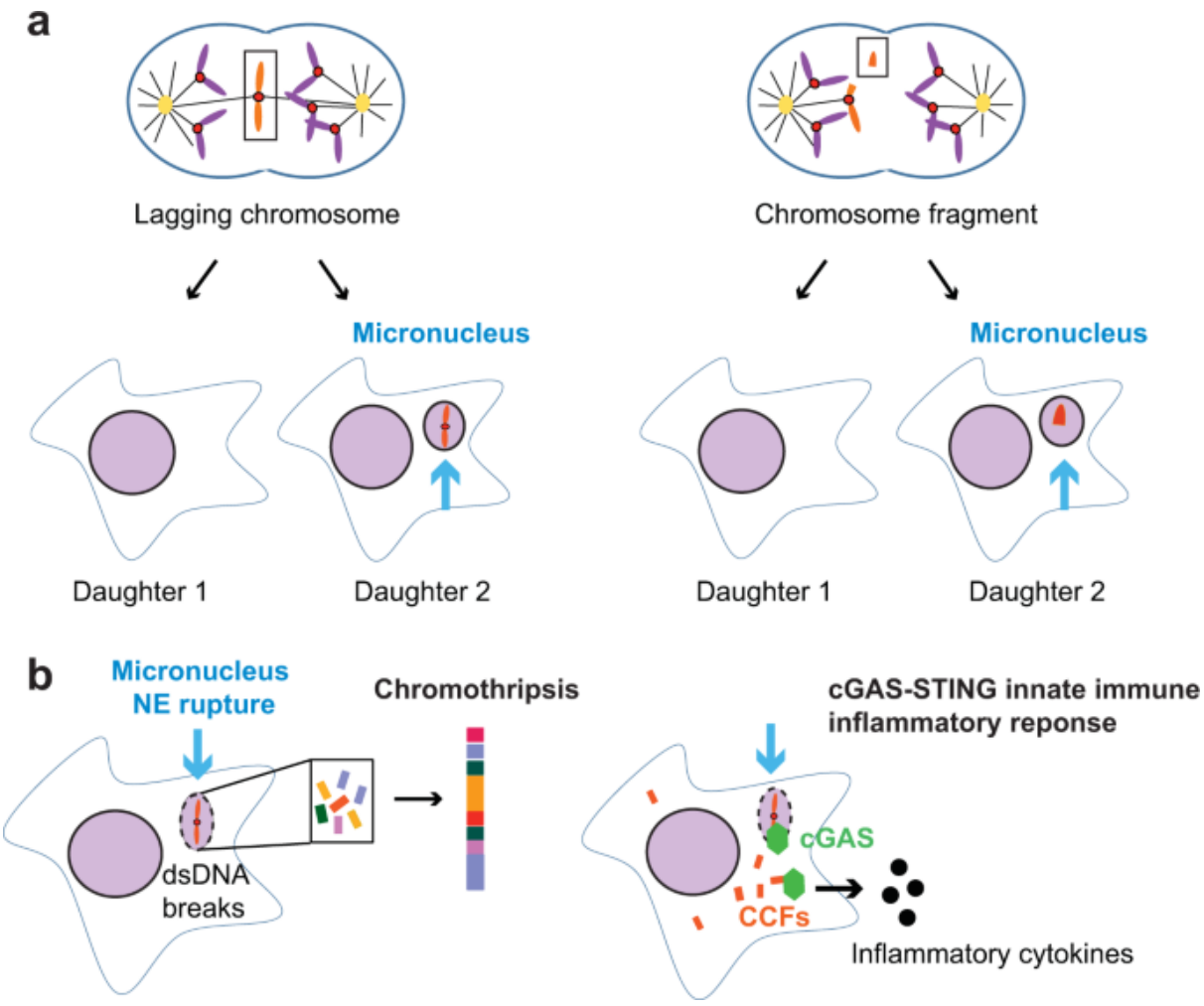

Figure 6: Formation of Micronuclei.

Micronuclei arise from lagging chromosomes (a) or chromosome fragments (b) following mitotic errors or DNA damage, respectively. Micronuclei are separate from the main nucleus and have fragile envelopes that are prone to rupture. This can lead to chromothripsis when chromosomes contained in micronuclei with a ruptured nuclear envelope acquire double strand DNA breaks. Double stranded DNA that is released into the cytosol, can be detected by the DNA sensor cyclic GMP-AMP Synthase (cGAS) triggering activation of the cyclic GMP-AMP Synthase, Stimulator of Interferon

genes (cGAS-STING) innate immune signalling pathway, promoting the release of inflammatory cytokines. Figure adapted from (Kwon et al., 2020).

Chromatin bridges are less well studied than MN but result from chromosome end-end fusions during telomere crisis, that can be visualised as a string of chromatin connecting the two segregating chromosomes at anaphase (Jiang and Chan, 2024). If these bridges break, they can also induce the formation of MN in the next round of cell division (Jiang and Chan, 2024). Like MN, they have also been shown to activate an innate immune response (Flynn et al., 2021).

One key innate immune signalling axis, thought to be activated is that of the cyclic GMP-AMP synthase (cGAS), stimulator of interferon genes (STING) pathway, that can act as a ‘double edge sword’ for cancer cells, through its ability to possess both pro-tumour and anti-tumour functions, dependent on the context, and stage of tumour progression (Section 1.3) (Kwon et al., 2020).

1.3. Nucleic Acid Sensing

1.3.1 Overview of The Innate Immune Response

The mammalian immune system consists of both the innate and adaptive response that work together to eliminate any pathogens (Marshall et al., 2018). The innate immune response provides a rapid first line of defence against invading pathogens, whilst the adaptive immune response is much more specific and results in immunological memory (Marshall et al., 2018).

Pathogen recognition initially occurs via pattern recognition receptors (PRRs) on the surface of immune cells that in turn recognise pathogen associated molecular patterns (PAMPs), which are small molecules that are found on the surface of pathogens, enabling them to be recognised as non-self by the host immune system (Tang et al., 2012). There are many different types of PRRs that are designed to recognise various PAMPs (Table; 1). When PAMPs are recognised by PRRs, innate immune signalling is initiated via the recruitment of innate immune cells such as macrophages and dendritic cells which can lead to the production of inflammatory cytokines (Li and Wu, 2021). This response then eventually leads to activation of the adaptive immune response through the recruitment of adaptive immune cells such as B and T cells (Li and Wu, 2021).

Furthermore, PRRs can be effective at recognising damage associated molecular patterns (DAMPs), which are endogenous molecules released by damaged or dying cells (Tang et al., 2012). Examples of DAMPs include; High mobility group box 1 (HMGB1), mitochondrial DNA (Mt DNA), heat shock proteins (HSPs) and extracellular histones (Roh and Sohn, 2018). Recognition of DAMPs can lead to the clearance of damaged or dying cells, but can also foster an inflammatory microenvironment, and in the case of cancer, this can support tumour cell survival and metastasis (Hernandez et al., 2016).

Table 1: Examples of PRRs and PAMPs

PRRs	PAMPs	Source and Location
Toll-like Receptor 4 (TLR4)	Lipopolysaccharide	Bacteria, cell surface
Toll-Like Receptor-3 (TLR3)	Double stranded RNA	Viruses, endosome
Retinoic Acid Inducible Gene I (RIG-I)/ Melanoma Differentiation-Associated Protein 5 (MDA5)	Double stranded RNA	Viruses, cytosol
Absent In Melanoma-2 (AIM-2)	Double stranded DNA	Viruses, bacteria, self-DNA, cytosol
Cyclic GMP-AMP Synthase (cGAS)	Cytosolic DNA	Viruses and intracellular bacteria, cytosol

Interestingly, evidence has suggested that the cGAS STING pathway which detects cytosolic DNA, particularly in the case of viral infection, also plays a role in cancer (Samson and Ablasser, 2022) (Section 1.3.4).

1.3.2 DNA sensing Pathways

DNA sensing pathways play important roles during an innate immune response, through the detection of DNA, released from various sources; including DNA from pathogens, damaged cells and MN (Chen et al., 2025). The primary sensor of cytosolic DNA is cGAS and its adaptor protein STING, which is termed the canonical response, and is thought to be associated with increased anti-tumour immune activity (Fig; 7) (section 1.3.2.1). Another DNA sensor, Interferon gamma inducible protein 16 (IFI16) plays a role in both canonical and non-canonical cGAS STING signalling but predominantly functions as part of the non-canonical response. This response operates independently of cGAS to activate STING and is thought to be associated with increased pro-tumour immune activity (Fig; 7) (section 1.3.2.2) (Dunphy et al., 2018).

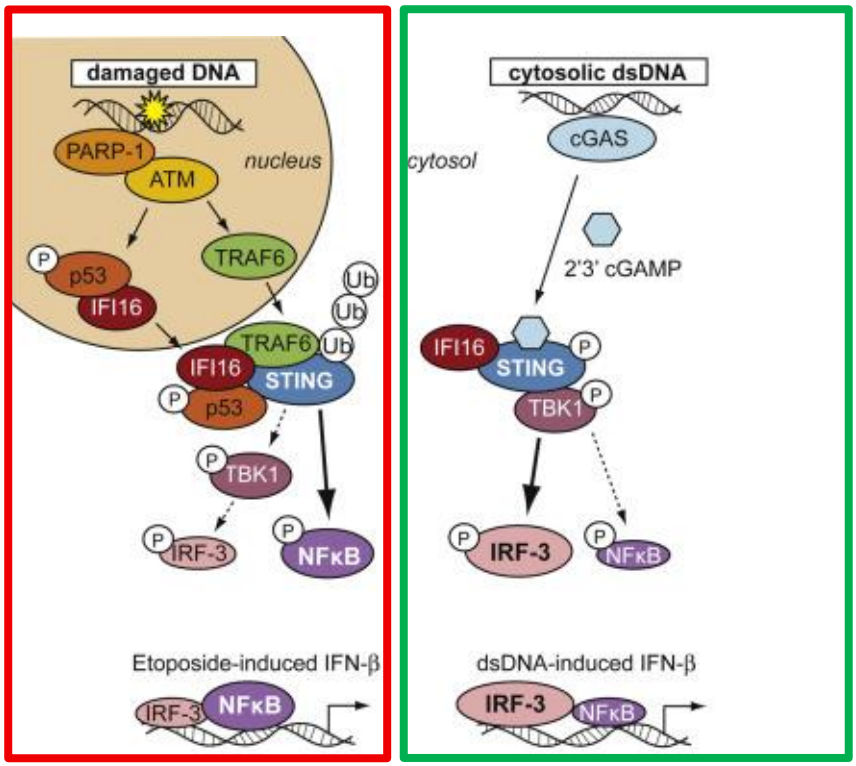

Figure 7: Overview of canonical and non-canonical cGAS STING activation.
Canonical stimulator of interferon genes (STING) activation (green) involves the release of cytosolic DNA that is detected by the DNA sensor cyclic GMP-AMP Synthase (cGAS). The second messenger Cyclic GMP-AMP Synthase (cGAMP) is then synthesised which binds to the adaptor protein STING at the endoplasmic reticulum (ER) before translocating to the golgi and binding Tank binding kinase 1

(TBK1). This leads to phosphorylation and activation of the transcription factor Interferon Regulatory factor 3 (IRF3) and leads to subsequent production of type I interferons and chemokines such as C-X-C motif chemokine ligand 10 (CXCL10). Non-canonical STING activation (red) is less well understood and operates independently of cGAS. Instead, damage is directly detected by the damage sensors Ataxia telangiectasia mutated (ATM) and poly (ADP-ribose) polymerase 1 (PARP1), coordinating with Interferon gamma inducible protein -16 (IFI16) and p53. This leads to an alternative STING complex forming that includes STING, tumour necrosis factor receptor associated- factor 6 (TRAF6) and IFI16, favouring nuclear factor kappa-light-chain-enhancer of activated B cells (NF- κB) activation over IRF3. This generates a more pro-inflammatory set of cytokines. Figure adapted from (Dunphy et al., 2018).

1.3.2.1 The Canonical cGAS STING Pathway

The cGAS STING pathway is the main detector of cytosolic DNA, and canonical cGAS STING activation, involving a type I IFN dependent response is the most well characterised (Yu and Liu, 2021, Motwani et al., 2019).

To initiate this response, cytosolic DNA is required which can be derived from multiple sources. This includes viral infections, where DNA is detected as a PAMP, as well as during DNA damage/cellular stress, where DNA serves as a DAMP (Yu and Liu, 2021). Whilst CGAS can localise to the nucleus, it is primarily a cytosolic DNA sensor, that recognises and binds double stranded DNA in a sequence-independent manner before synthesising the second messenger, cyclic guanosine monophosphate–adenosine monophosphate (cGAMP), which then serves to bind and activate the adaptor protein STING, localised to the endoplasmic reticulum (ER) (Liu and Xu, 2025). cGAS was first identified by Sun et al., (2013) upon fractionation of cytosolic extracts from a murine fibrosarcoma cell line, where it was shown to possess two DNA binding sites for its DNA sensing activity. STING on the other hand was first described by Ishikawa and Barber (2008), who showed that upon binding cGAS, STING undergoes a conformational change, via a signal from cGAMP enabling STING's activation and the initiation of downstream signalling. After, its activation, STING is then translocated out of the ER and through the Golgi apparatus (Ishikawa et al., 2009). STING re-localisation is a key indicator of its activation and can be visualised using fluorescence microscopy, where STING has been shown to accumulate in the Golgi and peri-nuclear regions, as distinct foci, post DNA transfection (Ishikawa et al., 2009). STING then recruits TANK-binding kinase 1 (TBK1), which phosphorylates itself, STING and the transcription factor, interferon regulatory factor-3 (IRF3) leading to its activation through phosphorylation (Ishikawa and Barber, 2008). STING also activates nuclear factor kappa- light-chain enhancer of activated B cells (NF-κB). Both IRF3 and NF-κB then translocate into the nucleus from the cytoplasm, resulting in the production of type-I- interferons, and other interferon-stimulated genes (ISGs) (Decout et al., 2021, Dvorkin et al., 2024). Ultimately this promotes an anti-viral response, further recruitment of adaptive immune cells and subsequent clearance of infection or damaged cells (Dvorkin et al., 2024).

It is also important to recognise that there are additional DNA sensors and one important one is IFI16. IFI16 is nuclear at steady state but can shuttle between the nucleus and cytoplasm, dependent on the context (Dunphy et al., 2018). It is thought that cooperation of IFI16 and cGAS in some cells is needed for full STING activation and a type I dependent IFN response. In a study conducted by Almine et al., (2017) using human immortalised keratinocytes (HaCaT cells), lacking cGAS and IFI16, the production of C-C motif chemokine ligand 5 (CCL5) and C-X-C motif chemokine ligand 10 (CXCL10) was impaired, highlighting the importance of IFI16 for STING activation. Similarly, IFI16 has been shown to be crucial for DNA sensing within human macrophages, as when IFI16 was depleted, downstream signalling was compromised, indicating the effects of IFI16 depletion on efficient DNA sensing (Jønsson et al., 2017). Furthermore, IFI16 plays a role in the non-canonical cGAS STING pathway favouring NF-κB activation over IRF3. One study showed that using two metastatic melanoma cell lines with IFI16 knockdown, the levels of phosphorylated p-65 (a subunit of the NF-κB family) was decreased (Kobayashi et al., 2024). This indicated that IFI16 is not only essential for a canonical cGAS STING response, but also a non-canonical NF-κB response. Despite this, research is still needed to further understand in what cells and what contexts IFI16 is needed for full STING activation.

1.3.2.2 The Non-Canonical cGAS STING Pathway

More recently, a non-canonical mode of cGAS STING activation has been identified in human epithelial cells, which is less well understood (Fig; 7) and is known to occur in response to etoposide (Dunphy et al., 2018). This alternative pathway is thought to take place independently of cGAS and involves the DNA damage sensors poly- (ADP-ribose) polymerase 1 (PARP-1) and ataxia telangiectasia mutated (ATM) together with the DNA binding protein IFI16 and tumour-suppressor protein p53 (Dunphy et al., 2018).This leads to the formation of an alternative STING signalling complex, that comprises STING, IFI16 and TNF-receptor associated factor 6 (TRAF6). This alternative complex, favours NF- κB activation over IRF3 and generates expression of a different, more pro-inflammatory set of cytokines, that could potentially favour a pro-tumour microenvironment (Dunphy et al., 2018). Interestingly, in this case NF-κB dependent signalling does not require STING phosphorylation or re-localisation to peri-nuclear foci, unlike canonical cGAS STING activation (Dunphy et al., 2018).

It Is also important to recognise, that just as STING can be activated independently of cGAS, cGAS can also function independently of STING, via translocation of cGAS into the nucleus where it blocks homologous recombination and promotes tumorigenesis (Jiang et al., 2019). This happens because of cGAS binding to the acidic patch of histones, blocking access of DNA repair proteins to DNA double strand breaks (Jiang et al., 2019).

1.3.3 The RNA Sensing Pathway

There are multiple RNA sensing pathways that can be activated via PAMPs and DAMPs binding PRRs. One key axis is the Retinoic acid inducible gene I and melanoma differentiation associated protein 5 (RIG-I/MDA-5) Fig; 9) (Rehwinkel and Gack, 2020).

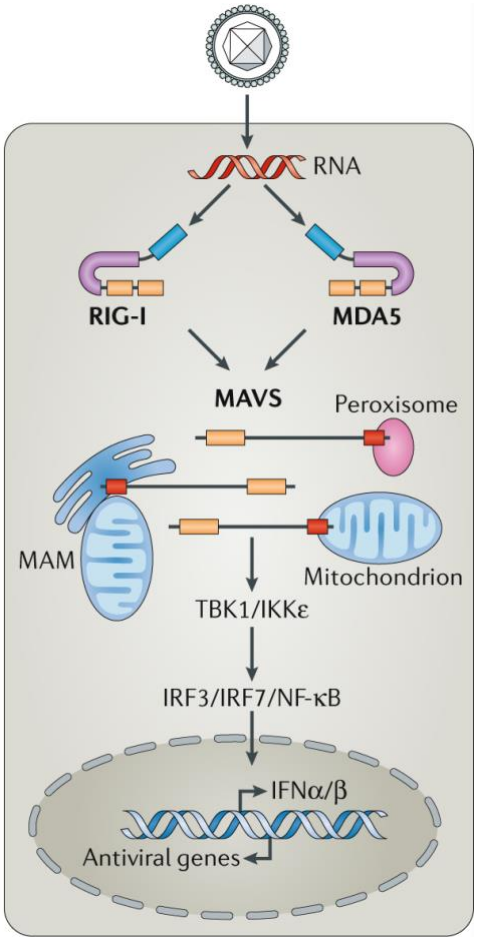

Figure 8: The RNA sensing pathway involving RIG-I like receptors

Retinoic acid inducible gene I (RIG-I) and melanoma differentiation associated protein 5 (MDA-5) detect viral RNA. These receptors then undergo conformational changes and interact with mitochondrial antiviral signalling protein (MAVS), anchored to mitochondrial associated membranes (MAMs) and peroxisomes. This sets of a signalling cascade to Tank binding kinase 1 (TBK1), in turn activating interferon regulatory factor 3 (IRF3), interferon regulatory factor 7 (IRF7) and nuclear factor kappa-light-chain-enhancer of activated B cells (NF-κB). Together, these induce the

expression of Type I interferons and other antiviral genes. Figure adapted from (Rehwinkel and Gack, 2020).

These are cytosolic receptors responsible for detecting double stranded viral RNA. Upon detection, this activates the signalling protein; mitochondrial antiviral signalling protein (MAVS). This then leads to activation of the transcription factors IRF3 and NF-kB, like the DNA sensing pathway and culminates in the production of type I interferons and pro-inflammatory cytokines (Rehwinkel and Gack, 2020).

1.3.4 The cGAS STING Pathway and its Role in Cancer

Cancer cells frequently possess cytosolic DNA, derived from multiple sources (Kwon and Bakhoum, 2020). Evidence suggests that this DNA, can exhibit both anti-tumorigenic and pro-tumorigenic effects that is dependent on the context and the stage of tumour progression. For instance primary tumours, may demonstrate a more intact and functional signalling pathway enabling DNA to elicit anti-tumorigenic effects through enhancing immune cell infiltration and subsequent immune activation (Wu et al., 2024). In contrast, metastatic tumours may face a different immune landscape, shifting to one which is more immunosuppressive and enabling tumour evasion of the immune system (Wu et al., 2024) However, it is also important to note that primary tumours are also capable of fostering an immunosuppressive tumour microenvironment (Wu et al., 2024). Here, DNA may elicit pro-tumorigenic effects through fostering chronic inflammatory signalling, that favours tumour survival and metastasis (Kwon and Bakhoum, 2020). There are many sources of DNA in tumours that can lead to subsequent innate immune activation (Fig; 10) (Wheeler and Unterholzner, 2023).

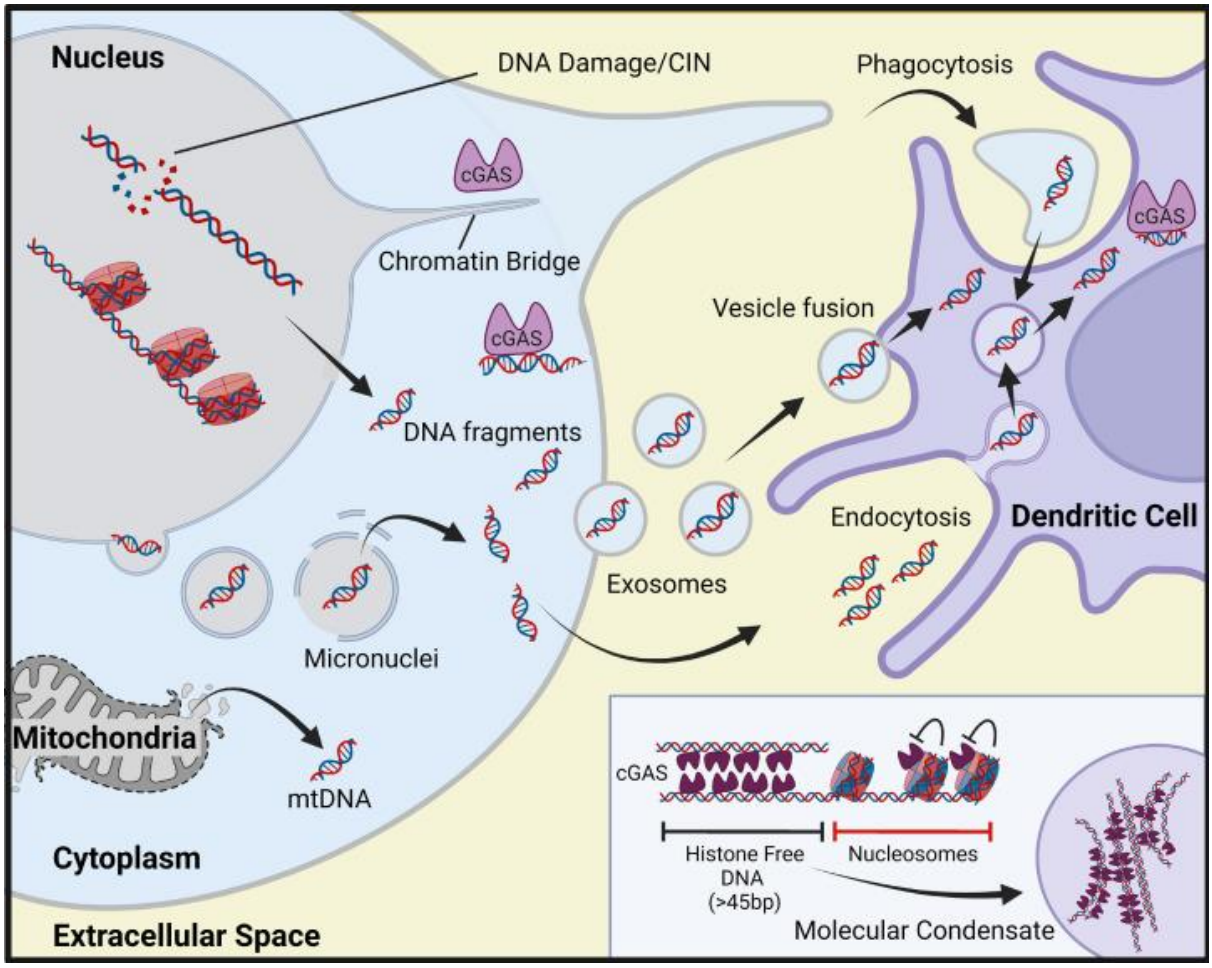

Figure 9: DNA Sources in Tumours and Innate Immune Activation.

Self-DNA in the cytosol can arise through exogeneous DNA damage (for example following radiation) as well as endogenous DNA damage, that arises from inherent chromosomal instability. Micronuclei, chromatin bridges and mitochondrial DNA are all potential sources of this double stranded DNA. This DNA can potentially activate an innate immune response via the cGAS STING signalling pathway. Figure adapted from (Wheeler and Unterholzner, 2023)

It is also important to note that mitochondrial DNA (mtDNA) can also activate the cGAS STING pathway in cancer, which is likely a result of cellular stress (Kim et al., 2023, Wheeler and Unterholzner, 2023). Cancer cells often undergo oxidative stress and subsequent mitochondrial dysfunction. This allows mtDNA to be released into the cytosol, likely through permeabilization of the mitochondrial membranes, allowing stimulation of the pathway (Kim et al., 2023). Interestingly, studies have suggested that mtDNA is more efficient at activating cGAS, compared to genomic DNA because

it does not contain nucleosomes and so the catalytic activity of cGAS is not reduced (Zierhut et al., 2019) However, this remains a controversy, with other studies suggesting that the presence of nucleosomes actually serves to increase cGAS activation (Dou et al., 2017).

Focusing on MN, research has primarily focused on how self-DNA from exogenous DNA damage induced MN rupture can trigger cGAS STING activation and contribute to anti-tumour immunity. For example, using single-cell RNA sequencing and fluorescent microscopy, a study conducted by Mackenzie et al., (2017) showed that upon micronuclear rupture after the induction of DNA damage by radiation; cGAS re-localised to MN in mouse embryonic fibroblasts and human U20S osteosarcoma cells. Furthermore, this generated a pro-inflammatory cGAS dependent response through cGAMP (Mackenzie et al., 2017). Similarly, using, MCF-10A epithelial cells, a study conducted by Harding et al., (2017) demonstrated that after irradiation, cGAS re-localised to ruptured MN and activated cGAS dependent signalling. Interestingly, however, in the study conducted by Mackenzie et al., (2017) 20% of intact MN could still recruit cGAS, suggesting that MN rupture may not be sufficient for cGAS activation. Agreeing with this observation, is a study conducted by Macdonald et al., (2023) who showed that MN rupture leads to but is not sufficient for cGAS activation, rather it is chromatin organisation that dictates recruitment.

Whilst evidence does suggest MN can promote cGAS STING activation, other studies suggest that activation of cGAS STING by MN could be dependent on progression through the cell cycle. For example, a study conducted by Sato and Hayashi., (2024) using live cell imaging showed that primary cGAS detection of DNA in micronuclei occurs when human colon cancer cells are in mitosis not interphase, which contradicts findings conducted by Mackenzie et al., (2017) and Harding et al., (2017) who suggested that the MN formed in interphase primarily activate cGAS. Interestingly, a recent study conducted by Flynn et al., (2021) suggested that it is chromatin bridges, not MN that activate the pathway, despite MN recruitment of cGAS. One possibility for this is the influence of chromatin state. Chromatins bridges lose their nucleosome integrity during elongation of the mitotic spindle in anaphase and therefore loss of these nucleosomes, may promote cGAS activation by facilitating its dimerization (Flynn et al., 2021). In contrast MN contain intact nucleosomes and when cGAS in

bound to these nucleosomes, its catalytic activity is reduced, therefore blocking its activation (Flynn et al., 2021). This agreed with findings suggested by Macdonald et al., (2023).

Some studies suggest that MN do not activate the cGAS STING pathway at all. A recent study conducted by Takaki et al., (2024) found that although radiation induced the formation of MN in human HeLa cervical cancer cells and these MN recruited cGAS, this did not activate the cGAS STING pathway. Furthermore, exposing these cells to other MN inducing agents still did not modulate cGAS STING activation. Taken together, this suggests that different cancer cells alter or evade the canonical cGAS STING pathway in some way and may act to promote a switch, favouring pro-tumour cGAS STING signalling.

1.3.4.1 Anti-tumour Functions of cGAS-STING Signalling

Many studies have implicated cGAS STING signalling in anti-tumour immunity, which is thought to occur early on in tumour development, acting to promote immune surveillance (Harding et al., 2017, Mackenzie et al., 2017, Bakhoum et al., 2018).

Initiation of this anti-tumour response occurs in response to both exogenous and endogenous DNA damage. This damage results in the formation of MN that can activate the cGAS STING pathway as described previously, initiating the canonical type I interferon response, and evidence suggests that it is a deficiency in the DNA damage response that upregulates pathway activation (Li and Chen, 2018).The pathway is mediated via p53 negatively regulating the exonuclease, three prime repair exonuclease 1 (TREX1) which makes cytosolic double stranded DNA from MN available for detection by cGAS (Wheeler and Unterholzner, 2023). This in turn leads to the secretion of various pro-inflammatory cytokines and chemokines, particularly type one interferons, that enhance the anti-tumour response (Fig; 9) (Kwon and Bakhoum, 2020). This occurs through the recruitment of immune cells such as CD8+ T cells and natural killer (NK) cells, which function to kill tumour cells once priming has occurred, which is further enhanced through the production of the key cytokine CXCL10 (Shen et al., 2015, Dou et al., 2017). Moreover, dendritic cells are activated which enhances their antigen presenting capacity to activate an adaptive immune response (Tan et al., 2008).

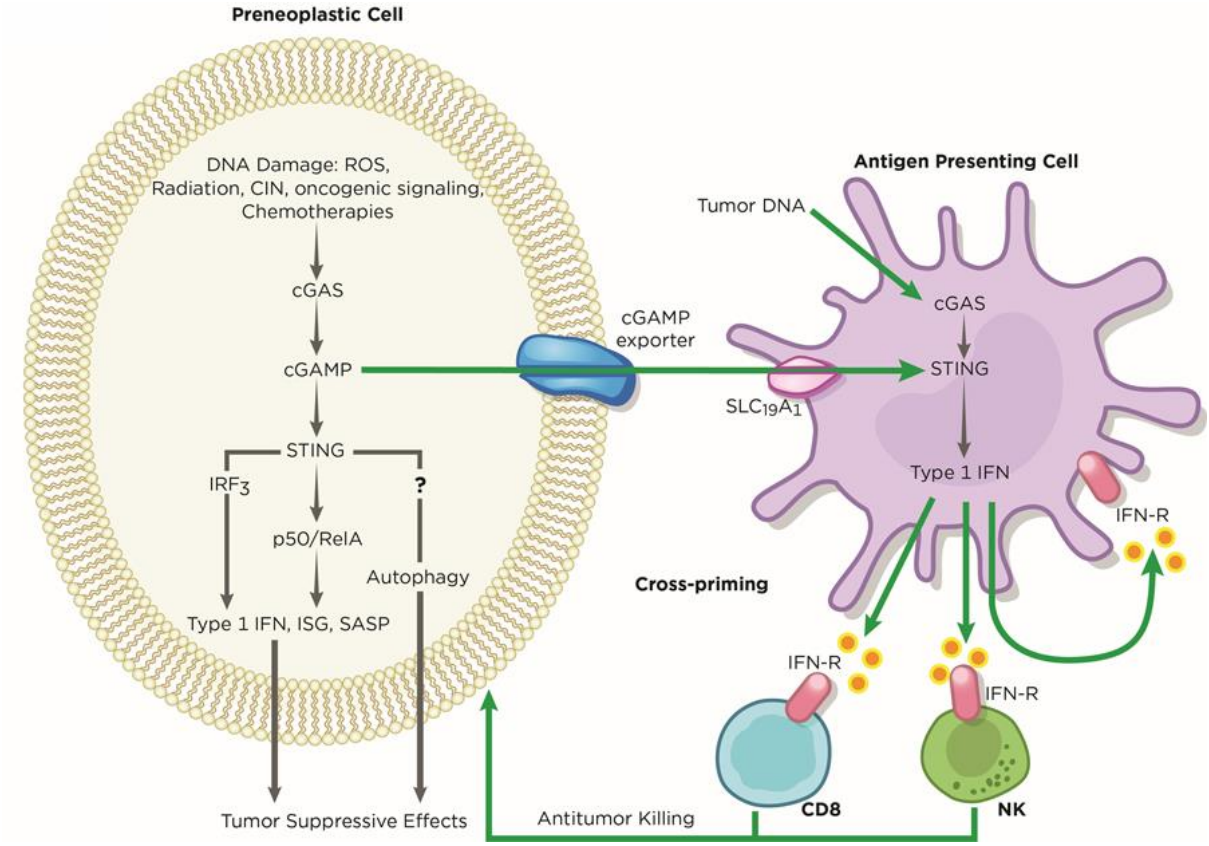

Figure 10: Anti-tumour functions of cGAS STING Signalling.

Early on in tumour development, it is thought that cyclic GMP-AMP synthase, Stimulator of Interferon genes (cGAS STING) functions to suppress tumours via cGAS detecting DNA damage. This then stimulates STING to upregulate expression of type I interferons and other interferon-stimulated genes. Furthermore, STING-mediated autophagy may occur to inhibit or delay tumour progression. Collectively, this allows crosstalk with neighbouring immune cells to regulate anti-tumour immunity. This can involve cyclic-guanosine-monophosphate adenosine monophosphate (cGAMP) and tumour DNA licencing antigen presenting cells to activate cGAS STING signalling, enabling immune cells to clear the tumour cells. Figure adapted from (Kwon and Bakhoum, 2020).

This response is characteristic of ‘hot tumours’ where there are high immune cell infiltration, active inflammatory responses and improved responsiveness to immunotherapies (Wang et al., 2023). This has shown promise in designing new therapies to activate DNA sensing and improve an anti-tumour immune response.

STING agonists are small molecules that work by mimicking natural ligands of STING or cGAMP to activate the cGAS STING pathway, discussed further in section 1.3.5 (Li et al., 2024). They have shown promise in enhancing an innate immune response in many cancers (Li et al., 2024, Meric-Bernstam et al., 2023). Despite this, in clinical trials, STING agonists have displayed little efficacy, due to factors such as toxic side effects, tumour heterogeneity as well as increasing resistance (Wang et al., 2024).

1.3.4.2 Pro-tumour Functions of cGAS STING Signalling

Tumour cells rarely activate the cGAS STING pathway, in response to self-DNA, compared with exogenous DNA (Kumar et al., 2023). This suggests an evolutionary mechanism, by which cancer cells can evade immune surveillance and facilitate tumorigenesis, by suppressing nuclear cGAS activity through an unknown mechanism. Cancer cells can display numerous strategies to evade immune surveillance and enable their survival. This involves re-wiring of the canonical cGAS STING pathway in some way directing its function towards increased pro-tumour signalling.

Firstly, cancer cells can alter expression of different components of the cGAS STING pathway to evade immune surveillance. For instance, transcriptional analysis of gastric cancer tumour samples revealed that a reduction in the expression of both cGAS and STING correlated with poor patient survival rates (Song et al., 2017). Agreeing with this finding was a study conducted by Yang et al., (2017) who showed that decreased cGAS expression correlated with poor survival rates of patients with lung adenocarcinoma. In contrast, other studies have highlighted how not decreased, but increased expression of STING and cGAS can also correlate with poor patient survival in colon cancer (Jiang et al., 2020). Increases in STING expression, leads to increased production of pro-inflammatory cytokines such as IL-6, which is a key cytokine in promoting cancer cell metastasis and survival. For example, depleting cGAS STING in triple negative breast cancer displaying CIN led to a reduction in IL-6 production and cell death (Hong et al., 2022). Furthermore, induction of DNA damage through radiation for instance enables cancer cells to upregulate TREX1 expression. TREX1 plays a role in degrading cytosolic DNA and therefore acts to suppress the anti-tumour response mediated by cGAS STING (Tani et al., 2024). In addition, cancer cells can suppress, cGAS activity through micro-nucleophagy and extracellular cGAMP hydrolysis, via expression of ectonucleotide pyrophosphatase phosphodiesterase 1 (ENPP1) on the surface of their membranes all aiding in cancer cell evasion of the immune system. (Zhao et al., 2021, An et al., 2024) Despite this, most tumours retain cGAS and STING expression in some way suggesting that their alteration in not the main factor driving immune evasion and further elucidation is needed to understand differences observed between different cancers (Kwon and Bakhoum, 2020).

In addition to altering expression of different components of the cGAS STING pathway, cancer cells can also promote chronic IFN signalling and induce low-grade inflammation, through downregulation of IFN's and upregulation of NF-κB. This leads to increased expression of interferon related DNA damage resistance signature genes, fostering a tumour-suppressive microenvironment that favours tumour invasion and metastasis (Gan et al., 2021). Furthermore, this NF-κB signalling can upregulate expression of programmed cell death ligand 1 (PD-L1), which suppresses T-cell activation and prevents cancer cells undergoing apoptosis (Jiang et al., 2020). Additionally, PD-L1 upregulation can also interfere with the production of interferons, whilst upregulation of the enzyme indoleamine-2,3-dioxygenase (IDO), can contribute to an immunosuppressive microenvironment (Spranger et al., 2013). A study conducted by Ahn et al., (2014) in primary human keratinocytes showed that 7,12-Dimethylbenz(a)anthracene (DMBA), cisplatin and etoposide can promote chronic inflammatory cytokine release in a STING-dependent manner. Similarly, a study conducted by Liang et al., (2017) showed that low grade inflammation can recruit suppressor cells that drives increased cell resistance to the effects of radiation, leading to colon cancer progression. Furthermore, using a model of brain cancer metastasis, a study conducted by Chen et al., (2016) revealed that cGAMP could be transferred through gap junctions to astrocytes, which activated STING. This then induced chronic signalling, promoted increased production of inflammatory cytokines and fostered tumour growth.

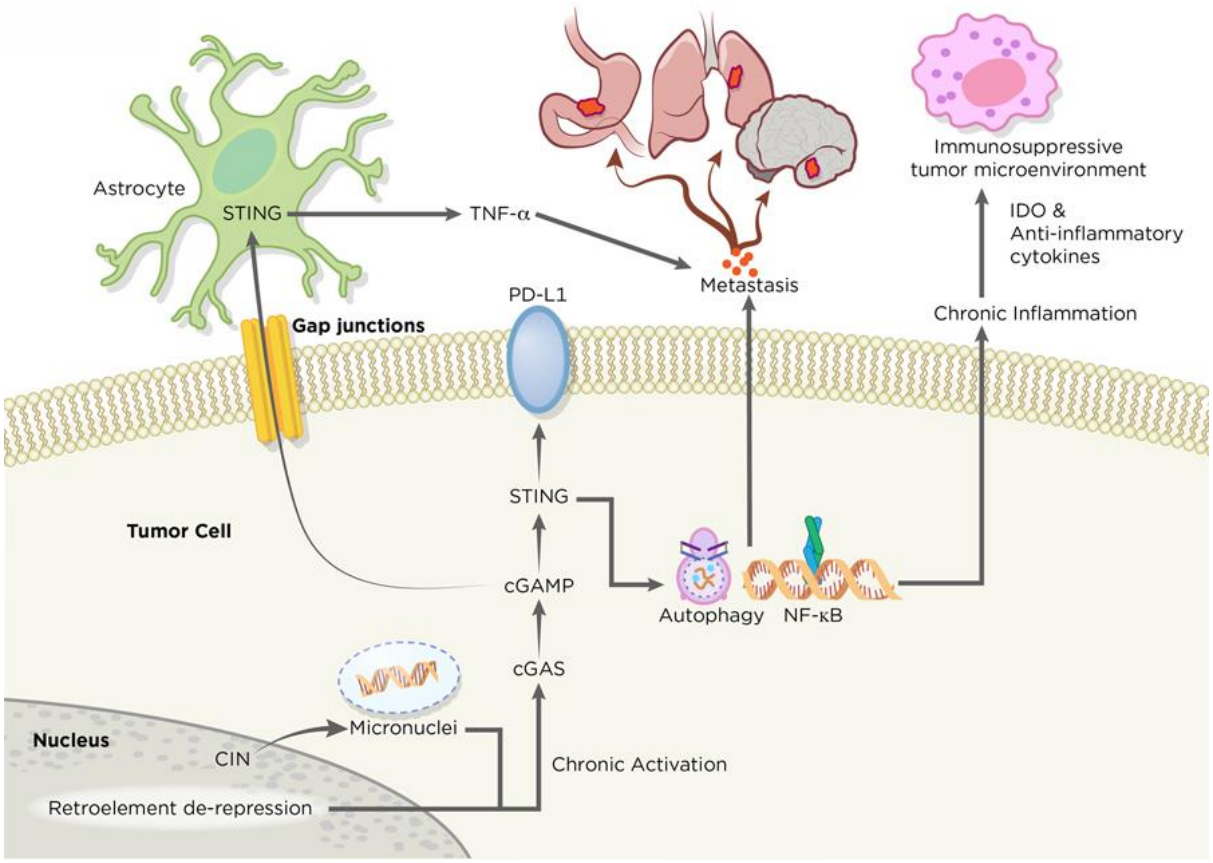

Figure 11: Pro-tumour functions of cGAS STING Signalling. In metastatic cells, micronuclei generated from tumours with high levels of chromosomal instability release their DNA into the cytosol. In turn chronic activation of Stimulator of interferon genes (STING) signalling leads to downregulation of interferon (IFN) production and upregulation of non-canonical nuclear factor kappa light chain enhancer of activated B cells (NF-κB) signalling. This leads to the production of anti-inflammatory cytokines and indoleamine-2,3-dioxygenase (IDO), which facilitates the establishment of an immunosuppressive microenvironment. Figure adapted from (Kwon and Bakhoum, 2020).

Emerging evidence suggests that tumour cells favour activation of the non-canonical cGAS STING pathway, that is NF-κB dependent, and this is closely related to tumour metastasis (Tian et al., 2022). This pathway favours NF-κB p65 activation over IRF3, resulting in a more pro-inflammatory gene expression profile that contributes to cancer cell proliferation and metastasis (Wheeler and Unterholzner, 2023). For example, a study conducted by Dunphy et al., (2018) showed that etoposide, a topoisomerase II poison elicits an NF-κB dependent immune response (independent of cGAS) within hours of treatment in immortalised HaCaT cells. Similarly, Ranoa et al., (2019)

revealed that in colorectal cancer, STING regulates the cell-cycle in a manner that functions independently of cGAS. This suggests that tumours can co-opt the cGAS STING pathway using different DNA sensors and adaptor proteins during chronic DNA damage or CIN.

Given that the cGAS STING pathway can display both pro-tumorigenic and anti-tumorigenic functions, it could pose potential as a therapeutic target, although this requires further research (Section 1.3.5).

1.3.5. The cGAS STING Pathway as a Therapeutic Target

Examples of therapies used to boost anti-tumour immunity are STING agonists, which are predominately small analogues of cGAMP that can act on STING and promote activation of an immune response. One example is that of 5.6-dimethylaxanthenone-4 acetic acid (DMXAA), that enabled an innate immune response through STING activation in mouse models of solid tumours but was not effective on human STING (Conlon et al., 2013). However, further research has led to the design of more promising cGAMP analogues for the treatment of human cancers. For example, cGAMP analogues enhanced anti-tumour functions of Chimeric Antigen receptor - Natural Killer cells (CAR-NK) cells in human models of pancreatic cancer (Da et al., 2022). Similar effects were seen using bacterial messengers such as cyclic di-adenosine monophosphate (c-di-AMP) in murine models of breast cancer (Vasiyani et al., 2021). There are also many STING agonists in human clinical trials. Examples include, ADU-S100 and MK-1454 trialled for patients with metastatic solid tumours or lymphomas, to which there was evidence of an anti-tumour response through CD8 infiltration (Kwon and Bakhoum, 2020). Despite this, there have been limited clinical benefits from these agonists in late-stage tumours in human clinical trials. This is likely a result of chronic activation of the cGAS STING pathway in metastatic tumours and therefore suppression of an anti-tumour immune response, or could reflect differences between mouse and human species and so requires further research (Kwon and Bakhoum, 2020).

It is also important to recognise how classic cancer therapies such as radiotherapy and chemotherapy can enhance anti-tumour functions of cGAS STING. These therapies can both cause DNA damage and produce MN which can activate the cGAS STING pathway. One example of a chemotherapeutic PARP inhibitor that elicits this effect is Olaparib used in the treatment of ovarian cancer, through eliciting a STING dependent response (Ding et al., 2018). Similarly, radiotherapy has demonstrated antitumour immunity by promoting cGAS STING activation, in non-small cell lung cancer (Yang et al., 2023). However, whether this is effective in different types of cancer still needs further understanding.

Whilst many late-stage tumours lose cGAS STING signalling, others can retain chronic low level activation, which can promote tumour progression and lead to the resistance of tumours to STING agonists (Gan et al., 2021). This had led to the development of STING Antagonists. Examples are the TBK1 inhibitors GSK-8612 and Cho-TBK1-HDO that have been shown to successfully suppress metastasis in mouse models of cholangiocarcinoma (Gao et al., 2023). Other examples include inhibitors of cGAS, including Suramin which has been shown to disrupt cGAS/DNA binding and therefore inhibit cGAS enzymatic activity in human THP-1 monocyte cells (Wang et al., 2018). Therefore, this provides an avenue for research into the use of these cGAS inhibitors to suppress cGAS STING signalling, particularly in many late-stage cancers.

Clearly, the cGAS STING pathway can be harnessed as a therapeutic target for the treatment of cancer. Despite this, tumour stage, CIN state, type of cancer and levels of cGAS STING activation all dictate the success of new and emerging therapies. Furthermore, even though many studies have linked CIN with activation of the cGAS STING pathway, there is limited literature that investigates STING signalling in the context of CA. It is known that centrosome clustering is the instigator of CIN (Milunović-Jevtić et al., 2016). Interestingly, however, only one study has investigated the effects of centrosome de-clustering on cGAS STING activation. this study found that centrosome de-clustering of irradiated human breast cancer cell lines induced cGAS STING activation of tumour associated immune cells, rather than cancer cells themselves (Kim et al., 2022). Therefore, further research is needed to understand cGAS STING pathway activation in different cancers, with varying levels of CA.

1.4. Project Aims

Strategies for the prevention and treatment of UM remain poor, because more than 50% of patients progress to incurable metastatic disease, for which there are no effective therapies (Rantala et al., 2019). As CA is known to occur in UM (Sabat-Pośpiech et al., 2022), which could lead to activation of an innate immune response, (Milunović-Jevtić et al., 2016) this could provide an alternative target. Although CA promotes tumorigenesis, it can be act as an ‘’Achilles heel” for cancer cells as they can avoid multipolar mitosis and subsequent cell death, mainly through centrosome clustering, mediated primarily through KIFC1 (Sabat-Pospiech et al., 2019). Despite this, even though centrosome clustering can promote cell survival, it can also generate large scale CIN, because of occasional merotelic kinetochore attachments that give rise to lagging chromosomes and eventual MN that could potentially activate the cGAS STING pathway (Milunović-Jevtić et al., 2016). Evidence from the literature seems to imply that activation of cGAS-STING by MN is a context-dependent phenomenon. Whilst in some cases it is a significant mechanism of immune activation, inducing anti-tumour functions (Harding et al., 2017, Mackenzie et al., 2017), it may be suppressed or absent in other scenarios. This could be through cancer cells downregulating or altering cGAS-STING signalling in some way to evade the innate immune system (Sato and Hayashi, 2024, Takaki et al., 2024, Dunphy et al., 2018, Flynn et al., 2021). Whilst it has been suggested that MN are potent activators of the cGAS-STING pathway in numerous studies, whether MN always activate the cGAS-STING pathway or only in certain contexts remains a matter of controversy. Furthermore, not many studies evaluate activation of the cGAS-STING pathway in cancers with and without CA particularly in the context of endogenous DNA damage. Overall, this contrasting evidence suggests a complex role for the cGAS-STING pathway, in which it operates through diverse mechanisms, dependent on the context.

Therefore, further research is needed to dissect the dual nature of this innate immune response, particularly in the context of CA, as well as how CA induced cGAS-STING activation may be exploited as a therapeutic target. This will be critical for developing strategies to enhance immune recognition and improve treatment options and prognostic outcomes for individuals with UM.

The aims of this project, therefore, are three-fold:

1) Perform exploratory analysis of expression of components of the cGAS STING pathway, using a transcriptomics data set from patient matched primary uveal melanoma (Mel270) and liver metastatic uveal melanoma (OMM2.3) cell lines. The primary uveal melanoma cell line is known to contain lower levels of centrosome amplification than the metastatic cell line and so will allow for a comparison of expression between the two.

2) Assess the relationship between centrosome amplification, micronuclei formation and cGAS STING activation in the above set of matched cell lines, using Immunofluorescence Confocal Microscopy and Western blotting.

3) Measure the activity of the cGAS STING pathway in the above set of matched cell lines, using key indicators of innate immune activation (such as IL-6 and CXCL10 release). This will be done using Enzyme Linked Immunosorbent Assays (ELISA).

2. Materials and Methods

Cell Culture

Cell lines were cultured in their appropriate complete growth medium (Table; 2) in T75 flasks. Cells were then incubated at 37°C, 5% CO_2 until passaging. To passage, cells were aspirated of media and twice dissociated with TrypleE Express (Gibco, Thermo-Fisher Scientific), before incubation for 10-20 minutes at 37°C, 5% CO_2. Cells were then resuspended as appropriate in complete medium, pipetting up and down to obtain a single cell suspension, before being transferred to a new T75 flask, containing fresh medium. All cell lines were passaged on average twice a week, when cells reached approximately 70-80% confluency. Cell lines were routinely tested for mycoplasma contamination.

Table 2: Composition of complete growth medium used and source of each cell line.

Cell Line	**Media Composition** (All reagents from Gibco, Thermo-Fisher Scientific)
Mel270 (Coupland Lab, University of Liverpool)	RPMI, 10% FBS, 1% PenStrep
OMM2.3 (Coupland Lab, University of Liverpool)	RPMI, 10% FBS, 1% PenStrep
HaCaT (German Cancer Research Institute)	DMEM, 10% FBS, 1% PenStrep
T24 (German Cancer Research Institute)	DMEM, 10% FBS, 1% PenStrep

Thawing and Freezing Cells

To thaw, cells were retrieved from liquid nitrogen and thawed at 37°C in a bead bath. Cells were then transferred to new T75 flasks and resuspended in complete growth medium before incubation at 37°C, 5% CO_2. To freeze, cells were twice dissociated using TrypleE Express before resuspending in fresh medium. Cells were then centrifuged at 1000 revolutions per minute (rpm) for 3 minutes, before being resuspended in freezing medium {5% dimethyl-sulfoxide (DMSO) (Sigma-Aldrich-MERCK) in cell media} and then transferred to cryogenic vials. Vials where then placed

in the -80°C freezer over night before being transferred to liquid nitrogen for long term storage.

Cell Counting

Cells were resuspended in complete medium before loading 10µL into a haemocytometer.

DNA and RNA Transfection

For herring's testis (HT DNA) (Sigma-Aldrich, MERCK) transfection; 1.8µL lipofectamine 2000 (Invitrogen, Thermo-Fisher Scientific) was first combined with 56.7µL optimem (Gibco, Thermo-Fisher Scientific), vortexed briefly and incubated at room temperature (RT) for 5 minutes. (HT) DNA at varying concentrations, dependent on the experiment (1, 2.5 or 5 µg/mL) was then added, mixed by pipetting and incubated at RT for 10 minutes before treating the cells for 1 hour, when investigating cGAS, IFI16 and STING and 3hrs when investigating IRF3 and NF-κB p65. For Poly(I:C) RNA transfections (Sigma-Aldrich, MERCK), the same process was repeated as for the DNA transfections, transfecting cells with poly(I:C) at varying concentrations, dependent on the experiment (0.1 or 1µg/mL). Mock transfections were also prepared (lipofectamine 2000 and optimem alone) as a negative control. HaCaT (immortalised human keratinocyte cells) or T24 (muscle invasive bladder cancer cells) were used as the positive controls.

Cell Treatments

Cells were treated with the chemotherapy agent; Etoposide (Sigma-Aldrich, MERCK) at 10µM and 50µM concentrations for 3 hrs. DMSO alone was also prepared to act as a negative control.

Immunofluorescence Staining and Confocal Microscopy

Mel270 (primary UM cells), OMM2.3 (metastatic UM cells) and HaCaT Cells were seeded on 13mm round glass coverslips in either a 6-well or 12-well plate at a concentration of $1x10^5$ cells/mL and incubated overnight at 37°C, 5% CO_2. Cells were washed with 1mL phosphate buffered saline (PBS) (Invitrogen, Thermo-Fisher Scientific, used at 1x working concentration, made from 10x stock concentration)

before being fixed with 1mL methanol (Sigma-Aldrich, MERCK) for 10 minutes at -20°C. Coverslips were removed from wells and transferred cell side up onto parafilm in a humidified chamber. Each coverslip was blocked in 100µL 5% FBS, 0.2% Tween-20 (Sigma-Aldrich, MERCK) in PBS for 1 hour at RT. Each coverslip was then treated with 100µL primary antibody (1:600 dilution) (Table; 4) in 5% FBS, 0.2% Tween-20 in PBS overnight at RT. Coverslips were then washed once with 100µL PBS before being treated with 100µL secondary antibody in 5% FBS, 0.2% Tween-20 in PBS (1:1500 dilution) (Table; 5). Coverslips were then left for 3 hours in the dark at RT. Coverslips were again washed in 100µL PBS before being mounted face down onto glass slides using 15µL of mowiol containing DAPI (Sigma-Aldrich, MERCK). Coverslips were then left to dry overnight at RT and stored long term at 4°C.

Cells were imaged using a Zeiss LSM880 confocal microscope.

Cell Lysis

To obtain cell lysates, hot lysis was performed. Mel270, OMM2.3 and HaCaT cells were seeded into 10cm dishes (5 million cells/dish) and incubated overnight at 37°C, 5% CO_2. Cells were aspirated of media before washing once in 900µL PBS. Laemmli lysis buffer (2% sodium dodecyl sulfate (SDS), 0.0625M Tris Base, pH.8, 10% Glycerol) (Sigma-Aldrich, MERCK) was added based on cell confluency before placing plates over a heat block (105 °C). cells were then scraped into screw cap tubes and heated for 10 minutes, vortexing every 2 minutes. Tubes were pulse centrifuged when cold and stored in the freezer until use (-20°C).

BCA Assay

To ascertain protein concentrations of the lysates a Bicinchoninic acid (BCA) assay was performed.

Lysates were diluted 1 in 3 in laemmli lysis buffer before 10µL of each lysate were added in duplicate in a 96-well plate, alongside 10µL of BCA standards in duplicate. As a control, 10µL of laemmli lysis buffer was also added in duplicate. BCA reagent (Thermo-Fisher Scientific) was prepared at a 50:1 ratio of reagent A to reagent B and mixed by pipetting. 200µL was then added to each well and incubated at 37°C for 30

minutes. After incubation, absorbance was read using the Tecan mPLEX plate reader set to 562nm.

SDS-Polyacrylamide Gel Electrophoresis (SDS-PAGE)

SDS-PAGE was carried out to separate proteins based on their molecular weight. A 12% resolving gel was made up, followed by a 4% stacking gel (Table; 3). 5mL of the 12% resolving gel mixture was poured between a short plate and tall plate held together in a Bio-rad Mini-PROTEAN Tetra Handcast cassette. 1mL ethanol was poured on top to seal and prevent the formation of bubbles. One set, the ethanol was soaked up with filter paper and 1mL stacking gel was added. A comb was then inserted and left to set. Prepared gels were kept in 4°C fridge for three weeks.

Table 3: Preparation of 12% Resolving gel and 4% Stacking gel for SDS-PAGE. Reagents are from Sigma-Aldrich, MERCK

Gel	Resolving gel	Stacking gel
Percentage	12%	4%
Milli-Q Water (MQW)	8.7mL	3.17mL
Tri's buffer Resolving (1.5M, pH 8.8) Stacking (0.5M pH 6.8)	 5mL -	 - 1.25mL
Acrylamide Bisacrylamide (40%)	6mL	0.5mL
SDS (10%)	200µL	50µL
Ammonium persulfate (APS) (10%)	100µL	20µL
Tetramethyl-ethylenediamine (TEMED)	20µL	5µL

The gels were transferred to a Bio-rad Mini Protean Tetra Handcast tank and 1x running buffer (25 mM Tris, 192 mM glycine, 0.1% SDS pH 8.3) was added. The comb

was removed and 40µg protein lysates mixed with 6x loading buffer (375 mM Tris-HCl 6.8 pH, 6% SDS (w/v), 30% glycerol (v/v), 9% beta-mercaptoethanol (BME) (v/v), 0.06%) bromophenol blue (w/v) was loaded into the gel wells, alongside 3µL of protein ladder (Thermo-Fisher Scientific). Gels were then run at 200 volts, 90mAmps for 120 minutes or longer until the dye front reached the bottom of the gel.

All reagents used to make the buffers from Thermo-Fisher Scientific

Western Blot Transfer and Antibody Probing

Once the gel had run, proteins were transferred onto a nitrocellulose membrane (Bio-rad). A stack was made up of 7x layers of blotting filters, nitrocellulose membrane, gel and then another 7x layers of blotting filters. 35mL transfer buffer (5x (biorad) made up to 1x with 600mL H2O and 200mL ethanol) was then added to moisten the blotting stack. Air bubbles were rolled out using a roller and the proteins were transferred using the Bio-rad Trans-blot Turbo transfer system, set to “high molecular weight, 1 mini gel for 10 minutes”.

After transfer, the blot was placed in ponceau red stain (Thermo-Fisher Scientific) for 1 minute to visualise protein bands. The blot was then rinsed in MQW water and then blocked in 5% marvel milk powder in tris-buffered saline (TBST) (Tween 20 0.1% (v/v), 20 mM Tris, 150 mM NaCl, pH7.4) on the rocker at RT for 1 hour. The blot was then incubated in primary antibodies on the rocker overnight at 4°C (1:1000 dilution) (Table; 4). The blot was then washed 3 x 5 minutes in TBST at RT on the rocker. Secondary antibodies were then added (1:10000) (Table; 5) and placed on the rocker at RT for 1 ½ hrs. The blot was then washed again 3 x 5 minutes in TBST on the rocker before rinsing in PBS.

The membranes were then visualised using the ibright FL1500 imaging software.

Enzyme- Linked Immunosorbent Assay (ELISA)

ELISA for the quantification of CXCL10 (Lot P405135) and IL-6 (Lot P439848) were carried out according to manufacturer’s instructions using duoset ELISA Kits (R&D systems). High-binding ELISA plates were coated with 100µL capture antibody

(2µg/mL) for both IL-6 and CXCL10 before incubation overnight at RT. Plates were then washed 3 times in PBS/0.05% Tween-20 before the addition of 300µL blocking solution (1% bovine serum albumin (BSA) in PBS). Plates were then incubated for 2 hours at RT. 7-point 2-fold dilutions were made of standards with a range of 600pg/mL to 9.38pg/mL (IL-6) and 2000pg/mL to 31.2pg/mL (CXCL10). Samples were diluted 1:20 (T24) or 1:2 (Mel270, OMM2.3) in reagent diluent. 100µL sample or standard was then added in triplicate and incubated at RT overnight. The plate was washed 3 times before addition of 100µL detection antibody prepared to working concentrations of 50ng/mL (IL-6) and 12.5ng/mL (CXCL10). Plates were incubated for 2 hours at RT. The plate was then washed again 3 times before addition of 100µL streptavidin-horseradish peroxidase (HRP) (1:40 dilution) for 20 minutes at RT. The plate was washed three times and 100µL 3,3',5,5'-Tetramethylbenzidine (TMB) ELISA substrate solution (Thermo-Fisher Scientific) was added for 20 minutes at RT. The reaction was then stopped via addition of 50µL of 0.18M H_2S04 (Sigma-Aldrich, MERCK). Plates were then read at 570nm using the Tecan Mplex plate reader.

MTS Assay

20µL of 3-(4,5-Dimethylthiazol-2-yl)-5-(3-carboxymethoxyphenyl)-2-(4-sulfophenyl)-2H-tetra-zolium (MTS) reagent (CellTiter 96® AQueous One Solution Cell Proliferation Assay (MTS) Promega) was added to each well before incubation for 4 hours at 37°C, 5% CO_2. Plates were then read using the tecan Mplex Plate reader, set to 450nm.

Cancer Transcriptomics

To explore expression of components of the cGAS STING pathway, a transcriptomics data set from patient matched primary uveal melanoma (Mel270) and liver metastatic uveal melanoma (OMM2.3) cell lines was analysed. A previously generated FPKM dataset was analysed by uploading to the iDEP software, a tool used for RNA-sequencing analysis. We conducted differential gene expression analysis by using an FDR cutoff of 0.1. A simple KEGG pathway analysis was then performed to illustrate differentially expressed genes, relevant to the cGAS STING pathway that was either upregulated or downregulated in Mel270 compared to OMM2.3 cells.

Statistical Analyses

Data analysis was performed using Excel and Graphpad Prism (V10.4.1). Where relevant, statistical analyses were performed in GraphPad Prism (V10.4.1). A shapiro-Wilk test was first used to assess normality. If the data was normally distributed, a two-tailed unpaired t-test was performed to assess statistical significance between groups. A p=value <0.05 was considered statistically significant. When comparing multiple treatment groups to control, a one-way ANOVA with Dunnett's multiple comparison test was performed, comparing each condition to DMSO control. *= p< 0.01. **=p<0.05 was considered statistically significant.

Table 4: Primary Antibodies used throughout project

Antibody	Company	Catalogue Number
cGAS	Cell Signalling Technology	15102S
STING	Cell Signalling Technology	13647S
γH2AX	Cell Signalling Technology	9718S
IFI16	Santa Cruz Biotechnology	sc-8023
p65	Cell Signalling Technology	6956S
IRF3	Cell Signalling Technology	4302S
Alpha-Tubulin	Sigma-Aldrich	T6199

Table 5: Secondary Antibodies used throughout project

Antibody	Company	Catalogue Number
Alexa-Fluor Plus 555nm	Invitrogen	A32732
Alexa-Fluor 488nm	Invitrogen	A32723
IRDye 680RD	LI-COR	926-68073
IRDye 800CW	LI-COR	926-32212

3. Results

3.1.1 Metastatic UM Cells Exhibit Increased Micronuclei Formation.

Many cancer cells contain MN which are structural hallmarks of CIN. MN are derived from two origins, whole chromosomes or chromosomal fragments that fail to incorporate into daughter nuclei during cell division (Kwon et al., 2020). It is known that metastatic cancers typically display higher levels of CIN than primary cancers. For example, the cell lines used in this study; OMM2.3 (metastatic UM cells) and Mel270 (primary UM cells) reflect this. OMM2.3 cells have been shown to display increased levels of CA in 32% of all mitotic cells , compared to only 10% in Mel270 cells (Sabat-Pośpiech et al., 2022).

Therefore, we hypothesised, that metastatic cancer cells would display an increased frequency of MN compared to their primary counterparts. To understand whether these MN could induce an innate immune response, it was first important to establish whether our selected patient matched UM cell lines ((Mel270 from a primary tumour; lower CA and OMM2.3 from a liver metastasis; higher CA), contained MN, using immunofluorescence microscopy.

Mel270 and OMM2.3 cells were grown on coverslips and 24 hours later, the cells were fixed and stained with DAPI (DNA stain) to detect MN. To quantify the extent of MN, multiple images were taken per cell line across three fields of view, where MN was visible (Fig; 12A, B). The number of MN was then expressed as a percentage of total cells (Fig; 12C) and compared to the published CA status of these cell lines, reported by Sabat Pośpiech et al., (2022) (Fig; 12D).

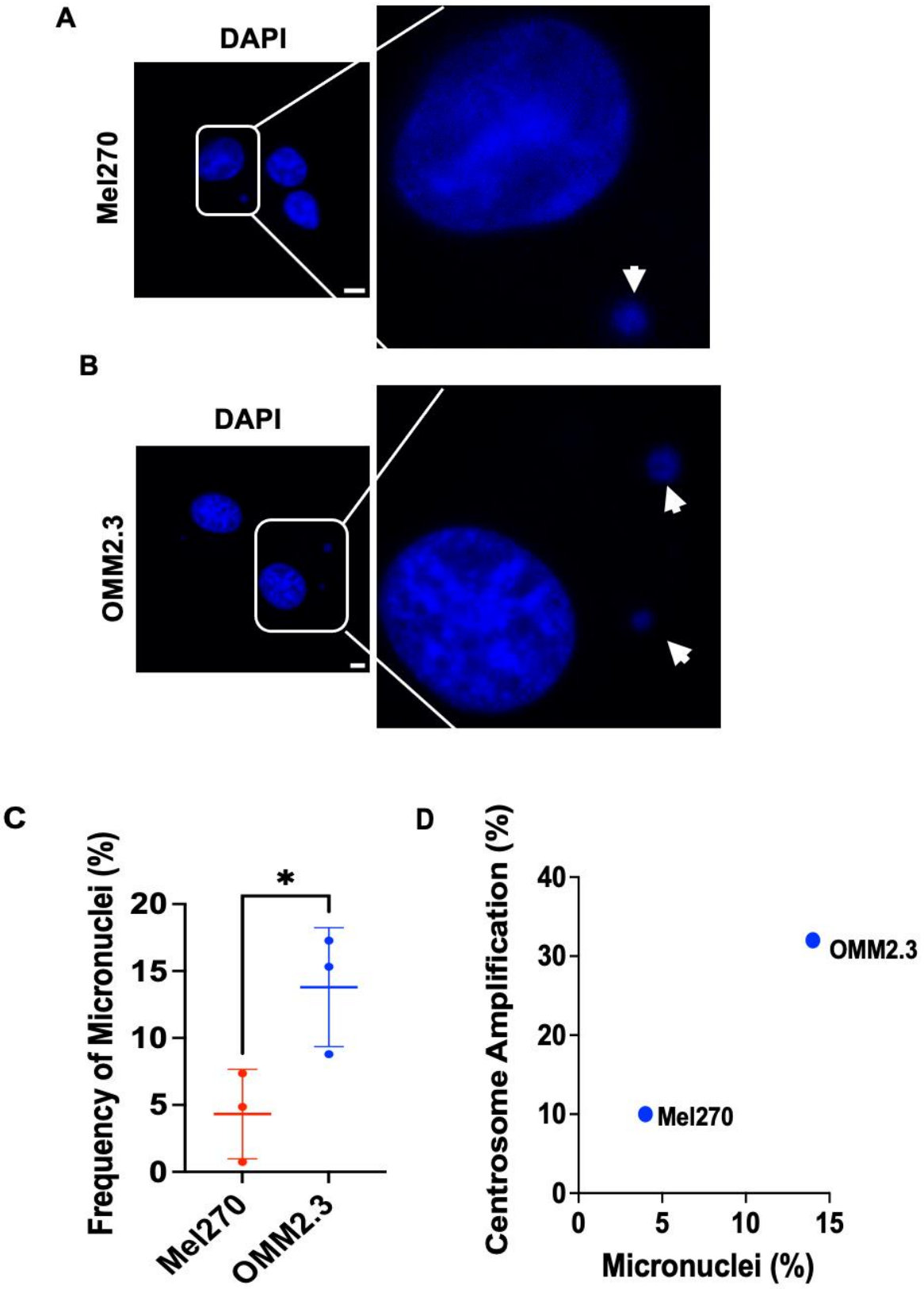
A
DAPI
Mel270
B
DAPI
OMM2.3
C
Frequency of Micronuclei (%)
20
15
10
5
0
*
Mel270
OMM2.3
D
Centrosome Amplification (%)
40
30
20
10
0
OMM2.3
Mel270
0
5
10
15
Micronuclei (%)

Figure 12: Increased MN frequency in Metastatic UM Cells.
Example immunofluorescent images of micronuclei observed in (**A)** Mel270 cells, (**B)** OMM2.3 cells. White arrows represent micronuclei. Scale bar = 5μm (**C)** Quantification of micronuclei as a % of total cells across three independent experiments (n=3). Data plotted as individual points +/- SD. Statistical analysis was performed using a two-tailed unpaired T-test; * p = 0.0419. D) Scatter plot of published % centrosome amplification status plotted against mean % micronuclei for both cell lines.

Upon examination of both Mel270 and OMM2.3 cells using Immunofluorescence, both cell lines exhibited MN formation (Fig; 12A, B). OMM2.3 cells displayed a significant increase in the frequency of MN compared to Mel270 cells (Fig; 12C), confirming that metastatic UM cells contain higher levels of CA and display elevated levels of CIN compared to primary UM cells (Fig; 12D).

3.1.2 UM Cells Contain Micronuclei Exhibiting DNA Damage

Based on the observation of MN in both cell lines in our first experiment (Fig; 12), we next sought to understand if these MN possessed DNA damage, using immunofluorescence microscopy.

Mel270 and OMM2.3 cells were grown on coverslips and 24 hours later, cells were fixed and stained with DAPI (DNA stain) and anti- γH2AX antibody, a marker used to detect the cell's response at sites of DNA damage. The anti-γH2AX antibody recognises a phosphorylated histone variant that is known to accumulate at sites of double strand breaks within DNA (Yuan et al., 2010). From this, MN that were γH2AX positive were counted by eye using the γH2AX channel (Fig; 13A, B) and plotted as a percentage of total MN (Fig; 13C).

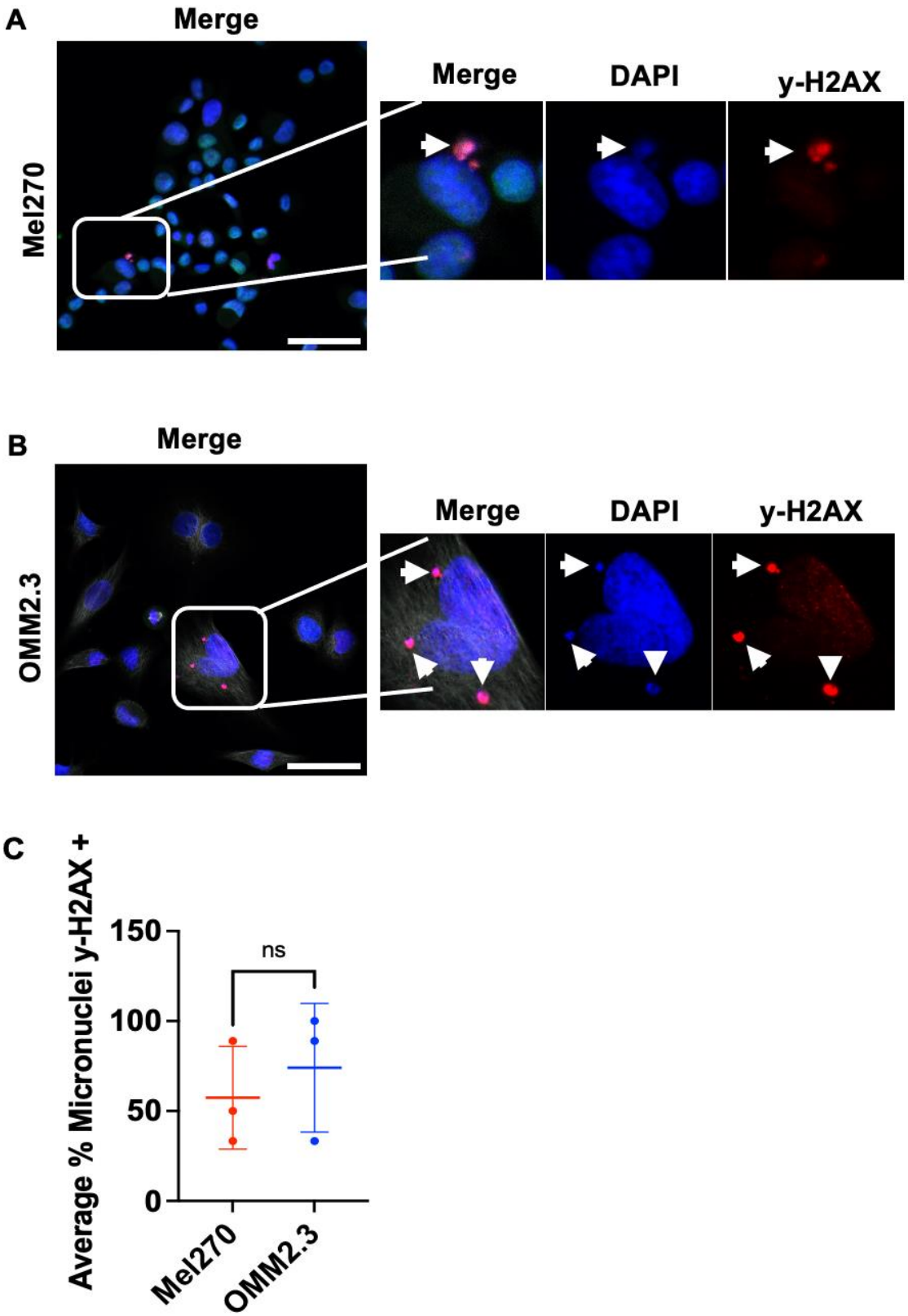
A
Merge
Mel270
Merge
DAPI
y-H2AX
B
Merge
OMM2.3
Merge
DAPI
y-H2AX
C
Average % Micronuclei y-H2AX +
150
100
50
0
ns
Mel270
OMM2.3

Figure 13: MN in UM cells Exhibit DNA damage

Example immunofluorescent images of y-H2AX positive MN observed in (**A)** Mel270 cells, (**B)** OMM2.3 cells. Scale bar on merge = 50µm. (**C)** Quantification of MN as a percentage that were γH2AX positive across three independent experiments (n=3). Data plotted as individual points +/- SD. Statistical analysis using a two-tailed unpaired T-test was performed, p = ns (not significant).

There was no significant difference between Mel270 and OMM2.3 cells in their % of MN that were γH2AX positive (Fig; 13C), with both cell lines containing over 50% of all MN that were γH2AX positive and therefore enriched for DNA damage (Fig; 13A, B). This was expected as MN have been shown to be key sites of ongoing DNA damage and are therefore frequently positive for γH2AX. This is particularly the case in cancer cells where there is elevated CIN, increased MN formation and envelope rupture (Xu et al., 2011, Medvedeva et al., 2007) This suggested that irrespective of CA status and genome instability, both cell lines had the potential to induce an innate immune response. However, it is important to note that metastatic cells possess greater numbers of MN and so will have a greater burden of DNA damage and whilst DNA damage has been associated with innate immune activation, not all MN do induce a response (Takaki et al., 2024, Sato and Hayashi, 2024). Therefore, it was important to investigate activation of this innate immune response further in our own cell lines.

3.1.3 Differential Expression of DNA Sensing Components at baseline and post (HT) DNA Transfection

As MN expressed high levels of DNA damage in both cell lines in our previous experiment (Fig; 13), we wanted to consider whether these MN may be capable of activating DNA sensing pathways. A key innate immune signalling axis is the cytosolic DNA sensing pathway cGAS STING. Rupture of MN has been shown in some contexts to leak DNA into the cytosol, leading to the recruitment of the DNA sensor cGAS and subsequent downstream type I interferon production through STING signalling. However, even though studies suggest that MN recruit cGAS and activate an innate immune response (Mackenzie et al., 2017, Harding et al., 2017), other studies show that recruitment of cGAS to MN is not sufficient to induce an interferon response (Takaki et al., 2024, Sato and Hayashi, 2024).

Therefore, to understand if cGAS, IFI16 and STING were intrinsically expressed in UM cells in the absence of stimulation or genotoxic stressors, cGAS, IFI16 and STING expression was first examined by western blot (Fig; 14). This would enable further understanding of whether UM cells possessed an intact DNA sensing pathway, under baseline conditions. Mel270 and OMM2.3 cells were lysed and proteins separated by gel electrophoresis. Proteins were transferred to a nitrocellulose membrane before probing for cGAS, STING and IFI16 (Fig; 14).

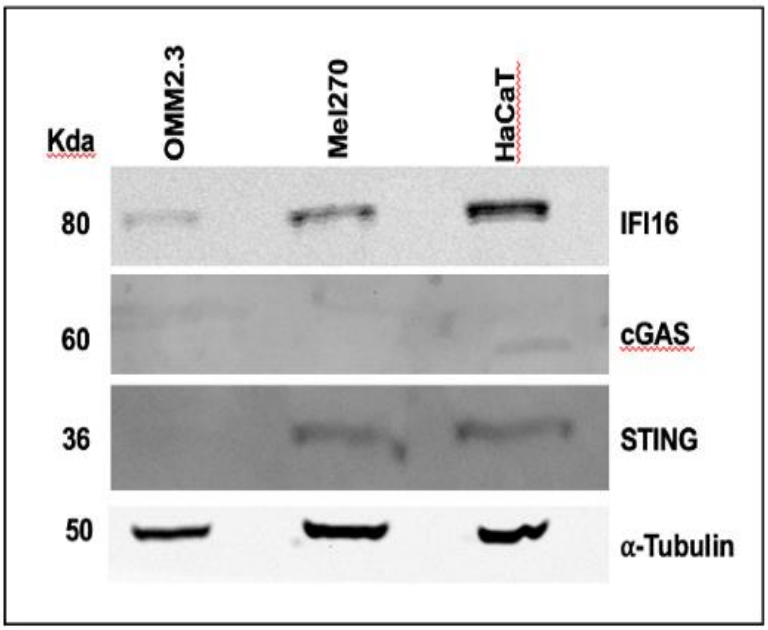

Figure 14: Differential Expression of DNA sensing Components at baseline. Western blot for cGAS, IFI16 and STING in Mel270, OMM2.3 Cells HaCaT cells were used as the positive control. Alpha-tubulin used as a loading control.

Unexpectedly and in contrast to findings in the literature, both primary and metastatic UM cells, with low and high CA respectively, were devoid of cGAS at baseline, when compared to HaCaT control cells (Fig; 14). A cell line dependent expression of IFI16 was observed, with levels being weaker in OMM2.3 cells that display higher CA(Fig; 14). STING was present in HaCaT control cells as expected but interestingly STING was only expressed in OMM2.3 cells(Fig; 14). This suggested that UM cells may possess altered or suppressed DNA sensing mechanisms as an immune evasion strategy. Furthermore, these findings also suggested that greater levels of CA, in the case of the metastatic cell line and therefore greater levels of genomic instability, may lead to further downregulation of DNA sensing components.

Given the absence of cGAS but cell line dependent expression of IFI16 observed in our UM cells (Fig; 14), we next examined IFI16 localisation using confocal microscopy to confirm findings observed in the western blot (Fig; 15).

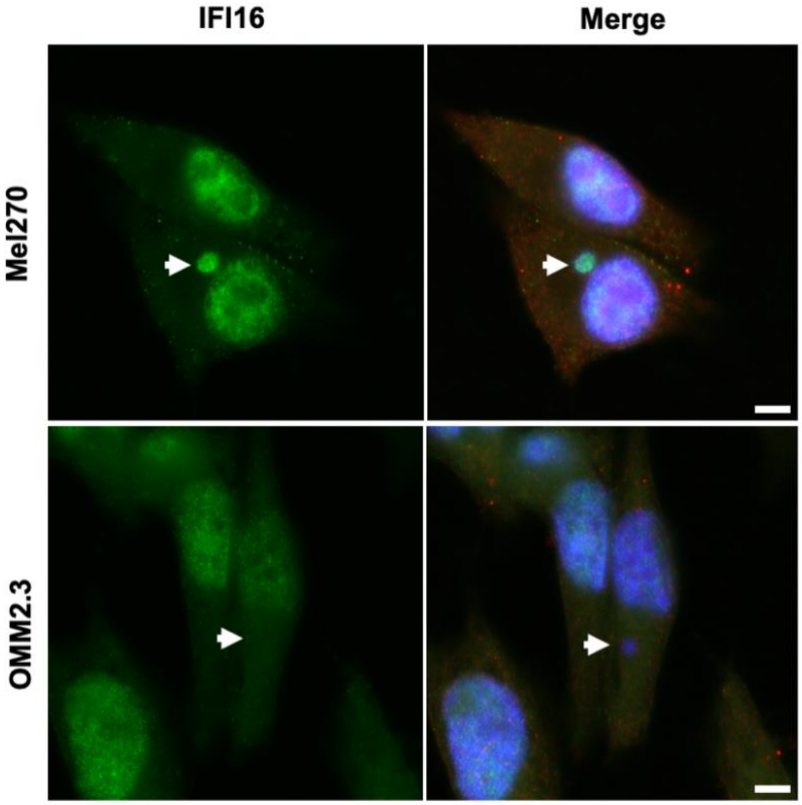

Figure 15: UM cells contain MN that vary in their levels of IFI16 expression at baseline

Representative immunofluorescent images of Mel270 and OMM2.3 cells, Scale bar on merge = 5µm. To note, cells were also stained with cGAS (red stain visible on merge images). However, individual cGAS channel omitted as not relevant to experiment.

Both cell lines contained MN, with individual MN varying in their levels of accumulation of IFI16 at baseline (Fig; 15). As expected, the metastatic OMM2.3 cells, with higher CA displayed weaker levels of IFI16 compared to primary mel270 cells, with lower CA, which agreed with findings observed in the western blot (Fig; 14).

To further assess whether UM cells retained any capacity to respond to cytosolic DNA, given the absence of cGAS, cells were transfected with 2.5µg/mL (HT) DNA, which serves as a source of exogenous double stranded DNA. This would enable us to test whether UM cells, could mediate DNA sensing via alternative DNA sensors such as

IFI16. To do this we investigated whether IFI16 co-localises with transfected DNA and/or MN in UM cells (Fig; 16). Human HaCaT cells were used as a positive control.

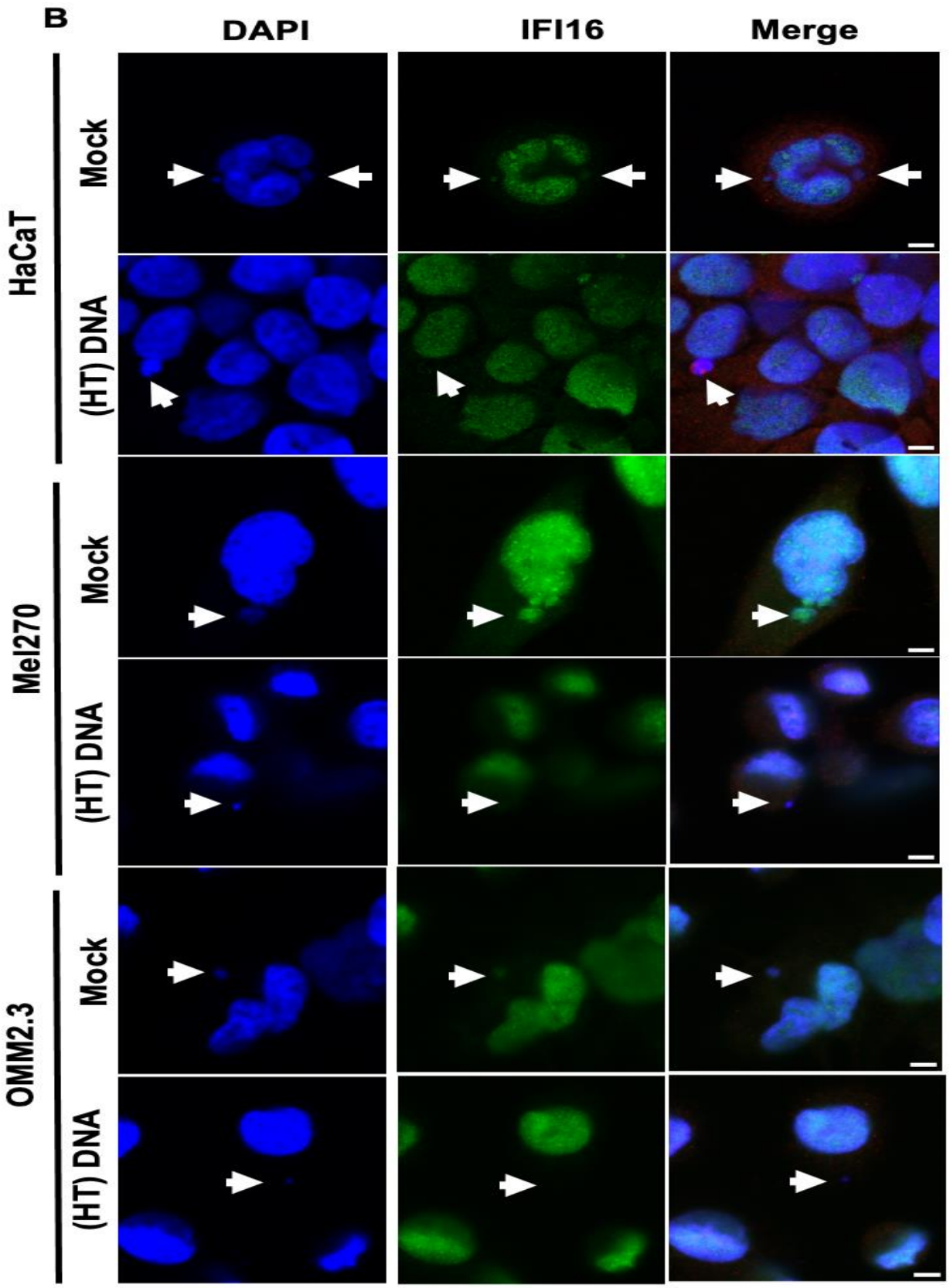
B
DAPI
IFI16
Merge
HaCaT
Mock
(HT) DNA
Mel270
Mock
(HT) DNA
OMM2.3
Mock
(HT) DNA

Figure 16: UM cells contain MN that vary in their levels of IFI16 expression post (HT) DNA transfection

Representative immunofluorescent images of Mel270 and OMM2.3 cells. Scale bar on merge = 5µm. To note, cells were also stained with cGAS (red stain visible on merge images). However, individual cGAS channel omitted as not relevant to experiment.

The same findings were observed post DNA-transfection with individual MN and clusters of transfected DNA varying in their levels of IFI16 expression both in mock and transfected cells for all cell lines. Again, lower levels of IFI16 were observed in MN of metastatic UM cells (higher CA) compared to primary UM cells (lower CA) and HaCaT control cells (Fig; 16). Taken together, this further supported downregulation or absence of a functional DNA sensing pathway in UM cells.

3.1.5 Absence of IRF3 and NF-κB p65 Nuclear Translocation in Response to (HT) DNA in UM Cells.

We next investigated whether downstream signaling remained functional. This was done by assessing activation of downstream transcription factors IRF3 and NF-κB p65. p65 (ReIA) is the major subunit of the NF-κB family that is responsible for mediating NF-κB signaling and inflammatory cytokine expression (Oeckinghaus and Ghosh, 2009). Both IRF3 and NF-κB p65 are known to translocate to the nucleus from the cytoplasm upon activation (Popli et al., 2022).

Cells were transfected with 2.5µg/mL (HT) DNA, which engages the cGAS STING pathway to activate predominately IRF3, but also NF-κB p65 for 3 hours. Cells were fixed and stained using anti-IRF3 and anti- NF-κB P65 before immunofluorescence was carried out (Fig;17).

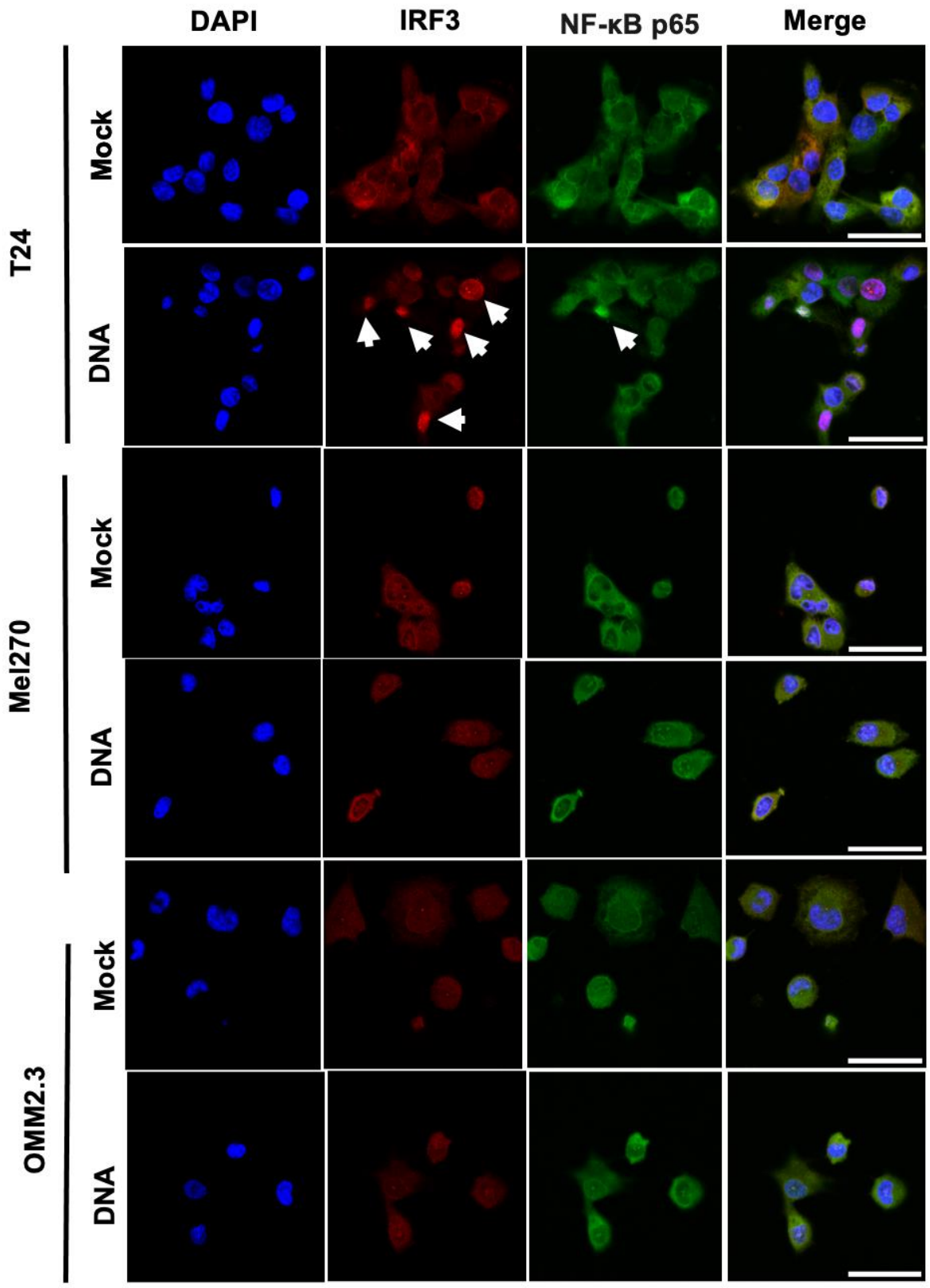
DAPI
IRF3
NF-κB p65
Merge
T24
Mock
DNA
Mel270
Mock
DNA
OMM2.3
Mock
DNA

Figure 17: IRF3 and NF-κB p65 do not translocate to the nucleus upon (HT) DNA transfection in UM cells.

Representative immunofluorescent images of T24, Mel270 and OMM2.3 cells. Scale bar on merge = 50μm. White arrows represent cases of IRF3 and NF-κB p65 nuclear translocation.

T24 cells are muscle invasive derived bladder cancer cells, that were used as the positive control as they are known to express a functional DNA sensing pathway. As expected, T24 cells, did exhibit robust nuclear translocation of both IRF3 and NF-κB p65 in response to (HT) DNA transfection, compared to mock. This confirmed that these cells possessed a functionally intact DNA sensing pathway and therefore validated the experimental setup (Fig; 17). In contrast, UM cells exhibited no detectable nuclear translocation of IRF3 and NF-κB p65 following (HT) DNA transfection, like mock controls (Fig; 17) further supporting absence of a functionally intact DNA sensing pathway in our UM cells.

3.1.6 IRF3 and NF-κB p65 Translocation Occurs in Response to Poly(I:C) RNA in UM Cells

Since there was an absence of IRF3 and NF-κB p65 nuclear translocation in UM cells, post (HT) DNA transfection (Fig; 17), we then wanted to understand if this defect was specific to the DNA sensing pathway or a result of a broader impairment of innate immune signaling pathways. To investigate this, we examined if our UM cells activated IRF3 and NF-κB p65 in response to cytosolic RNA.

To do this we transfected cells with 0.1µg/mL poly(I:C), which mimics double stranded-RNA. Rather than activate the cGAS STING signaling axis, poly(I:C) engages the RIG-I/MDA-5 pathway but this also leads to IRF3 and NF-κB p65 activation. Cells were then fixed at the 3-hour timepoint, stained for IRF3 and NF-κB p65 and immunofluorescence was then carried out (Fig; 18).

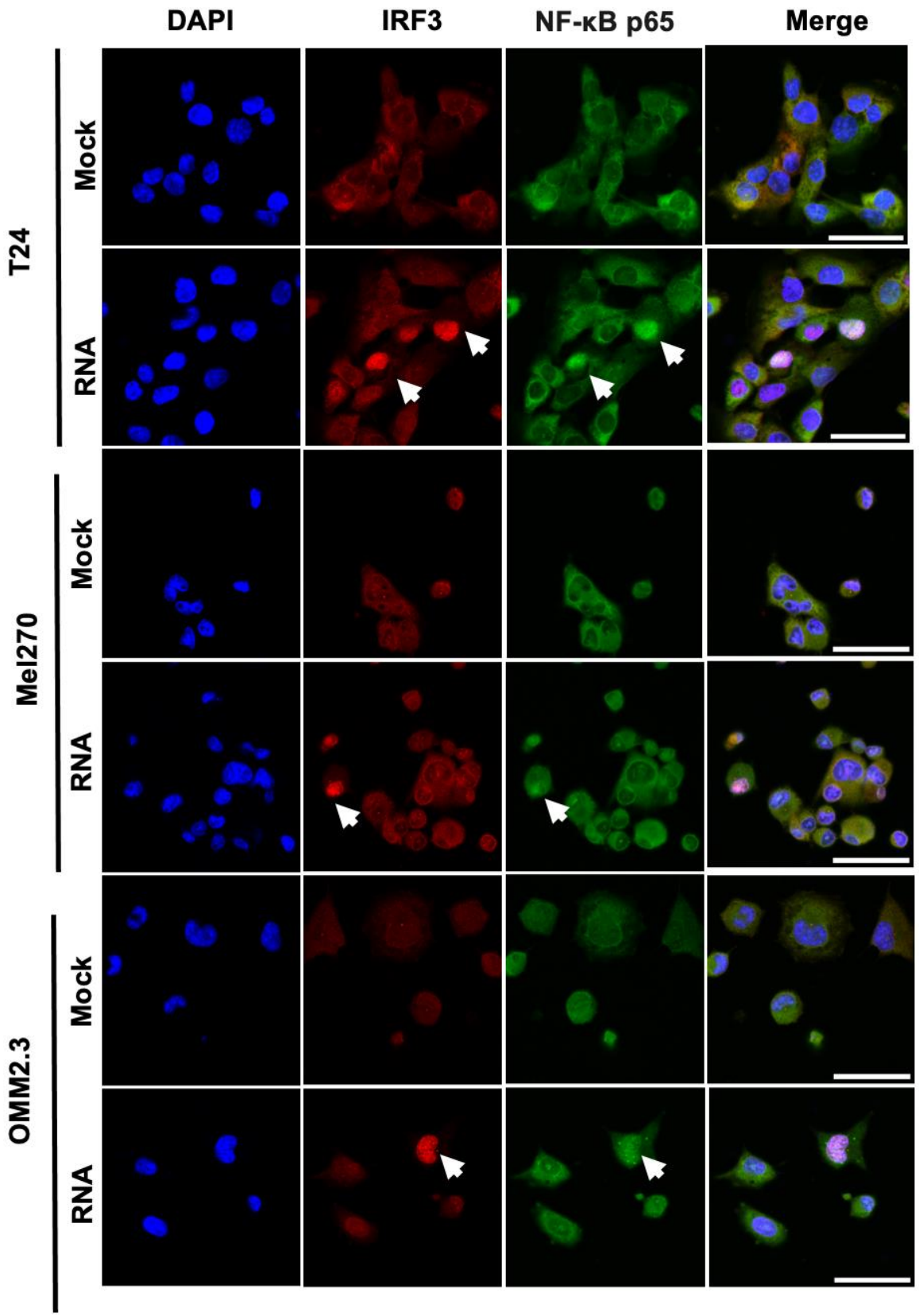
DAPI
IRF3
NF-κB p65
Merge
T24
Mock
RNA
Mel270
Mock
RNA
OMM2.3
Mock
RNA

Figure 18: Nuclear translocation of IRF3 and NF-κB p65 occurs upon poly(I:C) stimulation in UM cells.

Representative immunofluorescent images of T24, Mel270 and OMM2.3 cells. Scale bar on merge = 50μm. White arrows represent cases of IRF3 and NF-κB p65 nuclear translocation.

In contrast to (HT) DNA transfection (Fig; 17), UM cells exhibited translocation of IRF3 and NF-κB p65 to the nucleus following poly(I:C) RNA transfection, like T24 control cells (Fig; 18). This indicated that RNA-sensing pathways remained functional as cells responded to RNA stimulation.

3.1.5 Absence of IRF3 and NF-κB p65 Nuclear Translocation in Response to Etoposide in UM Cells.

Since UM cells appeared to lack functional cytosolic DNA sensing (Figures; 15, 16, 17,) but retained functional RNA sensing (Fig; 18), we were next interested to understand if alternative pathways might be engaged. Previous findings by Dunphy et al., (2018) showed that the chemotherapeutic agent etoposide promotes non-canonical STING activation through inducing inhibition of topoisomerase II in a cGAS independent manner. This then leads to the formation of DNA double strand breaks within the nucleus, which is recognized by the DNA damage factors ATM and PARP-1 and the DNA sensor IFI16; leading to an alternative STING signaling complex that favors NF-kB p65 activation over IRF3. We therefore tested if our two UM cell lines responded to etoposide.

To do this, we treated we treated Mel270, OMM2.3 UM cells and T24 (control cells) with 50μM Etoposide for 3 hours before fixing and staining for IRF3 and NF-κB p65. Immunofluorescence microscopy was then carried out (Fig; 19).

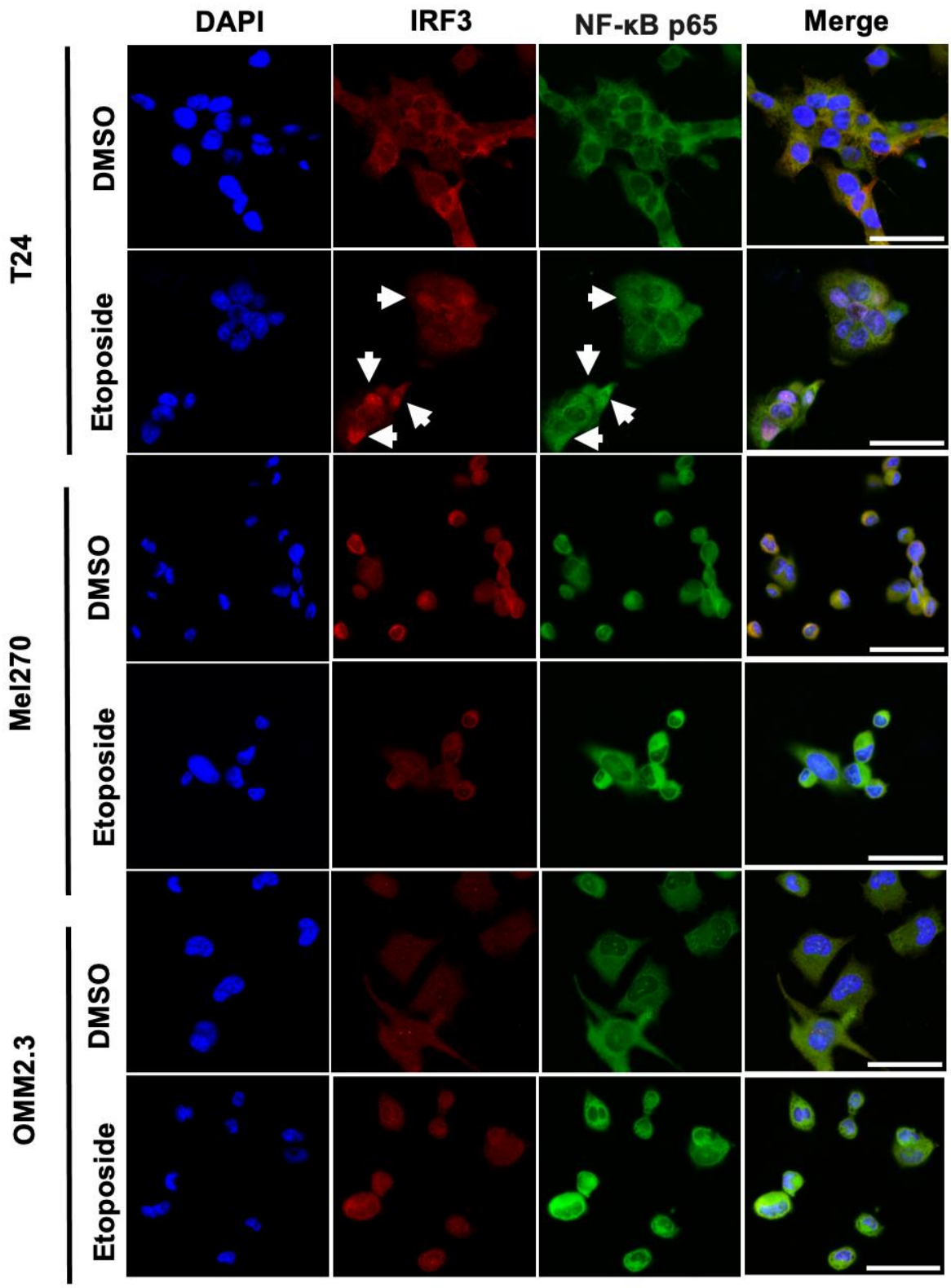
DAPI
IRF3
NF-κB p65
Merge
T24
Mel270
OMM2.3
DMSO
Etoposide
DMSO
Etoposide
DMSO
Etoposide

Figure 19: Absence of nuclear translocation of IRF3 and NF-κB p65 upon Etoposide treatment in UM cells.

Representative immunofluorescent images of T24, Mel270 and OMM2.3 cells. Scale bar on merge = 50μm. White arrows represent cases of IRF3 and NF-κB p65 nuclear translocation.

T24 control cells exhibited translocation of IRF3 and NF-κB p65, 3 hours post etoposide treatment as expected. In contrast, and like post (HT DNA) transfection, UM cells exhibited no nuclear translocation of both transcription factors (Fig; 19). These findings indicated that UM cells not only fail to respond to DNA sensing but also to DNA -damage induced signalling in response to etoposide.

3.1.7 Etoposide is the most Potent Reducer of Cell Viability across all cell lines.

As an additional experiment, we investigated the effect of nucleic acid transfections and etoposide treatment on cell viability. To do this, MTS cell viability assays were conducted (Fig; 20). This would allow us to assess whether impaired immune sensing correlated with altered sensitivity to nucleic acid transfections and Etoposide in our UM cells.

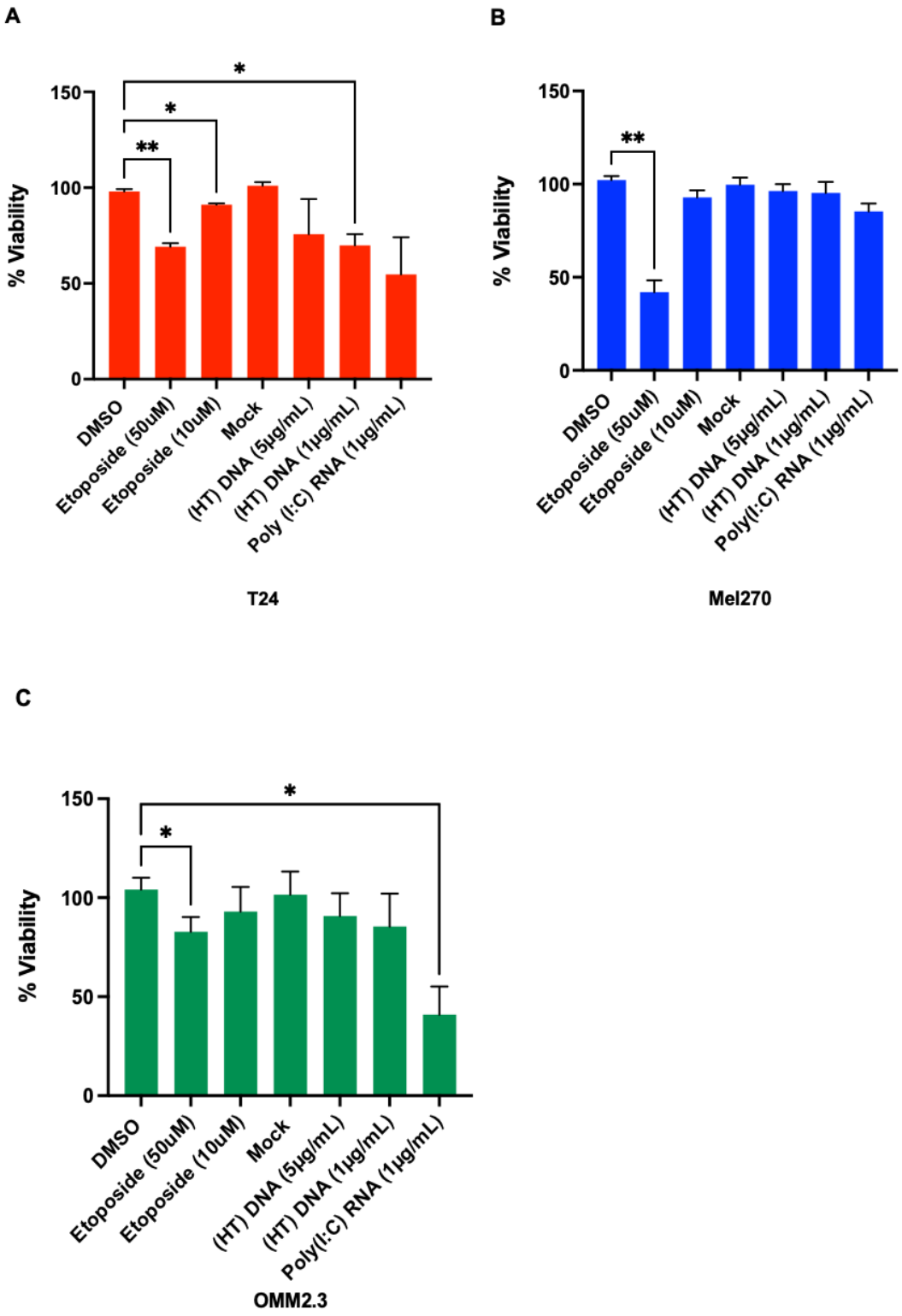
A
% Viability
150
100
50
0
*
*
**
DMSO
Etoposide (50uM)
Etoposide (10uM)
Mock
(HT) DNA (5µg/mL)
(HT) DNA (1µg/mL)
Poly (I:C) RNA (1µg/mL)
T24
B
% Viability
150
100
50
0
**
DMSO
Etoposide (50uM)
Etoposide (10uM)
Mock
(HT) DNA (5µg/mL)
(HT) DNA (1µg/mL)
Poly(I:C) RNA (1µg/mL)
Mel270
C
% Viability
150
100
50
0
*
*
DMSO
Etoposide (50uM)
Etoposide (10uM)
Mock
(HT) DNA (5µg/mL)
(HT) DNA (1µg/mL)
Poly(I:C) RNA (1µg/mL)
OMM2.3

Figure 20: 50μM Etoposide causes the greatest reduction in cell viability across all cell lines.

T24, Mel270 and OMM2.3 cells were treated with the chemotherapy agent Etoposide (10μM and 50μM concentrations) or transfected with (HT) DNA (1 and 5μg/mL) or Poly(I:C) RNA (1μg/mL) for 48hrs. DMSO and mock transfections acted as controls for treatments trialed. MTS reagent was then added to each well and incubated for 4 hours before reading the absorbance (490nm). Bar graphs were plotted as % viability by normalizing to the untreated cells, **(A)** T24, **(B)** Mel270, **(C)** OMM2.3. Data plotted as individual points (biological triplicates) per condition +/- standard deviation. A one-way ANOVA with Dunnett's multiple comparison test was performed, comparing each condition to DMSO control. *= $p < 0.01$. **=$p<0.05$ (statistically significant).

In T24 control cells, treatment with both concentrations of Etoposide significantly reduced cell viability compared with DMSO control, with 50μM causing the greatest reduction (Fig; 20A). Transfection with (HT) DNA also caused a modest reduction in cell viability, with lower concentrations (1μg/mL) having a significant effect. Poly(I:C) RNA transfection also produced a similar effect but to a lesser extent. In Mel270 cells, only the 50μM concentration of Etoposide caused a significant reduction in cell viability. In contrast nucleic acid transfections had minimal effects when compared to mock controls (Fig; 20B). Like mel270 cells, 50μM Etoposide again significantly reduced cell viability when compared to DMSO control in OMM2.3 cells, with (HT) DNA transfection producing minimal effects. In contrast to mel270 cells, Poly(I:C) RNA transfection, did significantly reduce cell viability in OMM2.3 cells (Fig; 20C).

3.1.8 UM cells induce IL-6 production in Response to Poly(I:C) RNA but not in response to Etoposide and (HT) DNA.

Our previous experiments revealed that our UM cells did not activate IRF3 or NF-κB p65 in response to Etoposide treatment and (HT) DNA transfection (Fig; 17, 19). However, cells retained the ability to respond to poly(I:C) RNA transfection (Fig; 18). Therefore, to further investigate the immune response of our UM cells, we next examined downstream inflammatory cytokine production. We first quantified IL-6 secretion, a key target of NF-κB p65, by ELISA (Fig; 21). To ensure results were not due to technical error, T24 cells were used as a positive control.

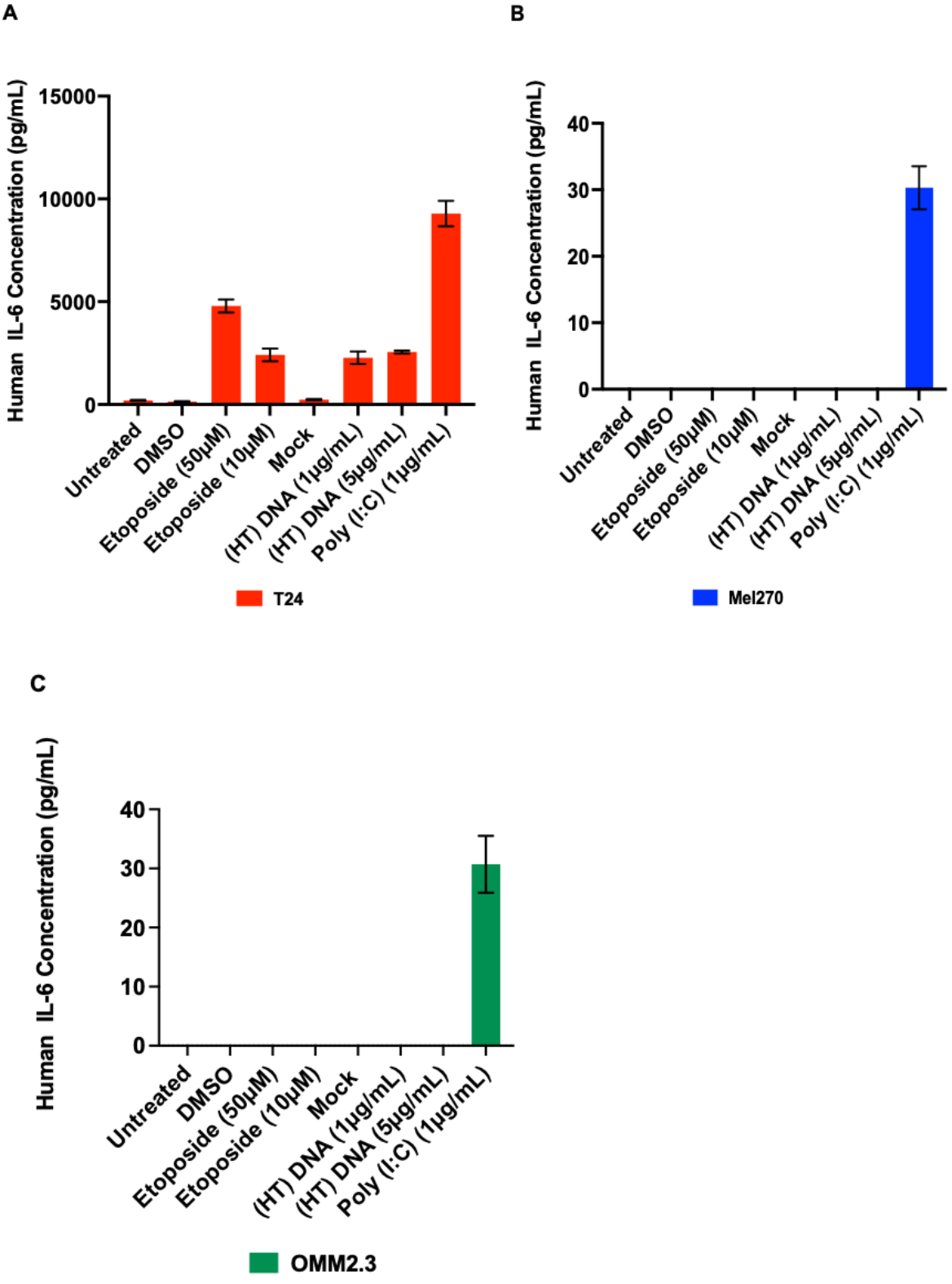
A
Human IL-6 Concentration (pg/mL)
15000
10000
5000
0
Untreated
DMSO
Etoposide (50µM)
Etoposide (10µM)
Mock
(HT) DNA (1µg/mL)
(HT) DNA (5µg/mL)
Poly (I:C) (1µg/mL)
T24
B
Human IL-6 Concentration (pg/mL)
40
30
20
10
0
Untreated
DMSO
Etoposide (50µM)
Etoposide (10µM)
Mock
(HT) DNA (1µg/mL)
(HT) DNA (5µg/mL)
Poly (I:C) (1µg/mL)
Mel270
C
Human IL-6 Concentration (pg/mL)
40
30
20
10
0
Untreated
DMSO
Etoposide (50µM)
Etoposide (10µM)
Mock
(HT) DNA (1µg/mL)
(HT) DNA (5µg/mL)
Poly (I:C) (1µg/mL)
OMM2.3

Figure 21: UM cells induce IL-6 production in Response to Poly(I:C) RNA but not in response to Etoposide and (HT) DNA.

IL-6 secretion measured via ELISA in **(A)** T24 cells **(B)** Mel270 cells **(C)** OMM2.3 cells, Cells were treated with the chemotherapy agent Etoposide (10μM and 50μM concentrations) or transfected with (HT) DNA (1 and 5μg/mL) or Poly(I:C) RNA (1μg/mL) for 24 hours before conducting ELISA according to manufacturer's protocol. Untreated, DMSO and mock transfections acted as controls for the treatments/transfections trialed. Data presented as biological triplicates +/- standard deviation. Experiment is representative of two repeat experiments. Statistical analysis was not performed due to the limited number of repeat experiments.

T24 control cells exhibited robust secretion of IL-6 post Etoposide treatment as well as post-stimulation with poly(I:C) and (HT) DNA, compared to controls (Fig; 21A) This confirmed validity of the assay in the detection of IL-6. In contrast, both Mel270 and OMM2.3 cells exhibited undetectable IL-6 secretion in response to Etoposide and (HT) DNA transfection. In contrast Poly(I:C) RNA transfection induced modest IL-6 secretion in both cell lines, compared to controls. However, this secretion was minimal when compared to the T24 control cells (Figures; 21B, C).

3.1.9 UM Cells induce CXCL10 production in Response to Poly(I:C) RNA but not in Response to Etoposide and (HT) DNA.

Based on the observation that IL-6 secretion did not occur in response to (HT) DNA and Etoposide treatment but did occur in response to poly(I:C) RNA in our UM cells (Fig; 21)., we next examined whether a similar effect was observed for CXCL10. CXCL10 is regulated by both IRF3 and NF-κB, and is a key chemokine produced in response to anti-viral DNA and RMA sensing pathways. Therefore, quantifying CXCL10 secretion by ELISA enabled us to further understand the broader innate immune activation occurring within our UM cells (Fig; 22).

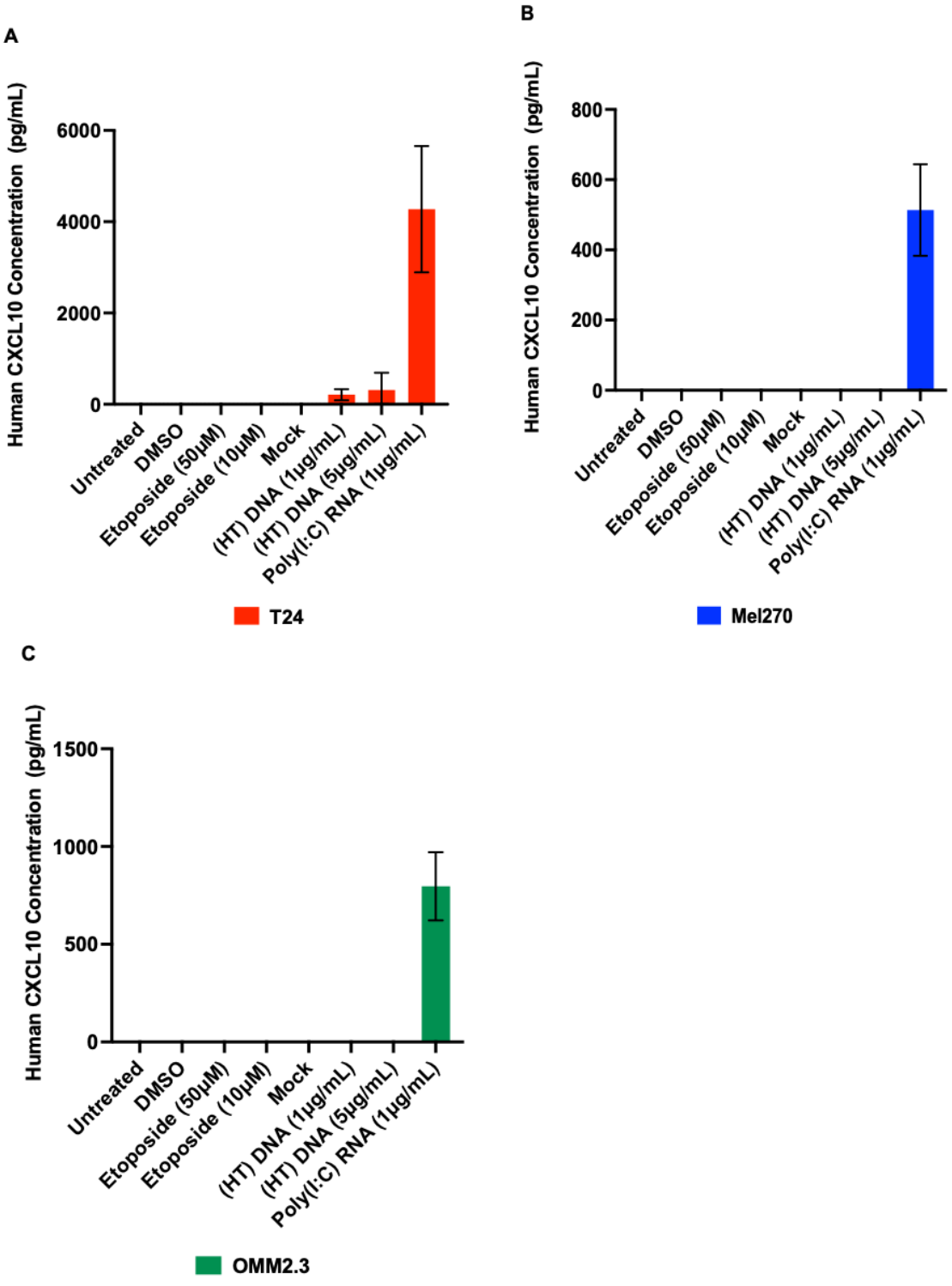
A
Human CXCL10 Concentration (pg/mL)
6000
4000
2000
0
Untreated
DMSO
Etoposide (50µM)
Etoposide (10µM)
Mock
(HT) DNA (1µg/mL)
(HT) DNA (5µg/mL)
Poly(I:C) RNA (1µg/mL)
T24
B
Human CXCL10 Concentration (pg/mL)
800
600
400
200
0
Untreated
DMSO
Etoposide (50µM)
Etoposide (10µM)
Mock
(HT) DNA (1µg/mL)
(HT) DNA (5µg/mL)
Poly(I:C) RNA (1µg/mL)
Mel270
C
Human CXCL10 Concentration (pg/mL)
1500
1000
500
0
Untreated
DMSO
Etoposide (50µM)
Etoposide (10µM)
Mock
(HT) DNA (1µg/mL)
(HT) DNA (5µg/mL)
Poly(I:C) RNA (1µg/mL)
OMM2.3

Figure 22: UM Cells induce CXCL10 production in Response to Poly(I:C) RNA but not in response to Etoposide and (HT) DNA.

CXCL10 secretion measured via ELISA in **(A)** T24 cells, **(B)** Mel270 cells **(C)** OMM2.3 Cells were treated with the chemotherapy agent Etoposide (10μM and 50μM concentrations) or transfected with (HT) DNA (1 and 5μg/mL) or Poly(I:C) RNA (1μg/mL) for 24 hours before conducting ELISA according to manufacturer's protocol. Untreated, DMSO and mock transfections acted as controls for the treatments/transfections trialed. Data presented as biological triplicates +/- standard deviation. Experiment is representative of two repeat experiments. Statistical analysis was not performed due to the limited number of repeat experiments

T24 control cells exhibited robust secretion of CXCL10 following (HT) DNA and Poly(I:C) RNA transfection, but not after etoposide treatment, compared to controls, again validating the assay (Fig; 22A). In contrast, Mel270 and OMM2.3 cells failed to secrete CXCL10 in response to Etoposide and (HT) DNA but did so in response to poly(I:C) RNA (Fig; 22B, C). However, like findings observed for IL-6 secretion, induced CXCL10 levels were not as high compared to T24 control cells.

3.1.10 Transcriptomic Analysis of the cGAS STING Pathway

To complement our protein and functional assays above, transcriptomic analyses was performed. Whilst this data was exploratory, this provided an insight into expression of different components of the DNA sensing pathway in Mel270 compared to OMM2.3 cells. A previously generated fragments per kilobase of transcript per million mapped reads (FPKM) dataset was analysed by uploading to the iDEP software, a tool used for RNA-sequencing analysis. We conducted differential gene expression analysis by using a false discovery rate (FDR) cutoff of 0.1. From this we identified 822 upregulated and 742 downregulated genes in Mel270 compared to OMM2.3 cells (Fig; 23A).

To determine if any of these components were differentially expressed in Mel270 compared to OMM2.3 cells, a KEGG pathway analysis was performed (Fig; 23B).

A

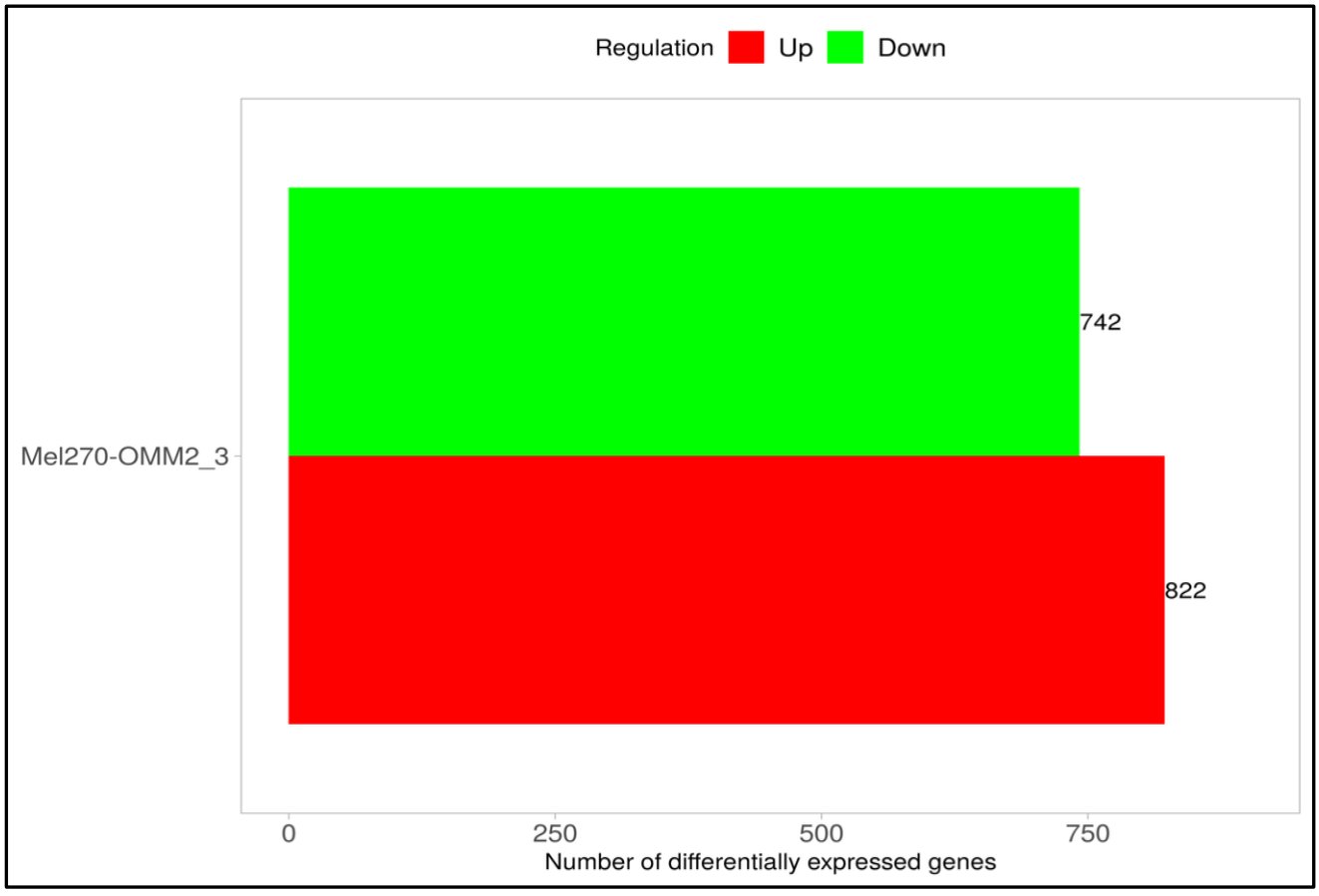

B

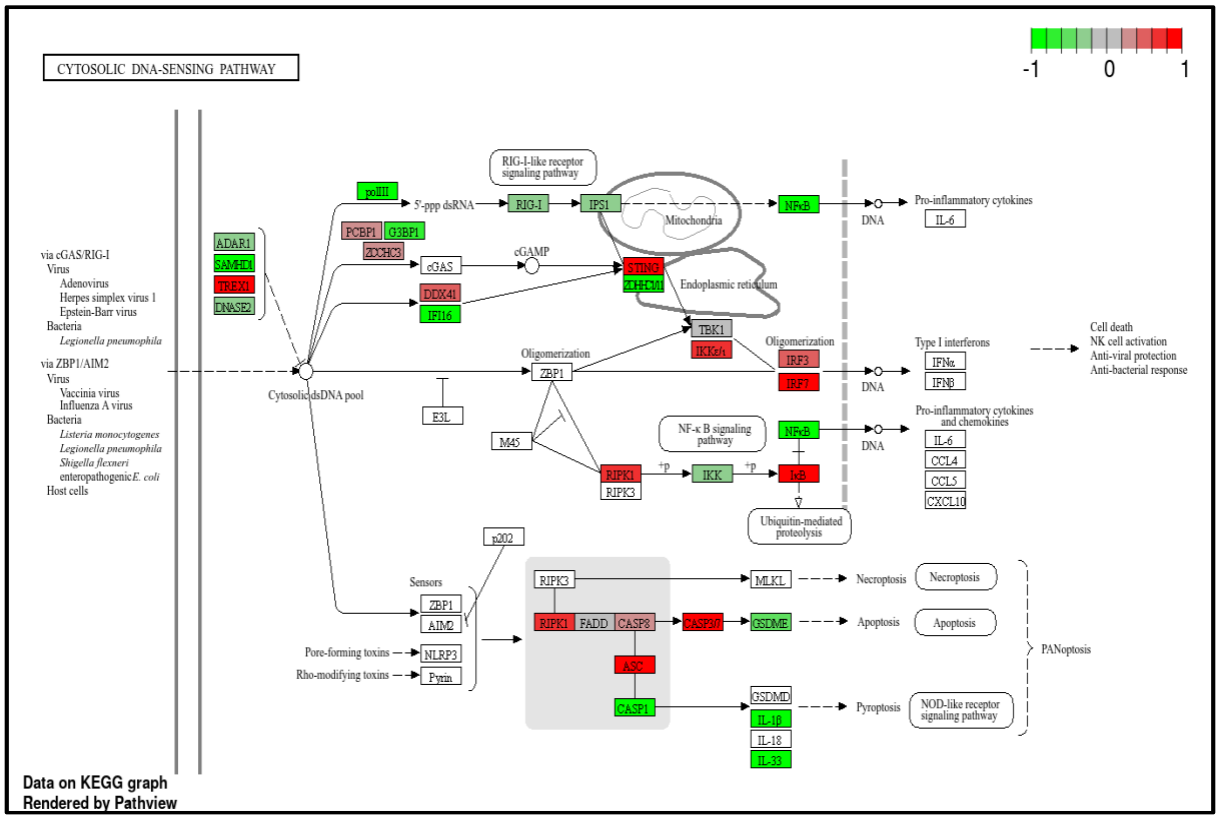

Figure 23: KEGG Pathway Analysis of Cytosolic DNA sensing pathway in Mel270 compared to OMM2.3 Cells.

A previously created FPKM (fragments per kilobase of transcript per million mapped reads) datasheet generated from RNA-sequencing data was used to analyze changes in gene expression between Mel270 and OMM2.3 Cells. The datasheet was uploaded to the iDEP software which returned a bar graph (A) displaying the number of differentially expressed genes in Mel270 compared to OMM2.3 cells. A 0.1 False discovery rate (FDR) cutoff was applied. (B) A KEGG analysis plot of the cytosolic DNA Sensing pathway. The pathway indicates changes in expression of genes of interest using a color gradient scheme for upregulation or downregulation. Red shows upregulation, green shows downregulation. Grey/white represents unchanged or not included in the original dataset respectively.

Transcriptomic analysis revealed that components of the cGAS STING pathway are differentially expressed between Mel270 and OMM2.3 cells. There were 822 genes upregulated in Mel270 compared to OMM2.3 cells (Fig; 23A). Focusing on components relevant to the cGAS STING axis, KEGG pathway analysis revealed

upregulation of STING and IRF3 but downregulation of other components including NF-kB and IFI16 in Mel270 cells compared to OMM2.3 cells (Fig; 23B). TBK1 remained unchanged, and cGAS was not reported in the original dataset (Fig; 23B). This did, however, confirm a link between varying levels of CA and genome instability and how cancers at different stages of tumour progression may utilise and or alter cGAS STING signalling, providing an avenue for further research.

5. Discussion

5.1 Introduction and Summary of Findings

CA is a recognised hallmark of many cancer types, including UM (Sabat-Pospiech et al., 2022), representing a double-edged sword for cancer cells (Sabat-Pośpiech et al., 2019). Cancer cells employ a mechanism known as centrosome clustering to cope with the levels of CA they express, by permitting the formation of a pseudo-bipolar spindle and enabling them to survive. However, this process is error prone and can lead to increased genomic instability (Sabat-Pośpiech et al., 2019). One consequence is the formation of MN that have been shown in some cases to activate the cGAS-STING pathway, a key innate immune signalling axis involved in the recognition of cytosolic DNA (Mackenzie et al., 2017, Harding et al., 2017). However, the cGAS STING pathway is not always activated and more recent studies have shown that MN fail to induce a cGAS dependent response (Takaki et al., 2024; Sato and Hayashi, 2024).

Despite many studies into the complex dual nature of activation of the cGAS STING pathway in cancer, the relationship and precise mechanisms by which CA influences the innate immune system remains underexplored, particularly in the context of UM. Therefore, this project aimed to further understand activation of the cGAS STING pathway in UM cells with varying levels of CA. To do this a patient-matched model of primary (Mel270) and metastatic (OMM2.3) UM cell lines were used that displayed lower and higher levels of CA respectively.

Our findings suggested that UM cells, regardless of CA status selectively suppress cytosolic DNA sensing, mediated by cGAS and STING and via alternate cGAS independent pathways, such as those that can be induced by the DNA damaging agent etoposide. This is likely a mechanism employed by UM cells to evade immune surveillance by downregulating a type I interferon response. Interestingly, the RNA sensing pathway, mediated through RIG-I/MDA-5 remained functionally intact, which highlighted the potential for exploitation as a therapeutic target. Furthermore, metastatic cells that exhibit higher levels of CA appeared to suppress DNA sensing to a greater extent than primary cells that exhibit lower levels of CA. This suggested possible enhancement of immune evasion strategies in cells with greater levels of CA and genome instability.

5.2 UM Cells Possess Impaired DNA Sensing

Our initial experiments revealed that even though both high and low CA UM cells contained MN (Fig; 12A, B), cells with higher levels of CA exhibited a significant increase in the number of MN formed (Fig; 12C). This suggested that higher CA leads to heightened genomic instability, consistent with findings conducted by Kwon and Bakhoum (2020) using various breast cancer cell lines, where MN were consistently increased in high vs low CA cells. This is also consistent with findings revealed by Sabat Pośpiech et al., (2022), who showed that metastatic OMM2.3 cells have higher levels of CA, compared to primary Mel270 cells, and therefore heightened genome instability (Fig; 12D). Additionally, both low and high CA containing UM cells contained micronuclei enriched for γH2AX, a marker of DNA double strand breaks (Fig; 13A, B), but no significant difference was observed between the two cell lines (Fig; 13C). MN are frequently positive for γH2AX indicating that there is ongoing DNA damage (Medvedeva et al., 2007). As over 50% of all MN in both cell lines were γH2AX positive, this suggested that MN displayed persistent DNA damage that could be predisposing MN to rupture and leading to the activation of cGAS in the cytosol.

However, surprisingly, when investigating cGAS expression our findings revealed that irrespective of CA status UM cells contained MN that were devoid of cGAS under baseline conditions (Fig;14) compared to HaCaT cells, which are human immortalised keratinocytes, known to express cGAS. This contrasted with findings from Mackenzie et al., (2017) and Harding et al., (2017) who showed that MN were enriched for cGAS in various human and mouse models irrespective of DNA damage. We therefore suggest that UM cells not only lack activation of the cGAS STING pathway but do not express cGAS altogether. This may represent an immune evasion mechanism, specific to UM cells only and one that has not been previously reported. However, in a recent preprint by MacDonald et al., (2023), it was revealed that nuclear chromatin, not nuclear envelope integrity, dictates cGAS recruitment to MN and that the ability of MN to trigger an immune response is dependent on the original state of DNA present before damage. As this was an aspect not explored here, it does provide an avenue for further investigation. Additionally, it is also important to note how other sources of DNA could potentially activate cGAS. For instance, Flynn et al., (2021) revealed that it is chromatin bridges, not MN that activate the cGAS STING pathway. In a separate

study, Zierhut et al., (2019) revealed that mtDNA is more efficient at activating cGAS due to the absence of nucleosomes. This highlights the complexity in how cGAS can be activated in different cell types and again as this was an aspect not explored in our study, provides an avenue for further research.

Furthermore, we observed that irrespective of CA status UM cells contain MN that display heterogeneity in their levels of IFI16 expression at baseline and post (HT) DNA transfection (Fig 14, 15, 16). As some MN were IFI16 positive and others were not, this suggested that there was variable IFI16 association with MN chromatin. As IFI16 is normally a nuclear protein associated with chromatin, the presence in MN, indicates that MN does not necessarily require nuclear envelope rupture for initiation of activation of an innate immune response. Despite this, IFI16 has been shown to be important for full cGAS activation in some studies (Almine et al., 2017, Jønsson et al., 2017). Furthermore, as a cell line dependent expression of IFI16 was observed, with weakest levels observed in metastatic UM cells with higher CA, this could contribute to impaired DNA sensing and suggests enhancement of immune evasion strategies in advanced UM. This could aid cell proliferation, survival and progression of metastatic UM cells.

In addition, we found that UM cells with lower CA retain STING, whereas UM cells with higher CA did not (Fig,14). This further suggested further suppression of DNA sensing when there is greater levels of CA. However, even though STING was present in cells with lower CA, it was likely not functional given no activation of the cGAS STING pathway was observed. Furthermore, translocation of the key transcription factors NF-kB p65 or IRF3 (Fig; 17), and secretion of the key cytokines IL-6 and CXCL10 (Fig; 21 and Fig; 22) did not occur at baseline and post DNA transfection, compared to T24 control cells, which confirmed a complete suppression and lack of a functional DNA sensing pathway in in our two tested UM cell lines. When performing cell viability assays, we noted that T24 cells responded to etoposide and showed increased sensitivity to nucleic acid transfections. This is consistent with the fact that T24 calls are known to possess an intact DNA sensing pathway (Fig; 20). In contrast Mel270 and OMM2.3 cells have impaired DNA sensing, and this was reflected in their differences in sensitivity to nucleic acid transfections and etoposide (Fig; 20).

These findings partly agree with Takaki et al., (2024), who demonstrated in six different cell lines (HaCaT, T24, SiHa, HeLa, WI-38 and HUVEC), self-DNA in MN fails to activate cGAS STING. However, our findings also diverge, as Takaki et al., (2024) also revealed that upon DNA transfection, the cGAS STING pathway is activated, as the cell lines they use all possess cGAS and STING expression. Similarly, in a study conducted by Sato and Hayashi (2024), experiments showed greater cGAS activation in mouse compared to human cells. However, their findings were limited to one cell line using an engineered reporter system and so this warrants further validation.

Multiple mechanisms have been discussed in the literature as explanations for cGAS STING suppression in different cancer types. One notable mechanism, appears to be epigenetic silencing through promoter methylation, causing reduced expression of these proteins (Konno et al., 2018, Falahat et al., 2021, Wu et al., 2018). This includes DNA hypermethylation, which has been observed in cutaneous malignant melanoma, (Xia et al., 2016). Additionally, post-translational modifications such as STING ubiquitination have been shown to affect trafficking of STING and IRF3 activation without impacting expression of STING (Ni et al., 2017). Whether similar mechanisms are at play in the UM cell lines we tested remains unknown. To test this, bisulphite sequencing or methylation specific PCR could be utilised to assess promoter methylation. Additionally, STING trafficking could be assessed through confocal microscopy, whilst ubiquitination could be investigated using immunoprecipitation. These experiments could provide explanations as to the suppressed cGAS-STING signalling we observed in our two tested UM cell lines.

Consistent with our protein-level and functional assays, basic transcriptomic analysis confirmed differential expression of components of the cGAS STING pathway in cells with high vs low CA (Fig 23.) This provides additional molecular evidence for the responses we observed in our experiments and provides further evidence for future exploration.

5.3 UM cells retain functional RNA sensing

Whilst DNA sensing was suppressed in UM cells lines, irrespective of CA status, stimulation with poly (I:C), elicited a response. Both cell lines exhibited nuclear translocation of the key transcription factors IRF3 and NF-kB p65 (Fig; 18) as well as secretion of the cytokines IL-6 and CXCL10 (Figures 21,22) in response to RNA stimulation. This agreed with findings conducted by Almine et al; (2017) who showed that human keratinocytes lacking cGAS or STING respond to poly(I:C) but not transfected DNA and furthermore suggested that DNA sensing was incomplete without IFI16 but IFI16 was not required for functional RNA sensing. Although it is important to note that translocation of transcription factors and secretion of cytokines was markedly reduced in comparison to T24 cells known to secrete IL-6 and CXCL10 and display translocation of IRF3 and NF-kB p65. RNA sensing primarily occurs through the RIG-I/MDA-5 pathway that normally detects viral or endogenous double stranded RNA. This then triggers MAVS protein, leading to downstream signalling that culminates in IRF3 and NF-κB p65 translocation to the nucleus and a type I IFN response (Rehwinkel and Gack, 2020). The fact that we observed a response to RNA but not DNA, confirms selective impairments of DNA sensing at the level of the upstream DNA sensors and STING as an immune evasion strategy in UM, whilst the shared signalling components such as TBK1 and IRF3 are still functional. Importantly, this suggests that RNA sensing pathways could provide a reliable therapeutic strategy for patients with UM, particularly in cases where DNA sensing cannot be activated.

STING agonists can be used to reactivate STING after suppression. Most STING agonists are analogues that mimic cyclic dinucleotides such as cGAMP and have shown promise in the clinic (Wang et al., 2024) For example MK-1454 and ADU-100, STING agonists has been shown to induce a strong type I interferon response and when combined with the antibodies pembrolizumab and spartalizumab have been effective at shrinking tumours in patients with lymphoma (Magand et al., 2023, Meric-Bernstam et al., 2023). However, as treatment effects were limited here, this means theirs is still no conclusive evidence for efficacy In any clinical trials, only in mouse models. As we did not try STING agonists in our study, testing a range of STING agonists on these UM cells could be useful. Furthermore, as our UM cells show response to poly(I:C), this could provide a target for upregulation of CXCL10 and a

boosted anti-tumour immune response. Therefore, MAVS or RNA agonists to stimulate RIG-I/MDA5 signalling could be developed for this purpose.

5.4 UM cells supress engagement of alternative cGAS-independent STING pathways

Whilst the most well understood pathway is canonical cGAS-dependent activation of STING, studies have highlighted the role for alternative pathways, in the context of DNA damage (Dunphy et al., 2018). These alternative or non-canonical pathways have been shown to operate independently of cGAS. In contrast to the anti-tumour immunity that is associated with canonical cGAS STING signalling, these alternative pathways are associated with more pro-tumour functions and specifically may contribute to chronic inflammation, thereby facilitating metastasis and proliferation (Dunphy et al., 2018).

As our findings showed a suppression of canonical DNA sensing through MN formation and therefore absence of canonical cGAS STING signalling in our UM cell lines, we next considered whether alternative pathways were at play. To do this we used etoposide, a well characterised topoisomerase 11 inhibitor and chemotherapy drug, that has been shown in the literature to elicit a type one interferon response via direct recognition of damaged DNA by the DNA damage sensors ATM and PARP1 (Dunphy et al., 2018).

Despite this, we saw no translocation of key transcription factors; IRF3 and NF-κB p65 to the nucleus or secretion of IL-6 and CXCL10 in response to etoposide in our UM cells (Figures; 19, 21, 22) In contrast T24 cells that have been derived from muscle invasive bladder cancer have been shown to induce canonical and non-canonical signalling under similar conditions. As there was both a lack of canonical and non-canonical DNA sensing, this suggested a broader impairment in DNA sensing that may be specific to UM cells. Previous findings from Dunphy et al. (2018) revealed a robust induction of innate immune activation within hours of etoposide induced DNA damage. However, it is important to note that this was in human keratinocytes and not cancer cells. Interestingly, there are not many papers that study the effects of induced DNA damage by etoposide in human cancer cells. However, one study revealed that using another DNA damaging agent, doxorubicin to cause DNA damage induced an NF-κB

non-canonical response, leading to increased IL-6 secretion in triple negative breast cancer cell lines (Vasiyani et al., 2021). This suggests variations between tumour types in DNA damage induced non-canonical activation of STING and provides an opportunity for further research into other DNA damaging agents, not just etoposide in promoting a non-canonical response. Therefore, our results suggest that keratinocytes and some cancer cells engage this response, but the two UM cell lines we tested do not.

5.5 Limitations and Future Directions

Despite the key insights provided by this project, there are several limitations, which must be acknowledged to provide opportunities for future research. Addressing these will be critical in the understanding of how cancers with varying levels of CA can evade immune detection, and how this can be harnessed to improve therapeutic outcomes.

In our study, we only focused on two UM cell lines (primary, lower levels of CA; and metastatic, higher levels of CA). Therefore, to get a broader understanding of how cancers with varying levels of CA evade immune detection, it would be useful to include a panel of cell lines, Moreover, expanding our investigations into other tumour types will address issues around tumour heterogeneity between cancers. Additionally, utilising multiple cancer types will help to determine if our findings are just specific to UM.

Furthermore, time constraints made it difficult to draw firm conclusions from this study and more repeats would be needed to validate any conclusions drawn. One difficulty was the ability of accurately distinguishing micronuclei from transfected DNA within the cells, as they both appear as small DAPI positive structures in confocal microscopy. IFI16 can localise to micronuclei but can also co-localise with transfected DNA in the cytoplasm. Further work could incorporate Lamin B1 as a marker for nuclear envelope staining or use live-cell imaging using fluorescently tagged transfected DNA. This would allow us to specifically identify micronuclei versus cytoplasmic DNA and increase the reliability of our interpretations.

In addition, further experiments are needed to uncover the precise mechanisms by which these UM cells escape immune detection. For example, future work should

consider whether the loss of cGAS and or STING is due to epigenetic silencing such as promoter methylation, post transcriptional regulation or post-translational modifications. In addition, restoring cGAS or STING expression could help determine if immune activity can be rescued and therefore confirm the importance of cGAS and STING in immune evasion. Finally in vivo modelling using mouse models to capture a realistic picture of the tumour microenvironment under physiologically relevant conditions is needed. This will come through gaining further understanding of cancer cells interactions with different immune cell subsets. Using mouse models will enable us to gain a further understanding of the anti-tumour immune response and provide reasons as to why STING agonists appear to be more effective in murine models, compared to humans. Mining of publicly available datasets using databases such as The Cancer Genome Atlas Program could reveal a correlation between pathway activity, mutations and epigenetics as well as clinical responses to immunotherapies. Furthermore, using patient-derived samples could enable analyses of STING and cGAS expression at the protein and mRNA level and enable us to correlate findings with immune cells infiltration using experimental techniques such as flow cytometry or single-cell RNA sequencing. Together, this could enable the assignment of patients to different subgroups for future targeted therapies.

5.7 Conclusion

This project highlights the importance of understanding innate immune modulation in cancers exhibiting CA. Our findings indicate that UM cells evade immune detection through selectively suppressing the cGAS-STING DNA sensing pathway, with this suppression greater in metastatic cells that display higher levels of CA and genome instability. However, the exact mechanisms underlying this suppression warrants further investigation. These findings have important implications for emerging therapeutic strategies and highlight the need to further investigate innate immune pathway modulation to enhance anti-tumour immunity in UM.

6. Bibliography

AHN, J., XIA, T., KONNO, H., KONNO, K., RUIZ, P. & BARBER, G. N. 2014. Inflammation-driven carcinogenesis is mediated through STING. *Nat Commun,* 5**,** 5166.

ALMINE, J. F., O'HARE, C. A. J., DUNPHY, G., HAGA, I. R., NAIK, R. J., ATRIH, A., CONNOLLY, D. J., TAYLOR, J., KELSALL, I. R., BOWIE, A. G., BEARD, P. M. & UNTERHOLZNER, L. 2017. IFI16 and cGAS cooperate in the activation of STING during DNA sensing in human keratinocytes. *Nature Communications,* 8**,** 14392.

AN, Y., ZHU, J., XIE, Q., FENG, J., GONG, Y., FAN, Q., CAO, J., HUANG, Z., SHI, W., LIN, Q., WU, L., YANG, C. & JI, T. 2024. Tumor Exosomal ENPP1 Hydrolyzes cGAMP to Inhibit cGAS-STING Signaling. *Adv Sci (Weinh),* 11**,** e2308131.

ARNANDIS, T., MONTEIRO, P., ADAMS, S. D., BRIDGEMAN, V. L., RAJEEVE, V., GADALETA, E., MARZEC, J., CHELALA, C., MALANCHI, I., CUTILLAS, P. R. & GODINHO, S. A. 2018. Oxidative Stress in Cells with Extra Centrosomes Drives Non-Cell-Autonomous Invasion. *Dev Cell,* 47**,** 409-424.e9.

BAI, H., BOSCH, J. J. & HEINDL, L. M. 2023. Current management of uveal melanoma: A review. *Clin Exp Ophthalmol,* 51**,** 484-494.

BAKHOUM, S. F., NGO, B., LAUGHNEY, A. M., CAVALLO, J. A., MURPHY, C. J., LY, P., SHAH, P., SRIRAM, R. K., WATKINS, T. B. K., TAUNK, N. K., DURAN, M., PAULI, C., SHAW, C., CHADALAVADA, K., RAJASEKHAR, V. K., GENOVESE, G., VENKATESAN, S., BIRKBAK, N. J., MCGRANAHAN, N., LUNDQUIST, M., LAPLANT, Q., HEALEY, J. H., ELEMENTO, O., CHUNG, C. H., LEE, N. Y., IMIELENSKI, M., NANJANGUD, G., PE'ER, D., CLEVELAND, D. W., POWELL, S. N., LAMMERDING, J., SWANTON, C. & CANTLEY, L. C. 2018. Chromosomal instability drives metastasis through a cytosolic DNA response. *Nature,* 553**,** 467-472.

BANERJEE, I., BEHL, B., MENDONCA, M., SHRIVASTAVA, G., RUSSO, A. J., MENORET, A., GHOSH, A., VELLA, A. T., VANAJA, S. K., SARKAR, S. N., FITZGERALD, K. A. & RATHINAM, V. A. K. 2018. Gasdermin D Restrains Type I Interferon Response to Cytosolic DNA by Disrupting Ionic Homeostasis. *Immunity,* 49**,** 413-426.e5.

BASTO, R., BRUNK, K., VINADOGROVA, T., PEEL, N., FRANZ, A., KHODJAKOV, A. & RAFF, J. W. 2008.

BOVERI, T. 2008. Concerning the origin of malignant tumours by Theodor Boveri. Translated and annotated by Henry Harris. *J Cell Sci,* 121 Suppl 1**,** 1-84.

BÜRCKSTÜMMER, T., BAUMANN, C., BLÜML, S., DIXIT, E., DÜRNBERGER, G., JAHN, H., PLANYAVSKY, M., BILBAN, M., COLINGE, J., BENNETT, K. L. & SUPERTI-FURGA, G. 2009. An orthogonal proteomic-genomic screen identifies AIM2 as a cytoplasmic DNA sensor for the inflammasome. *Nat Immunol,* 10**,** 266-72.

CHAN, J. Y. 2011. A Clinical Overview of Centrosome Amplification in Human Cancers. *International Journal of Biological Sciences,* 7**,** 1122-1144.

CHEN, Z., BEHRENDT, R., WILD, L., SCHLEE, M. & BODE, C. 2025. Cytosolic nucleic acid sensing as driver of critical illness: mechanisms and advances in therapy. *Signal Transduction and Targeted Therapy,* 10**,** 90.

CHEN, Q., BOIRE, A., JIN, X., VALIENTE, M., ER, E. E., LOPEZ-SOTO, A., JACOB, L., PATWA, R., SHAH, H., XU, K., CROSS, J. R. & MASSAGUÉ, J. 2016. Carcinoma-astrocyte gap junctions promote brain metastasis by cGAMP transfer. *Nature,* 533**,** 493-498.

CHUNG, C., SEO, W., SILWAL, P. & JO, E.-K. 2020. Crosstalks between inflammasome and autophagy in cancer. *Journal of Hematology & Oncology,* 13.

CONDUIT, P. T., WAINMAN, A. & RAFF, J. W. 2015. Centrosome function and assembly in animal cells. *Nature Reviews Molecular Cell Biology,* 16**,** 611-624.
CONLON, J., BURDETTE, D. L., SHARMA, S., BHAT, N., THOMPSON, M., JIANG, Z., RATHINAM, V. A., MONKS, B., JIN, T., XIAO, T. S., VOGEL, S. N., VANCE, R. E. & FITZGERALD, K. A. 2013. Mouse, but not human STING, binds and signals in response to the vascular disrupting agent 5,6-dimethylxanthenone-4-acetic acid. *J Immunol,* 190**,** 5216-25.
CRASTA, K., GANEM, N. J., DAGHER, R., LANTERMANN, A. B., IVANOVA, E. V., PAN, Y., NEZI, L., PROTOPOPOV, A., CHOWDHURY, D. & PELLMAN, D. 2012. DNA breaks and chromosome pulverization from errors in mitosis. *Nature,* 482**,** 53-8.
DA, Y., LIU, Y., HU, Y., LIU, W., MA, J., LU, N., ZHANG, C. & ZHANG, C. 2022. STING agonist cGAMP enhances anti-tumor activity of CAR-NK cells against pancreatic cancer. *Oncoimmunology,* 11**,** 2054105.
DECOUT, A., KATZ, J. D., VENKATRAMAN, S. & ABLASSER, A. 2021. The cGAS–STING pathway as a therapeutic target in inflammatory diseases. *Nature Reviews Immunology,* 21**,** 548-569.
DEYOUNG, K. L., RAY, M. E., SU, Y. A., ANZICK, S. L., JOHNSTONE, R. W., TRAPANI, J. A., MELTZER, P. S. & TRENT, J. M. 1997. Cloning a novel member of the human interferon-inducible gene family associated with control of tumorigenicity in a model of human melanoma. *Oncogene,* 15**,** 453-7.
DING, L., KIM, H. J., WANG, Q., KEARNS, M., JIANG, T., OHLSON, C. E., LI, B. B., XIE, S., LIU, J. F., STOVER, E. H., HOWITT, B. E., BRONSON, R. T., LAZO, S., ROBERTS, T. M., FREEMAN, G. J., KONSTANTINOPOULOS, P. A., MATULONIS, U. A. & ZHAO, J. J. 2018. PARP Inhibition Elicits STING-Dependent Antitumor Immunity in Brca1-Deficient Ovarian Cancer. *Cell Rep,* 25**,** 2972-2980.e5.
DOU, Z., GHOSH, K., VIZIOLI, M. G., ZHU, J., SEN, P., WANGENSTEEN, K. J., SIMITHY, J., LAN, Y., LIN, Y., ZHOU, Z., CAPELL, B. C., XU, C., XU, M., KIECKHAEFER, J. E., JIANG, T., SHOSHKES-CARMEL, M., TANIM, K., BARBER, G. N., SEYKORA, J. T., MILLAR, S. E., KAESTNER, K. H., GARCIA, B. A., ADAMS, P. D. & BERGER, S. L. 2017. Cytoplasmic chromatin triggers inflammation in senescence and cancer. *Nature,* 550**,** 402-406.
DUNPHY, G., FLANNERY, S. M., ALMINE, J. F., CONNOLLY, D. J., PAULUS, C., JØNSSON, K. L., JAKOBSEN, M. R., NEVELS, M. M., BOWIE, A. G. & UNTERHOLZNER, L. 2018. Non-canonical Activation of the DNA Sensing Adaptor STING by ATM and IFI16 Mediates NF-κB Signaling after Nuclear DNA Damage. *Molecular Cell,* 71**,** 745-760.e5.
DVORKIN, S., CAMBIER, S., VOLKMAN, H. E. & STETSON, D. B. 2024. New frontiers in the cGAS-STING intracellular DNA-sensing pathway. *Immunity,* 57**,** 718-730.
FDA (2022) *FDA approves tebentafusp-tebn for unresectable or metastatic uveal melanoma*. U.S. Food & Drug Administration. 25 January. Available at: https://www.fda.gov/drugs/resources-information-approved-drugs/fda-approves-tebentafusp-tebn-unresectable-or-metastatic-uveal-melanoma (Accessed: 17 September 2025).
FALAHAT, R., BERGLUND, A., PUTNEY, R. M., PEREZ-VILLARROEL, P., AOYAMA, S., PILON-THOMAS, S., BARBER, G. N. & MULÉ, J. J. 2021. Epigenetic reprogramming of tumor cell-intrinsic STING function sculpts antigenicity and T cell recognition of melanoma. *Proc Natl Acad Sci U S A,* 118.

FLYNN, P. J., KOCH, P. D. & MITCHISON, T. J. 2021. Chromatin bridges, not micronuclei, activate cGAS after drug-induced mitotic errors in human cells. *Proc Natl Acad Sci U S A,* 118.

FU, Y., XIAO, W. & MAO, Y. 2022. Recent Advances and Challenges in Uveal Melanoma Immunotherapy. *Cancers (Basel),* 14.

GAO, C. Q., CHU, Z. Z., ZHANG, D., XIAO, Y., ZHOU, X. Y., WU, J. R., YUAN, H., JIANG, Y. C., CHEN, D., ZHANG, J. C., YAO, N., CHEN, K. Y. & HONG, J. 2023. Serine/threonine kinase TBK1 promotes cholangiocarcinoma progression via direct regulation of β-catenin. *Oncogene,* 42**,** 1492-1507.

GAN, Y., LI, X., HAN, S., LIANG, Q., MA, X., RONG, P., WANG, W. & LI, W. 2021. The cGAS/STING Pathway: A Novel Target for Cancer Therapy. *Front Immunol,* 12**,** 795401.

GANEM, N. J., GODINHO, S. A. & PELLMAN, D. 2009. A mechanism linking extra centrosomes to chromosomal instability. *Nature,* 460**,** 278-82.

GODINHO, S. A., PICONE, R., BURUTE, M., DAGHER, R., SU, Y., LEUNG, C. T., POLYAK, K., BRUGGE, J. S., THÉRY, M. & PELLMAN, D. 2014. Oncogene-like induction of cellular invasion from centrosome amplification. *Nature,* 510**,** 167-71.

GREGAN, J., POLAKOVA, S., ZHANG, L., TOLIĆ-NØRRELYKKE, I. M. & CIMINI, D. 2011. Merotelic kinetochore attachment: causes and effects. *Trends Cell Biol,* 21**,** 374-81.

GÜÇ, E., TREVEIL, A., LEACH, E., BROOMFIELD, A., CAMERA, A., CLUBLEY, J., NIETO GARCIA, P., KAZACHENKA, A., KHANOLKAR, R., DEL CARPIO, L., HEYN, H., HASSEL, J. C., SACCO, J. J., STANHOPE, S., COLLINS, L., PIULATS, J. M., RANADE, K. & BENLAHRECH, A. 2025. Tebentafusp, a T cell engager, promotes macrophage reprogramming and in combination with IL-2 overcomes macrophage immunosuppression in cancer. *Nat Commun,* 16**,** 2374.

HARBOUR, J. W., ONKEN, M. D., ROBERSON, E. D., DUAN, S., CAO, L., WORLEY, L. A., COUNCIL, M. L., MATATALL, K. A., HELMS, C. & BOWCOCK, A. M. 2010. Frequent mutation of BAP1 in metastasizing uveal melanomas. *Science,* 330**,** 1410-3.

HARDING, S. M., BENCI, J. L., IRIANTO, J., DISCHER, D. E., MINN, A. J. & GREENBERG, R. A. 2017. Mitotic progression following DNA damage enables pattern recognition within micronuclei. *Nature,* 548**,** 466-470.

HELGADOTTIR, H. & HÖIOM, V. 2016. The genetics of uveal melanoma: current insights. *Appl Clin Genet,* 9**,** 147-55.

HERNANDEZ, C., HUEBENER, P. & SCHWABE, R. F. 2016. Damage-associated molecular patterns in cancer: a double-edged sword. *Oncogene,* 35**,** 5931-5941.

HOLLAND, A. J., LAN, W. & CLEVELAND, D. W. 2010. Centriole duplication: A lesson in self-control. *Cell Cycle,* 9**,** 2731-6.

HONG, C., SCHUBERT, M., TIJHUIS, A. E., REQUESENS, M., ROORDA, M., VAN DEN BRINK, A., RUIZ, L. A., BAKKER, P. L., VAN DER SLUIS, T., PIETERS, W., CHEN, M., WARDENAAR, R., VAN DER VEGT, B., SPIERINGS, D. C. J., DE BRUYN, M., VAN VUGT, M. & FOIJER, F. 2022. cGAS-STING drives the IL-6-dependent survival of chromosomally instable cancers. *Nature,* 607**,** 366-373.

ISHIKAWA, H. & BARBER, G. N. 2008. STING is an endoplasmic reticulum adaptor that facilitates innate immune signalling. *Nature,* 455**,** 674-678.

ISHIKAWA, H., MA, Z. & BARBER, G. N. 2009. STING regulates intracellular DNA-mediated, type I interferon-dependent innate immunity. *Nature,* 461**,** 788-92.

JAGER, M. J., SHIELDS, C. L., CEBULLA, C. M., ABDEL-RAHMAN, M. H., GROSSNIKLAUS, H. E., STERN, M. H., CARVAJAL, R. D., BELFORT, R. N., JIA, R., SHIELDS, J. A. & DAMATO, B. E. 2020. Uveal melanoma. *Nat Rev Dis Primers,* 6**,** 24.

JIANG, H. & CHAN, Y. W. 2024. Chromatin bridges: stochastic breakage or regulated resolution? *Trends in Genetics,* 40**,** 69-82.

JIANG, H., XUE, X., PANDA, S., KAWALE, A., HOOY, R. M., LIANG, F., SOHN, J., SUNG, P. & GEKARA, N. O. 2019. Chromatin-bound cGAS is an inhibitor of DNA repair and hence accelerates genome destabilization and cell death. *Embo j,* 38**,** e102718.

JIANG, M., CHEN, P., WANG, L., LI, W., CHEN, B., LIU, Y., WANG, H., ZHAO, S., YE, L., HE, Y. & ZHOU, C. 2020. cGAS-STING, an important pathway in cancer immunotherapy. *J Hematol Oncol,* 13**,** 81.

JØNSSON, K. L., LAUSTSEN, A., KRAPP, C., SKIPPER, K. A., THAVACHELVAM, K., HOTTER, D., EGEDAL, J. H., KJOLBY, M., MOHAMMADI, P., PRABAKARAN, T., SØRENSEN, L. K., SUN, C., JENSEN, S. B., HOLM, C. K., LEBBINK, R. J., JOHANNSEN, M., NYEGAARD, M., MIKKELSEN, J. G., KIRCHHOFF, F., PALUDAN, S. R. & JAKOBSEN, M. R. 2017. IFI16 is required for DNA sensing in human macrophages by promoting production and function of cGAMP. *Nature Communications,* 8**,** 14391.

JOHANSSON, P. A., BROOKS, K., NEWELL, F., PALMER, J. M., WILMOTT, J. S., PRITCHARD, A. L., BROIT, N., WOOD, S., CARLINO, M. S., LEONARD, C., KOUFARIOTIS, L. T., NATHAN, V., BEASLEY, A. B., HOWLIE, M., DAWSON, R., RIZOS, H., SCHMIDT, C. W., LONG, G. V., HAMILTON, H., KIILGAARD, J. F., ISAACS, T., GRAY, E. S., ROLFE, O. J., PARK, J. J., STARK, A., MANN, G. J., SCOLYER, R. A., PEARSON, J. V., VAN BAREN, N., WADDELL, N., WADT, K. W., MCGRATH, L. A., WARRIER, S. K., GLASSON, W. & HAYWARD, N. K. 2020. Whole genome landscapes of uveal melanoma show an ultraviolet radiation signature in iris tumours. *Nature Communications,* 11**,** 2408.

KALIKI, S. & SHIELDS, C. L. 2017. Uveal melanoma: relatively rare but deadly cancer. *Eye,* 31**,** 241-257.

KIM, J., KIM, H.-S. & CHUNG, J. H. 2023. Molecular mechanisms of mitochondrial DNA release and activation of the cGAS-STING pathway. *Experimental & Molecular Medicine,* 55**,** 510-519.

KIM, S., CHOE, M. H., OH, J. S. & KIM, J. S. 2022. Centrosome de-clustering of cancer cells induces cGAS-STING-mediated innate immunity of tumor-associated tumor cells in response to irradiation. *Biochem Biophys Res Commun,* 636**,** 24-30.

KOBAYASHI, Y., BUSTOS, M. A., HAYASHI, Y., YU, Q. & HOON, D. 2024. Interferon-induced factor 16 is essential in metastatic melanoma to maintain STING levels and the immune responses upon IFN-γ response pathway activation. *J Immunother Cancer,* 12.

KOCH, E. A. T., HEPPT, M. V. & BERKING, C. 2024. The Current State of Systemic Therapy of Metastatic Uveal Melanoma. *American Journal of Clinical Dermatology,* 25**,** 691-700.

KONNO, H., YAMAUCHI, S., BERGLUND, A., PUTNEY, R. M., MULÉ, J. J. & BARBER, G. N. 2018. Suppression of STING signaling through epigenetic silencing and missense mutation impedes DNA damage mediated cytokine production. *Oncogene,* 37**,** 2037-2051.

KRANTZ, B. A., DAVE, N., KOMATSUBARA, K. M., MARR, B. P. & CARVAJAL, R. D. 2017. Uveal melanoma: epidemiology, etiology, and treatment of primary disease. *Clin Ophthalmol,* 11**,** 279-289.

KRUPINA, K., GOGINASHVILI, A. & CLEVELAND, D. W. 2021. Causes and consequences of micronuclei. *Curr Opin Cell Biol,* 70**,** 91-99.

KUMAR, V., BAUER, C. & STEWART, J. H. 2023. Cancer cell-specific cGAS/STING Signaling pathway in the era of advancing cancer cell biology. *European Journal of Cell Biology,* 102**,** 151338.

KWON, J. & BAKHOUM, S. F. 2020. The Cytosolic DNA-Sensing cGAS-STING Pathway in Cancer. *Cancer Discov,* 10**,** 26-39.

KWON, J., LEE, D. & LEE, S.-A. 2023. BAP1 as a guardian of genome stability: implications in human cancer. *Experimental & Molecular Medicine,* 55**,** 745-754.

KWON, M., LEIBOWITZ, M. L. & LEE, J.-H. 2020. Small but mighty: the causes and consequences of micronucleus rupture. *Experimental & Molecular Medicine,* 52**,** 1777-1786.

LEONARD-MURALI, S., BHASKARLA, C., YADAV, G. S., MAURYA, S. K., GALIVETI, C. R., TOBIN, J. A., KANN, R. J., ASHWAT, E., MURPHY, P. S., CHAKKA, A. B., SOMAN, V., CANTALUPO, P. G., ZHUO, X., VYAS, G., KOZAK, D. L., KELLY, L. M., SMITH, E., CHANDRAN, U. R., HSU, Y.-M. S. & KAMMULA, U. S. 2024. Uveal melanoma immunogenomics predict immunotherapy resistance and susceptibility. *Nature Communications,* 15**,** 2863.

LEVINE, M. S., BAKKER, B., BOECKX, B., MOYETT, J., LU, J., VITRE, B., SPIERINGS, D. C., LANSDORP, P. M., CLEVELAND, D. W., LAMBRECHTS, D., FOIJER, F. & HOLLAND, A. J. 2017. Centrosome Amplification Is Sufficient to Promote Spontaneous Tumorigenesis in Mammals. *Dev Cell,* 40**,** 313-322.e5.

LIANG, H., DENG, L., HOU, Y., MENG, X., HUANG, X., RAO, E., ZHENG, W., MAUCERI, H., MACK, M., XU, M., FU, Y. X. & WEICHSELBAUM, R. R. 2017. Host STING-dependent MDSC mobilization drives extrinsic radiation resistance. *Nat Commun,* 8**,** 1736.

LI, J., DIAO, H., GUAN, X. & TIAN, X. 2020. Kinesin Family Member C1 (KIFC1) Regulated by Centrosome Protein E (CENPE) Promotes Proliferation, Migration, and Epithelial-Mesenchymal Transition of Ovarian Cancer. *Med Sci Monit,* 26**,** e927869.

LI, D. & WU, M. 2021. Pattern recognition receptors in health and diseases. *Signal Transduction and Targeted Therapy,* 6**,** 291.

LI, K., WANG, J., ZHANG, R., ZHOU, J., ESPINOZA, B., NIU, N., WANG, J., JURCAK, N., ROZICH, N., OSIPOV, A., HENDERSON, M., FUNES, V., LYMAN, M., BLAIR, A. B., HERBST, B., HE, M., YUAN, J., TRAFTON, D., YUAN, C., WICHROSKI, M., LIU, X., FU, J. & ZHENG, L. 2024. Overcome the challenge for intratumoral injection of STING agonist for pancreatic cancer by systemic administration. *J Hematol Oncol,* 17**,** 62.

LI, T. & CHEN, Z. J. 2018. The cGAS-cGAMP-STING pathway connects DNA damage to inflammation, senescence, and cancer. *J Exp Med,* 215**,** 1287-1299.

LI, Y., SHI, J., YANG, J., GE, S., ZHANG, J., JIA, R. & FAN, X. 2020. Uveal melanoma: progress in molecular biology and therapeutics. *Ther Adv Med Oncol,* 12**,** 1758835920965852.

LIU, Y. & XU, P. 2025. cGAS, an innate dsDNA sensor with multifaceted functions. *Cell Insight,* 4**,** 100249.
MACDONALD, K. M., NICHOLSON-PUTHENVEEDU, S., TAGELDEIN, M. M., KHASNIS, S., ARROWSMITH, C. H. & HARDING, S. M. 2023. Antecedent chromatin organization determines cGAS recruitment to ruptured micronuclei. *Nature Communications,* 14**,** 556.
MACKENZIE, K. J., CARROLL, P., MARTIN, C. A., MURINA, O., FLUTEAU, A., SIMPSON, D. J., OLOVA, N., SUTCLIFFE, H., RAINGER, J. K., LEITCH, A., OSBORN, R. T., WHEELER, A. P., NOWOTNY, M., GILBERT, N., CHANDRA, T., REIJNS, M. A. M. & JACKSON, A. P. 2017. cGAS surveillance of micronuclei links genome instability to innate immunity. *Nature,* 548**,** 461-465.
MAGAND, J., ROY, V., MEUDAL, H., ROSE, S., QUESNIAUX, V., CHALUPSKA, D. & AGROFOGLIO, L. A. 2023. Synthesis of Novel 3',3'-cyclic Dinucleotide Analogues Targeting STING Protein. *Asian Journal of Organic Chemistry,* 12**,** 76-86.
MARSHALL, J. S., WARRINGTON, R., WATSON, W. & KIM, H. L. 2018. An introduction to immunology and immunopathology. *Allergy, Asthma & Clinical Immunology,* 14**,** 49.
MARTHIENS, V., RUJANO, M. A., PENNETIER, C., TESSIER, S., PAUL-GILLOTEAUX, P. & BASTO, R. 2013. Centrosome amplification causes microcephaly. *Nature Cell Biology,* 15**,** 731-740.
MARTIN, M., MASSHÖFE, L., TEMMING, P., RAHMANN, S., METZ, C., BORNFELD, N., VAN DE NES, J., KLEIN-HITPASS, L., HINNEBUSCH, A. G., HORSTHEMKE, B., LOHMANN, D. R. & ZESCHNIGK, M. 2013. Exome sequencing identifies recurrent somatic mutations in EIF1AX and SF3B1 in uveal melanoma with disomy 3. *Nat Genet,* 45**,** 933-6.
MEDVEDEVA, N. G., PANYUTIN, I. V., PANYUTIN, I. G. & NEUMANN, R. D. 2007. Phosphorylation of histone H2AX in radiation-induced micronuclei. *Radiat Res,* 168**,** 493-8.
MERIC-BERNSTAM, F., SWEIS, R. F., KASPER, S., HAMID, O., BHATIA, S., DUMMER, R., STRADELLA, A., LONG, G. V., SPREAFICO, A., SHIMIZU, T., STEEGHS, N., LUKE, J. J., MCWHIRTER, S. M., MÜLLER, T., NAIR, N., LEWIS, N., CHEN, X., BEAN, A., KATTENHORN, L., PELLETIER, M. & SANDHU, S. 2023. Combination of the STING Agonist MIW815 (ADU-S100) and PD-1 Inhibitor Spartalizumab in Advanced/Metastatic Solid Tumors or Lymphomas: An Open-Label, Multicenter, Phase Ib Study. *Clin Cancer Res,* 29**,** 110-121.
MILUNOVIĆ-JEVTIĆ, A., MOONEY, P., SULERUD, T., BISHT, J. & GATLIN, J. C. 2016. Centrosomal clustering contributes to chromosomal instability and cancer. *Current Opinion in Biotechnology,* 40**,** 113-118.
MITTAL, K., OGDEN, A., REID, M. D., RIDA, P. C., VARAMBALLY, S. & ANEJA, R. 2015. Amplified centrosomes may underlie aggressive disease course in pancreatic ductal adenocarcinoma. *Cell Cycle,* 14**,** 2798-809.
MOTWANI, M., PESIRIDIS, S. & FITZGERALD, K. A. 2019. DNA sensing by the cGAS-STING pathway in health and disease. *Nat Rev Genet,* 20**,** 657-674.
NATHAN, P., HASSEL, J. C., RUTKOWSKI, P., BAURAIN, J. F., BUTLER, M. O., SCHLAAK, M., SULLIVAN, R. J., OCHSENREITHER, S., DUMMER, R., KIRKWOOD, J. M., JOSHUA, A. M., SACCO, J. J., SHOUSHTARI, A. N., ORLOFF, M., PIULATS, J. M., MILHEM, M., SALAMA, A. K. S., CURTI, B., DEMIDOV, L., GASTAUD, L., MAUCH,

C., YUSHAK, M., CARVAJAL, R. D., HAMID, O., ABDULLAH, S. E., HOLLAND, C., GOODALL, H. & PIPERNO-NEUMANN, S. 2021. Overall Survival Benefit with Tebentafusp in Metastatic Uveal Melanoma. *N Engl J Med,* 385**,** 1196-1206.
NI, G., KONNO, H. & BARBER, G. N. 2017. Ubiquitination of STING at lysine 224 controls IRF3 activation. *Sci Immunol,* 2.
OECKINGHAUS, A. & GHOSH, S. 2009. The NF-kappaB family of transcription factors and its regulation. *Cold Spring Harb Perspect Biol,* 1**,** a000034.
ONKEN, M. D., MAKEPEACE, C. M., KALTENBRONN, K. M., CHOI, J., HERNANDEZ-AYA, L., WEILBAECHER, K. N., PIGGOTT, K. D., RAO, P. K., YUEDE, C. M., DIXON, A. J., OSEI-OWUSU, P., COOPER, J. A. & BLUMER, K. J. 2021. Targeting primary and metastatic uveal melanoma with a G protein inhibitor. *J Biol Chem,* 296**,** 100403.
ORTEGA, M. A., FRAILE-MARTÍNEZ, O., GARCÍA-HONDUVILLA, N., COCA, S., ÁLVAREZ-MON, M., BUJÁN, J. & TEUS, M. A. 2020. Update on uveal melanoma: Translational research from biology to clinical practice (Review). *Int J Oncol,* 57**,** 1262-1279.
PANNU, V., MITTAL, K., CANTUARIA, G., REID, M. D., LI, X., DONTHAMSETTY, S., MCBRIDE, M., KLIMOV, S., OSAN, R., GUPTA, M. V., RIDA, P. C. & ANEJA, R. 2015. Rampant centrosome amplification underlies more aggressive disease course of triple negative breast cancers. *Oncotarget,* 6**,** 10487-97.
PIEMONTE, K. M., ANSTINE, L. J. & KERI, R. A. 2021. Centrosome Aberrations as Drivers of Chromosomal Instability in Breast Cancer. *Endocrinology,* 162.
POPLI, S., CHAKRAVARTY, S., FAN, S., GLANZ, A., ARAS, S., NAGY, L. E., SEN, G. C., CHAKRAVARTI, R. & CHATTOPADHYAY, S. 2022. IRF3 inhibits nuclear translocation of NF-κB to prevent viral inflammation. *Proc Natl Acad Sci U S A,* 119**,** e2121385119.
PRAKASH, A., PAUNIKAR, S., WEBBER, M., MCDERMOTT, E., VELLANKI, S. H., THOMPSON, K., DOCKERY, P., JAHNS, H., BROWN, J. A. L., HOPKINS, A. M. & BOURKE, E. 2023. Centrosome amplification promotes cell invasion via cell-cell contact disruption and Rap-1 activation. *J Cell Sci,* 136.
RAFF, J. W. & BASTO, R. 2017. Centrosome Amplification and Cancer: A Question of Sufficiency. *Developmental Cell,* 40**,** 217-218.
RAMASAMY, P., MURPHY, C. C., CLYNES, M., HORGAN, N., MORIARTY, P., TIERNAN, D., BEATTY, S., KENNEDY, S. & MELEADY, P. 2014. Proteomics in uveal melanoma. *Exp Eye Res,* 118**,** 1-12.
RANOA, D. R. E., WIDAU, R. C., MALLON, S., PAREKH, A. D., NICOLAE, C. M., HUANG, X., BOLT, M. J., ARINA, A., PARRY, R., KRON, S. J., MOLDOVAN, G. L., KHODAREV, N. N. & WEICHSELBAUM, R. R. 2019. STING Promotes Homeostasis via Regulation of Cell Proliferation and Chromosomal Stability. *Cancer Res,* 79**,** 1465-1479.
RANTALA, E. S., HERNBERG, M. & KIVELÄ, T. T. 2019. Overall survival after treatment for metastatic uveal melanoma: a systematic review and meta-analysis. *Melanoma Res,* 29**,** 561-568.
REHWINKEL, J. & GACK, M. U. 2020. RIG-I-like receptors: their regulation and roles in RNA sensing. *Nature Reviews Immunology,* 20**,** 537-551.
RELIMPIO-LÓPEZ, I., GARRIDO-HERMOSILLA, A. M., ESPEJO, F., GESSA-SORROCHE, M., COCA, L., DOMÍNGUEZ, B., DÍAZ-GRANDA, M. J., PONTE, B., CANO, M. J., RODRÍGUEZ DE LA RÚA, E., CARRASCO-PEÑA, F., MÍGUEZ, C., SAAVEDRA, J.,

ONTANILLA, A., CAPARRÓS-ESCUDERO, C., RÍOS, J. J. & TERRÓN, J. A. 2022. Clinical Outcomes after Surgical Resection Combined with Brachytherapy for Uveal Melanomas. *J Clin Med,* 11.

ROBERTSON, A. G., SHIH, J., YAU, C., GIBB, E. A., OBA, J., MUNGALL, K. L., HESS, J. M., UZUNANGELOV, V., WALTER, V., DANILOVA, L., LICHTENBERG, T. M., KUCHERLAPATI, M., KIMES, P. K., TANG, M., PENSON, A., BABUR, O., AKBANI, R., BRISTOW, C. A., HOADLEY, K. A., IYPE, L., CHANG, M. T., ABDEL-RAHMAN, M. H., AKBANI, R., ALLY, A., AUMAN, J. T., BABUR, O., BALASUNDARAM, M., BALU, S., BENZ, C., BEROUKHIM, R., BIROL, I., BODENHEIMER, T., BOWEN, J., BOWLBY, R., BRISTOW, C. A., BROOKS, D., CARLSEN, R., CEBULLA, C. M., CHANG, M. T., CHERNIACK, A. D., CHIN, L., CHO, J., CHUAH, E., CHUDAMANI, S., CIBULSKIS, C., CIBULSKIS, K., COPE, L., COUPLAND, S. E., DANILOVA, L., DEFREITAS, T., DEMCHOK, J. A., DESJARDINS, L., DHALLA, N., ESMAELI, B., FELAU, I., FERGUSON, M. L., FRAZER, S., GABRIEL, S. B., GASTIER-FOSTER, J. M., GEHLENBORG, N., GERKEN, M., GERSHENWALD, J. E., GETZ, G., GIBB, E. A., GRIEWANK, K. G., GRIMM, E. A., HAYES, D. N., HEGDE, A. M., HEIMAN, D. I., HELSEL, C., HESS, J. M., HOADLEY, K. A., HOBENSACK, S., HOLT, R. A., HOYLE, A. P., HU, X., HUTTER, C. M., JAGER, M. J., JEFFERYS, S. R., JONES, C. D., JONES, S. J. M., KANDOTH, C., KASAIAN, K., KIM, J., KIMES, P. K., KUCHERLAPATI, M., KUCHERLAPATI, R., LANDER, E., LAWRENCE, M. S., LAZAR, A. J., LEE, S., LERAAS, K. M., LICHTENBERG, T. M., LIN, P., LIU, J., LIU, W., LOLLA, L., LU, Y., IYPE, L., MA, Y., et al. 2017. Integrative Analysis Identifies Four Molecular and Clinical Subsets in Uveal Melanoma. *Cancer Cell,* 32**,** 204-220.e15.

ROH, J. S. & SOHN, D. H. 2018. Damage-Associated Molecular Patterns in Inflammatory Diseases. *Immune Netw,* 18**,** e27.

RYNIAWEC, J. M. & ROGERS, G. C. 2021. Centrosome instability: when good centrosomes go bad. *Cellular and Molecular Life Sciences,* 78**,** 6775-6795.

SABAT-POSPIECH, D., FABIAN-KOLPANOWICZ, K., PRIOR, I. A., COULSON, J. M. & FIELDING, A. B. 2019. Targeting centrosome amplification, an Achilles' heel of cancer. *Biochem Soc Trans,* 47**,** 1209-1222.

SABAT-POŚPIECH, D., FABIAN-KOLPANOWICZ, K., KALIRAI, H., KIPLING, N., COUPLAND, S. E., COULSON, J. M. & FIELDING, A. B. 2022. Aggressive uveal melanoma displays a high degree of centrosome amplification, opening the door to therapeutic intervention. *J Pathol Clin Res,* 8**,** 383-394.

SABINO, D., GOGENDEAU, D., GAMBAROTTO, D., NANO, M., PENNETIER, C., DINGLI, F., ARRAS, G., LOEW, D. & BASTO, R. 2015. Moesin Is a Major Regulator of Centrosome Behavior in Epithelial Cells with Extra Centrosomes. *Current Biology,* 25**,** 879-889.

SACCO, J. J., CARVAJAL, R. D., BUTLER, M. O., SHOUSHTARI, A. N., HASSEL, J. C., IKEGUCHI, A., HERNANDEZ-AYA, L., NATHAN, P., HAMID, O., PIULATS, J. M., RIOTH, M., JOHNSON, D. B., LUKE, J. J., ESPINOSA, E., LEYVRAZ, S., COLLINS, L., HOLLAND, C. & SATO, T. 2024. Long-term survival follow-up for tebentafusp in previously treated metastatic uveal melanoma. *J Immunother Cancer,* 12.

SAMSON, N. & ABLASSER, A. 2022. The cGAS–STING pathway and cancer. *Nature Cancer,* 3**,** 1452-1463.

SATO, Y. & HAYASHI, M. T. 2024. Micronucleus is not a potent inducer of the cGAS/STING pathway. *Life Sci Alliance,* 7.

SEKINO, Y., OUE, N., KOIKE, Y., SHIGEMATSU, Y., SAKAMOTO, N., SENTANI, K., TEISHIMA, J., SHIOTA, M., MATSUBARA, A. & YASUI, W. 2019. KIFC1 Inhibitor CW069 Induces Apoptosis and Reverses Resistance to Docetaxel in Prostate Cancer. *J Clin Med,* 8.

SHEN, Y. J., LE BERT, N., CHITRE, A. A., KOO, C. X., NGA, X. H., HO, S. S., KHATOO, M., TAN, N. Y., ISHII, K. J. & GASSER, S. 2015. Genome-derived cytosolic DNA mediates type I interferon-dependent rejection of B cell lymphoma cells. *Cell Rep,* 11**,** 460-73.

SILVA-RODRÍGUEZ, P., FERNÁNDEZ-DÍAZ, D., BANDE, M., PARDO, M., LOIDI, L. & BLANCO-TEIJEIRO, M. J. 2022. GNAQ and GNA11 Genes: A Comprehensive Review on Oncogenesis, Prognosis and Therapeutic Opportunities in Uveal Melanoma. *Cancers (Basel),* 14.

SINGH, A., DENU, R. A., WOLFE, S. K., SPERGER, J. M., SCHEHR, J., WITKOWSKY, T., ESBONA, K., CHAPPELL, R. J., WEAVER, B. A., BURKARD, M. E. & LANG, J. M. 2020. Centrosome amplification is a frequent event in circulating tumor cells from subjects with metastatic breast cancer. *Mol Oncol,* 14**,** 1898-1909.

SONG, S., PENG, P., TANG, Z., ZHAO, J., WU, W., LI, H., SHAO, M., LI, L., YANG, C., DUAN, F., ZHANG, M., ZHANG, J., WU, H., LI, C., WANG, X., WANG, H., RUAN, Y. & GU, J. 2017. Decreased expression of STING predicts poor prognosis in patients with gastric cancer. *Sci Rep,* 7**,** 39858.

SPRANGER, S., SPAAPEN, R. M., ZHA, Y., WILLIAMS, J., MENG, Y., HA, T. T. & GAJEWSKI, T. F. 2013. Up-regulation of PD-L1, IDO, and T(regs) in the melanoma tumor microenvironment is driven by CD8(+) T cells. *Sci Transl Med,* 5**,** 200ra116.

SUN, L., WU, J., DU, F., CHEN, X. & CHEN, Z. J. 2013. Cyclic GMP-AMP synthase is a cytosolic DNA sensor that activates the type I interferon pathway. *Science,* 339**,** 786-91.

TAKAKI, T., MILLAR, R., HILEY, C. T. & BOULTON, S. J. 2024. Micronuclei induced by radiation, replication stress, or chromosome segregation errors do not activate cGAS-STING. *Mol Cell,* 84**,** 2203-2213.e5.

TAN, Y. H., LIU, M., NOLTING, B., GO, J. G., GERVAY-HAGUE, J. & LIU, G. Y. 2008. A Nanoengineering Approach for Investigation and Regulation of Protein Immobilization. *Acs Nano,* 2**,** 2374-2384.

TANG, D., KANG, R., COYNE, C. B., ZEH, H. J. & LOTZE, M. T. 2012. PAMPs and DAMPs: signal 0s that spur autophagy and immunity. *Immunol Rev,* 249**,** 158-75.

TANI, T., MATHSYARAJA, H., CAMPISI, M., LI, Z. H., HARATANI, K., FAHEY, C. G., OTA, K., MAHADEVAN, N. R., SHI, Y., SAITO, S., MIZUNO, K., THAI, T. C., SASAKI, N., HOMME, M., YUSUF, C. F. B., KASHISHIAN, A., PANCHAL, J., WANG, M., WOLF, B. J., BARBIE, T. U., PAWELETZ, C. P., GOKHALE, P. C., LIU, D., UPPALURI, R., KITAJIMA, S., CAIN, J. & BARBIE, D. A. 2024. TREX1 Inactivation Unleashes Cancer Cell STING-Interferon Signaling and Promotes Antitumor Immunity. *Cancer Discov,* 14**,** 752-765.

TIAN, Z., ZENG, Y., PENG, Y., LIU, J. & WU, F. 2022. Cancer immunotherapy strategies that target the cGAS-STING pathway. *Front Immunol,* 13**,** 996663.

VAN DE NES, J. A. P., KOELSCHE, C., GESSI, M., MÖLLER, I., SUCKER, A., SCOLYER, R. A., BUCKLAND, M. E., PIETSCH, T., MURALI, R., SCHADENDORF, D. & GRIEWANK, K. G. 2017, Activating CYSLTR2 and PLCB4 Mutations in Primary Leptomeningeal Melanocytic Tumors. *J Invest Dermatol,* 137**,** 2033-2035.

VASIYANI, H., SHINDE, A., ROY, M., MANE, M., SINGH, K., SINGH, J., GOHEL, D., CURRIM, F., VAIDYA, K., CHHABRIA, M. & SINGH, R. 2021. The analog of cGAMP, c-di-AMP, activates STING mediated cell death pathway in estrogen-receptor negative breast cancer cells. *Apoptosis,* 26**,** 293-306.
WANG, L., GENG, H., LIU, Y., LIU, L., CHEN, Y., WU, F., LIU, Z., LING, S., WANG, Y. & ZHOU, L. 2023. Hot and cold tumors: Immunological features and the therapeutic strategies. *MedComm (2020),* 4**,** e343
WANG, B., YU, W., JIANG, H., MENG, X., TANG, D. & LIU, D. 2024. Clinical applications of STING agonists in cancer immunotherapy: current progress and future prospects. *Front Immunol,* 15**,** 1485546.
WANG, M., SOORESHJANI, M. A., MIKEK, C., OPOKU-TEMENG, C. & SINTIM, H. O. 2018. Suramin potently inhibits cGAMP synthase, cGAS, in THP1 cells to modulate IFN-β levels. *Future Med Chem,* 10**,** 1301-1317.
WANG, X., WANG, M., LI, X. Y., LI, J. & ZHAO, D. P. 2019. KIFC1 promotes the proliferation of hepatocellular carcinoma in vitro and in vivo. *Oncol Lett,* 18**,** 5739-5746.
WHEELER, O. P. G. & UNTERHOLZNER, L. 2023. DNA sensing in cancer: Pro-tumour and anti-tumour functions of cGAS-STING signalling. *Essays Biochem,* 67**,** 905-918.
WU, B., ZHANG, B., LI, B., WU, H. & JIANG, M. 2024. Cold and hot tumors: from molecular mechanisms to targeted therapy. *Signal Transduction and Targeted Therapy,* 9**,** 274.
XIA, T., KONNO, H. & BARBER, G. N. 2016. Recurrent Loss of STING Signaling in Melanoma Correlates with Susceptibility to Viral Oncolysis. *Cancer Res,* 76**,** 6747-6759.
XIAO, Y. X., SHEN, H. Q., SHE, Z. Y., SHENG, L., CHEN, Q. Q., CHU, Y. L., TAN, F. Q. & YANG, W. X. 2017. C-terminal kinesin motor KIFC1 participates in facilitating proper cell division of human seminoma. *Oncotarget,* 8**,** 61373-61384.
XU, B., SUN, Z., LIU, Z., GUO, H., LIU, Q., JIANG, H., ZOU, Y., GONG, Y., TISCHFIELD, J. A. & SHAO, C. 2011. Replication stress induces micronuclei comprising of aggregated DNA double-strand breaks. *PLoS One,* 6**,** e18618.
YANG, H., WANG, H., REN, J., CHEN, Q. & CHEN, Z. J. 2017. cGAS is essential for cellular senescence. *Proc Natl Acad Sci U S A,* 114**,** E4612-e4620.
YANG, C., LIANG, Y., LIU, N. & SUN, M. 2023. Role of the cGAS-STING pathway in radiotherapy for non-small cell lung cancer. *Radiation Oncology,* 18**,** 145.
YANG, J., MANSON, D. K., MARR, B. P. & CARVAJAL, R. D. 2018. Treatment of uveal melanoma: where are we now? *Ther Adv Med Oncol,* 10**,** 1758834018757175.
YAVUZYIGITOGLU, S., KOOPMANS, A. E., VERDIJK, R. M., VAARWATER, J., EUSSEN, B., VAN BODEGOM, A., PARIDAENS, D., KILIÇ, E. & DE KLEIN, A. 2016. Uveal Melanomas with SF3B1 Mutations: A Distinct Subclass Associated with Late-Onset Metastases. *Ophthalmology,* 123**,** 1118-28.
YU, L. & LIU, P. 2021. Cytosolic DNA sensing by cGAS: regulation, function, and human diseases. *Signal Transduction and Targeted Therapy,* 6**,** 170.
YUAN, J., ADAMSKI, R. & CHEN, J. 2010. Focus on histone variant H2AX: to be or not to be. *FEBS Lett,* 584**,** 3717-24.
ZHANG, W., ZHAI, L., WANG, Y., BOOHAKER, R. J., LU, W., GUPTA, V. V., PADMALAYAM, I., BOSTWICK, R. J., WHITE, E. L., ROSS, L. J., MADDRY, J., ANANTHAN, S., AUGELLI-SZAFRAN, C. E., SUTO, M. J., XU, B., LI, R. & LI, Y. 2016. Discovery of a novel inhibitor of kinesin-like protein KIFC1. *Biochem J,* 473**,** 1027-35.

ZHAO, M., WANG, F., WU, J., CHENG, Y., CAO, Y., WU, X., MA, M., TANG, F., LIU, Z., LIU, H. & GE, B. 2021. CGAS is a micronucleophagy receptor for the clearance of micronuclei. *Autophagy,* 17**,** 3976-3991.

ZIERHUT, C., YAMAGUCHI, N., PAREDES, M., LUO, J. D., CARROLL, T. & FUNABIKI, H. 2019. The Cytoplasmic DNA Sensor cGAS Promotes Mitotic Cell Death. *Cell,* 178**,** 302-315.e23.